ParisTech
INSTITUT DES SCIENCES ET TECHNOLOGIES
PARIS INSTITUTE OF TECHNOLOGY

AgroParisTech
INSTITUT DES SCIENCES ET INDUSTRIES DU VIVANT ET DE L'ENVIRONNEMENT
PARIS INSTITUTE OF TECHNOLOGY FOR LIFE, FOOD AND ENVIRONMENTAL SCIENCES

Ecole Doctorale ABIES
Agriculture Agriculture Alimentation Food Biologie Biology Environnement Environment Santé Health

Doctorat ParisTech

T H È S E

pour obtenir le grade de docteur délivré par

L'Institut des Sciences et Industries du Vivant et de l'Environnement

(AgroParisTech)

Spécialité : Science de l'environment

présentée et soutenue publiquement par

Yuan ZHANG

4 novembre, 2011

Modelling the dynamic of organic micro-pollutants during composting process of French organic wastes : Application for bioremediation of Chinese polluted soil

Directeur de thèse : **Patricia GARNIER & Yong-Guan ZHU**
Co-encadrement de la thèse : **Sabine HOUOT**

Jury

M. Yves COQUET, Professeur, AgroParisTech	Examinateur
M. Kai-Song ZHANG, Professeur, IUE-CAS	Examinateur
M. Chao-Xiang LIU, Professeur, IUE-CAS	Examinateur
M. Tian-Ling ZHENG, Professeur, Xiamen University	Examinateur
M. Chang-Zhou YAN, Professeur, IUE-CAS	Examinateur
M. Wen-Sui LUO, Professeur, IUE-CAS	Rapporteur
M. Zong-Ze SHAO, Professeur, Third institute of Oceanography	Rapporteur
M. Yong-Guan ZHU, Professeur, IUE-CAS	Directeur (Partie Chine)
Mme. Patricia GARNIER, CR, INRA-EGC	Directeur (Partie France)
Mme. Sabine HOUOT, Professeur, INRA-EGC	Co-directeur (Partie France)

AgroParisTech
INRA-EGC
78850 Thiverval-Grignon, site de Grignon, BP01

ACKNOWLEDGEMENT

The realization of my PHD could not be possible without the supports and the generosities from a great number of persons. I make firstly a point of thanking very sincerely to Ms. Patricia GARNIER and Mr. Yongguan ZHU, who in charge of me in France and in China respectively, for the relevance of their advices and the confidence that they invested in me, as well as their great help during my whole PHD period. Thanks to Ms. Francois LAUNAY and Corinnes FIERS, secretary of scientific direction in l'Ecole Doctorale ABIES, for their scientific directions and her extensive supports.

I want also to make a point of expressing my gratitude towards Ms. Sabine HOUOT, responsible of Equip Soil, who gave me a lot of technical directions and experimental conveniences, Mr. Enrique BARRIUSO, director of UMR INRA-AgroParisTech EGC, where I was complete my PHD for the part of France.

I prefer to say thanks to Egide with the program PHC-PFCC, who provides me the financial support when I was in France during my PHD period.

I would like to appreciate Yves COQUET , who provides me the chance to do my Master ' s Degree in AgroParisTech, and who leads to enter the soil science.

I want to thanks to Gwenaelle LASHERMES, my cooperator, who gives me a lot of help not only in the aspect of study but also in the aspect of life since I did my training course in the year of 2007. I would like to appreciate Mr. Jeremy DOUBLET and Cedric FRANCOU, who provide me the database so that I can complete the calibration of our model with more convenience.

I would like to thank to Mr. Nunan NAOISE, Mr. Jean-philipe STERYER, Ms. Muriel JOLLY, Ms. Marjolaine DESCHAMPS, Valerie BERGHEAUD, Ms. Min QIAO, and Nathalie BERNET, Clement PELTRE… for their academic and technical supports during my PHD in China and in France.

I would like to thank Chunnu GENG, JingJing PENG, Xuping JIAN, Gang LI, Bo XU, and Hongbo LI …who give me a lot of help during my period of study in Xiamen.

Finally, I prefer to make a point of testifying my affection with all the persons in UMR INRA-AgroParisTech in France and at RCEES-CAS in China, who took care about me and encouraged me during my PHD period. They thus contributed to make a good experience for me.

For all, I’d like to say thank you from my heart!

Summary:

ACKNOWLEDGEMENT 1

LIST OF FIGURES 7

LIST OF TABLES 12

LIST OF ABBREVIATIONS 13

ABSTRACT 15

RESUME 17

GENERAL INTRODUCTION 19

CHAPTER 1 LITERATURE REVIEW 23

1.1 Presentation of composting 23

1.1.1 Temperature 23

1.1.2 Areation (ventilation) 23

1.1.3 Free Air Space (FAS) 24

1.1.4 Moisture content 25

1.1.5 C/N ratio 26

1.1.6 pH value 26

1.1.7 The fate of microorganisms during the composting process 26

1.2 Evolution of organic matter (OM) during composting 27

1.2.1 The mesophilic phase 27

1.2.2 The thermophilic phase 27

1.2.3 The cooling phase 27

1.2.4 The maturation phase 28

1.3 Bioremediation of contaminated soil by composting 28

1.3.1 Contaminated soil by PAHs 28

1.3.2. Potential bioremediation of PAH-contaminated soils by composting 29

1.3.3 Evolution of PAHs during composting 30

1.4 Modelling the dynamics of OM and OP during the composting 31

1.4.1 Summary of environmental conditions 31

1.4.2 Summary of OM models 33

1.4.3 Summary of OP models 37

1.5 Objectives of the thesis 40

1.6 References 42

PART I: MODELING ORGANIC CARBON AND ORGANIC POLLUTANT DYNAMICS DURING COMPOSTING OF ORGANIC WASTES 51

CHAPTER 2: MODELLING OF ORGANIC MATTER DYNAMIC DURING THE COMPOSTING PROCESS 52

2.1 Abstract 52
2.2 Introduction 53
2.3 Materials and Methods 54
2.3.1 The model 54
2.3.2 Data acquisition for the model calibration 58
2.3.3 Calibration and evaluation of the model 60
2.4 Results and Discussion 63
2.4.1 Estimation of model parameters 63
2.4.2 Evaluation of calibrated model 67
2.4.3 Sensitivity analysis 73
2.5 Conclusion 75
2.6 Acknowledgements 76

CHAPTER 3: A MODEL COUPLING ORGANIC CARBON AND ORGANIC POLLUTANT DYNAMICS DURING COMPOSTING 81

3.1 Abstract 81
3.2 Introduction 82
3.3 Description of the COP_Compost model 83
3.3.1 Organic C module 83
3.3.2 Organic pollutant module 86
3.3.3 Model coupling OC and OP modules 86
3.4 Data acquisition for model calibration and evaluation 87
3.4.1 Data acquisition for calibration and evaluation of the OC module 87
3.4.2 Data acquisition for OP module calibration 88
3.4.3 Data acquisition for the coupling between OC and OP modules 89
3.5 Model calibration and evaluation 89
3.5.1 Calibration and evaluation of the OC module 89
3.5.2 Calibration and evaluation of the OP module 91
3.6 Results and discussion 92
3.6.1 Calibration of the OC module 92
3.6.2 Evaluation of the OC module 93
3.6.3 Calibration of the OPs module 96
3.7 Conclusions 101
3.8 Acknowledgements 102
3.9 References 103

CHAPTER 4: SENSITIVITY ANALYSIS OF COP_COMPOST MODEL FOR THE DEGRADATION OF ORGANIC MICROPOLLUTANTS DURING COMPOSTING PROCESS 107

4.1 Abstract 107
4.2 Introduction 107

4.3 Materials and methods....109
4.3.1 Presentation of COP_Compost model....109
4.3.2 Software / Interface (MATLAB & Excel)....112
4.3.3 Experimental Data for model calibration and evaluation....115
4.3.4 Model calibration for OP module....117
4.3.5 Sensitivity analysis....118
4.4 Results and discussion....119
4.4.1 Calibration of OP module....119
4.5 Sensitivity analysis....124
4.5.1 Sensitivity of pyrene and simazine to all parameters....124
4.5.2 Sensitivity to initial conditions....126
4.6 Conclusion....129
4.7 Acknowledgements....130
4.8 References....131

PART II: APPLICATION OF COP_COMPOST MODEL TO BIOREMEDIATION OF PAH CONTAMINATED SOIL....135

TROUGH COMPOST....135

CHAPTER 5: REMEDIATION OF POLYCYCLIC AROMATIC HYDROCARBON (PAH) CONTAMINATED SOIL THROUGH COMPOSTING WITH FRESH ORGANIC WASTES....136

5.1 Abstract....136
5.2 Introduction....137
5.3 Materials and methods....138
5.3.1 Experimental design....138
5.3.2 Contaminated soil....139
5.3.3 Mixture of wastes....139
5.3.4 Initial soil/waste mixtures....139
5.3.5 Specific added microorganisms....140
5.3.6 Bioreactors....140
5.3.7 Temperature and moisture....141
5.3.8 Sample collection....141
5.3.9 Organic matter analysis....142
5.3.10 PAHs analysis....142
5.3.11 PAH sorption....143
5.3.12 PLFA analysis....144
5.3.13 Statistical analysis....144
5.4 Results & Discussion....145
5.4.1 Dry mass....145
5.4.2 Organic matter analysis....146
5.4.3 Fate of PAHs....147

5.4.4 PLFA profiling 150
5.5 Conclusion 153
5.6 Acknowledgements 154
5.7 References 155

CHAPTER 6: MODELLING REMEDIATION OF POLYCYCLIC AROMATIC HYDROCARBON (PAH) CONTAMINATED SOIL THROUGH COMPOSTING WITH COP-COMPOST MODEL 161

6.1 Materials and Methods 161
6.1.1 Contaminated soil 161
6.1.2 Mixture of wastes 161
6.1.3 Initial soil/waste mixtures 161
6.1.4 Bioreactors 162
6.1.5 Temperature and moisture 162
6.1.6 Sample collection 162
6.1.7 Organic matter analysis 163
6.1.8 PAHs analysis 163
6.1.9 PAH sorption 164
6.1.10 Statistical analysis 164
6.1.11 COP_Compost model 165
6.1.12 Model application 167
6.2 Data acquisition for model simulation 167
6.2.1 Organic matter analysis 167
6.2.2 Organic micro-pollutant analysis 168
6.3 Results and discussion 170
6.3.1 OM simulation 170
6.3.2 OP simulation 171
6.3.2.2 Simulations with coupling model 173

PART III: GENERAL CONCLUSION AND PERSPECTIVES 177

APPENDIX: EQUATIONS OF THE COP-COMPOST MODEL 185

LIST OF FIGURES

Figure 1.1_A)**:** Microbial succession during the composting process (Epstein, 1997)

1.1_B): Idealized temperature variation in the compost during the composting process

Figure 1.2: Model describing the flux of C and N in the course OM decompositionin the field of soil: Model STICS (Nicolardot et al., 2001)

Figure 1.3: Schematic Representation of ADM1 model: conversion of a process of the anaerobic digestion (Batstone et al., 2002)

Figure 1.4: Schema of the model of Kasier (1996)

Figure 1.5: Multi-compartiment model (Xue and Selim, 1995; Shelton and Doherty, 1997)

Figure 1.6: Model of Saffih-Hdadi (2003)

Figure 2.1: General schema of the composting model of organic matter

Figure 2.2: Van Soest biochemical fractions of the initial composting mixtures used for model calibration and validation (Francou et al., 2008; Doublet et al., 2011). R1 to R6 are mixtures based on green waste (Francou et al., 2008); P1 to P6 mixtures are based on sewage sludge (Doublet et al., 2011). Mixtures marked with a "C" constituted the calibration dataset, and those marked with a "V" were randomly selected to constitute the validation dataset.

Figure 2.3: The evolution of the temperature during the composting process for P1 (Doublet, 2008) and R1 (Francou, 2003).

Figure 2.4: Experimental evolutions of the HEM, CEL and LIC fractions during the eight composting experiments of the calibration dataset. Symbols represent experimental values; dotted lines represent experimental medians. Solid lines represent the simulated evolutions obtained with first order kinetics, including the hydrolysis constants K_3, K_4 and K_5 for the HEM, CEL and LIC, respectively. The symbols ● represents the mixtures based on green waste (Francou, 2003; Francou et al., 2008); the symbols ▲ represents the mixtures based on sewage sludge (Doublet et al., 2011).

Figure 2.5: Example of the experimental (points) and simulated (lines) evolutions of the SOL and H2O fractions, and the CO_2 and microbial biomass during composting obtained with the calibration procedure of the model (seven parameters being fixed and six optimised for each composting experiment). In

this case, the P1 mixture displayed a median quality of fitting to the calibration dataset. Regarding SOL, the heavy black curve represents the total SOL fraction composed of SOL-S and SOL-F.

Figure 2.6: Example of the experimental (points) and simulated (lines) evolutions of the biochemical fractions and CO_2 during composting and obtained using the calibrated model (all parameters being fixed and described in Table 2.3; for the six parameters previously optimised, the mean of the optimised values was taken). In this case, the R4 mixture displayed a median quality of fitting to the validation dataset.

Figure 2.7: Comparison of observed and simulated, initial and final, biochemical composition of the composting experiments in the validation dataset. "exp_ini" expresses initial observed data of Van Soest fractions (% of TOM); "exp_final" expresses final observed data of Van Soest fractions; "simul_final" expresses final simulated data of Van Soest fractions.

Figure 2.8: Analysis of model sensitivity to the CO_2 fraction for 10 model parameters (Y, u_{max}, K_S, m_B, K_3, Y_{H2O}, K_2, K_1, K_5, K_4).

Figure 3.1: Schematic representation of the COP-Compost model. The total OC is divided into six pools based on biochemical fractionation. Parameters and variables are described in Table 3.1.

Figure 3.2: Experimental (symbols) and simulated (lines) data on biochemical fractions, carbon dioxide, water, microbial biomass (simulated only), and temperature (experimental only) during composting. The simulations were obtained using the OC module. The symbols represent the mean ± standard errors of experimental values of the six composting replicates.

Figure 3.3: Relationships between experimental and simulated values of biochemical fractions, carbon dioxide and water. Full dots: data used for OC module calibration (Mixtures P1, P2, P3, P5, R1, R3, R5, R6), empty dots and grey triangles: data used for validation (P4, P6, R2, R4 and L, respectively). The dotted line is the 1:1 line.

Figure 3.4: Experimental (symbols) and simulated (lines) data on soluble, sorbed, non-extractable, and mineralized LAS during composting. The simulations were obtained successively with Runs A, B, C, D for compost LAS-3 which presented a median quality of fitting. Symbols represent experimental values ± standard

errors.

Figure 3.5: Relationships between experimental and simulated values for soluble, sorbed, non-extractable and mineralized OPs for the four OPs, with Run B. The dotted line is the 1: 1 line.

Figure 3.6: Experimental and simulated distribution kinetics during the composting of ^{14}C between mineralized, soluble, sorbed and NER fractions, from ^{14}C-labeled glyphosate, LAS, fluoranthene and NP applied at the beginning of composting experiments. Simulations were obtained using the proposed calibration of the model coupling OC and OPs. GLY-2, LAS-2, FLT-2, and NP-1 represent the median quality of simulations. Area plots represent simulations and hatched histograms represent experimental values.

Figure 4.1: The presentation of COP_Compost model

Figure 4.2: The structure of MATLAB interface

Figure 4.3: Example of simulation (curves) of the experimental data (points) set corresponding to the composting mixture R4 used for the evaluation of the model. The simulations were done using the average estimated parameters of Table 4.2.

Figure 4.4: Comparison between simulated results and observed data (obtained from Hartlieb et al., 2003) for the 4 fractions (soluble, sorbed, NER and mineralised fraction) of pyrene (Fig.4-A) and simazine (Fig.4-B).

Figure 4.5: Comparison of observed data of simazine (obtained from Hartlieb et al., 2003) and simulated results using the model with adding a specific microbial population.

Figure 4.6: Sensitivity coefficient of the different model parameters for the 4 fractions of pyrene (Fig.4.6-A) and simazine, with adding the specific microbial population (Fig.4.6-B).

Figure 4.7: The sensitivity of pyrene to the initial quality of organic matters. Initial quantity of fraction of pyrene was: W_0 (Soluble) = 4.8; S_0 (Sorbed) = 91; NER_0 (non extractable) = 4.6 (gC / 100g TOCi). GW+SS = mixture of P3 (Doublet, 2008); GW+BIO+P = R4 (Francou, 2003); Manure =Fumier_Bovin. GW: Green wastes; SS: Sewage sludge; BIO: biowastes; P: Papers. Figures in line A represent the organic compositions characterized by the method of Van Soest. Figures in line B are the evolution of microbial biomasses in each organic waste. Line C shows the evolution of 4 OP fractions coupled with different organic wastes.

Figure 4.8: The sensitivity of simazine to the initial quality of organic matters. Initial quantity of fraction of pyrene was: W_0 (Soluble) = 51.6; S_0 (Sorbed) = 43.3; NER_0 (non extractable) = 5.1 (gC / 100g TOCi). Figures in line A are the evolution of microbial biomasses in each organic waste. Line B shows the evolution of 4 OP fractions coupled with different organic wastes.

Figure 4.9: The sensitivity of each fraction (soluble, sorbed, non-extractable and mineralized fraction) of simazine (Line A) and pyrene (Line C) to the initial quantity of microbial biomass; Line B corresponds the evolution of microbial biomass.

Figure 5.1: Design of bioreactor (volume of 1L).

Figure 5.2: Evolution of dry mass during composting for the different treatments (S, W, SW and SWB).

Figure 5.3: Loss of carbon mass (Fig.5.3-A) and percentage of total initial organic carbon mineralisation calculated according to the loss of carbon mass (Fig.5.3-B).

Figure 5.4: Changes of the biochemical fractions during composting in the W treatment (100% wastes) using the Van Soest method.

Figure 5.5: Evolution of total PAHs during composting (mean ± standard deviation) in the different treatments (S, W, SW and SWB); first order adjusted kinetics of dissipation in the SW and SWB treatments.

Figure 5.6: Evolution of small (2- and 3-rings), medium (4-rings) and large (5- and 6-rings) PAHs concentrations in soil during composting.

Figure 5.7: (5.7-A) Organic carbon-normalisaed sorption coefficient of FLT and PHE in initial soil, waste and soil-waste mixtures; (5.7-B) Evolution of Organic carbon-normalisaed sorption coefficient during composting in the soil-waste mixture (SW treatment). Different letters (a, b and c) within rows are significantly different ($p < 0.05$) according to one way-ANOVA analysis.

Figure 5.8: Principal component analysis of PLFA data. PC1 & PC2 represents different dates of composting course. Principal component 1 (PC1) explained 68.1% of the variation, while PC2 explained 14.5%. ■: Experimental data of Treatment S; ●: Data of Treatment W; ♦: Data of Treatment SW; ▲: Data of Treatment SWB. Different colours represented data with different date. Black = Day 0; Deep gray = Day 14; Gray = Day 35; Black circle = Day 42 and Gray

circle = Day 60.

Figure 5.9: G+/G- (Fig.5.9-A) and Fungal/Bacterial PLFA ratio (Fig.5.9-B) in different treatments during composting process.

Figure 6.1: Schematical presentation for COP_Compost model

Figure 6.2: Evolution of Van Soest fractions after 60 days of composting

Figure 6.3: Evolution of 16 USEPA-PAHs concentration during composting

Figure 6.4: Evolution of Kd value for FLT and PHE

Figure 6.5: Comparison between simulated and observed dataset for the end of composting (Curve: Simulated data; Points: Observed data)

Figure 6.6: Relationships between experimental and simulated values for soluble, sorbed, non-extractable (NER) and mineralized fraction (^{14}C-CO_2) of FLT, with Test A and B. The first line corresponds test A and second line represent test B.

Figure 6.7: Relationships between experimental and simulated values for soluble, sorbed, non-extractable (NER) and mineralized fraction (^{14}C-CO_2) of PHE, with Test A and B. The first line corresponds test A and second line represent test B.

Figure 6.8: Relationships between experimental and simulated values for soluble, sorbed, non-extractable (NER) and mineralized fraction (^{14}C-CO_2) of FLT, with the coupling model. The first line corresponds Test A and second line represents Test B.

Figure 6.9: Relationships between experimental and simulated values for soluble, sorbed, non-extractable (NER) and mineralized fraction (^{14}C-CO_2) of PHE, with the coupling model. The first line corresponds Test A and second line represents Test B.

LIST OF TABLES

Table 1.1: The different functions of temperature

Table 1.2: Organic matter modelling in the field of soil and composting

Table 1.3: Comparisons between the OM model in soil and during composting

Table 1.4: Three orders of the microbial growth μ

Table 1.5: Summary of OP models

Table 1.6: The equations for model of Saffih-Hdadi (2003)

Table 2.1: Used Petersen's matrix (1965) for composting model

Table 2.2: Modelling Efficiency during the calibration stage using the eight data set of composting P1, P2, P3, P5, R1, R3, R5 and R6

Table 2.3: Parameter values taken from the literature, estimated with the calibration procedure and used in the calibrated model. The parameter values used in the calibrated model are highlighted.

Table 2.4: Statistics to evaluate the calibrated model. The eight composting experiments (P1, P2, P3, P5, R1, R3, R5 and R6) of the calibration dataset were used.

Table 3.1: Variables and parameters in the COP-Compost model

Table 3.2: Statistical evaluation of the goodness-of-fit of the OC module

Table 3.3: Parameter values and evaluation statistics of OP simulations of Runs A, B, C, and D for the four OPs (units are given in Table 3.1).

Table 3.4: Statistical evaluation of model efficiency in the simulations obtained using the model coupling OC and OP modules, and with Run B.

Table 4.1: Equations for OP module

Table 4.2: Variables and parameters in the COP-Compost model

Table 4.3: Parameter values and evaluation statistics of OP simulations (units given in Table 4.2)

Table 5.1: Small, medium and large PAHs removal percentage for Treatment SW and SWB

Table 6.1: Statistical evaluation of the goodness-of-fit of the OC module

Table 6.2: The parameters applied in the OP module for simulating the observed data

Table 6.3: Statistical evaluation of the goodness-of-fit of the OP module

Table 6.4: Parameter values and evaluation statistics of OP simulations

LIST OF ABBREVIATIONS

DM = Dry mass

FLT = Fluoranthene

GLY = Glyphosate

LAS = Sodium linear alkylbenzene sulfonate

NP = Nonyphenols

OM = Organic Matter

OP = Organic pollutant

PAH = Polycyclic aromatic hydrocarbon

PHE = Phenanthrene

TOC = Total organic matter

Variables of COP_Compost model / biochemical fractions

H2O = organic C soluble in hot water

SOL = soluble fraction in neutral detergent

SOL-S = Proportion of organic C in the soluble fraction in neutral detergent with slow degradation (pool Ci=1)

SOL-F = Proportion of organic C in the soluble fraction in neutral detergent with fast degradation (pool Ci=2)

HEM = Hemicellulose (pool Ci=3)

CEL = Cellulose (pool Ci=4)

LIC = Lignin (pool Ci=5)

X = Microbial biomass

W = Soluble OP in water

S = Sorbed OP extracted with solvent

NER = Non-extractable residues OP (bound residues)

Parameters of COP_Compost model

K_1 = Hydrolysis constant of pool Ci=1 (SOL-S)

K_2 = Hydrolysis constant of pool Ci=2 (SOL-F)

K_3 = Hydrolysis constant of pool Ci=3 (HEM)

K_4 = = Hydrolysis constant of pool Ci=4 (CEL)

K_5 = Hydrolysis constant of pool Ci=5 (LIC)

Y = Assimilation yield of the available OC for microbial biomass

μ_{max} = Maximal specific growth rate for microbial biomass

Ks = Saturation constant for Monod kinetic

T_{min} = Minimum temperature for microbial growth

T_{max} = Maximum temperature for microbial growth

T_{opt} = Optimum temperature for microbial growth

m_B = Death constant for microbial biomass

Y_{mcs} = Availability yield for dead microbial biomass

Kd = Sorption coefficient of organic C

Kd_1 = Sorption coefficient of Ci=1 (SOL-S)

Kd_2 = Sorption coefficient of Ci=2 (SOL-F)

Kd_3 = Sorption coefficient of Ci=3 (HEM)

Kd_4 = Sorption coefficient of Ci=4 (CEL)

Kd_5 = Sorption coefficient of Ci=5 (LIC)

Fr = Non-extractable residue formation rate

dr = OP degradation rate

NER_0 = Non-extractable residues in the initial mixture

ABSTRACT

With the increasing of people's living standards, more and more urban wastes are produced everyday with a huge quantity. The big amount of wastes have not only occupied precious land resource, influenced the industry seriously and agricultural production, but also introduced various pollutants, which will harm human's life and health. Compost processing can help urban wastes to be recycled by transforming the organic matter into fertilizer and be returned to nature. Also it can be used as a bioremediation method for the polluted soil. The mathematical model is an efficient tool for understanding and modifying the composting process, predicting the stability of compost products, and then assuring the harmfulness of pollutants for agriculture.

Our objective in this study was to construct a model describing the dynamics of organic micro-pollutants during the composting and parameterize the model under the interface of MATLAB. This model should be used according to users' needs with 3 modules: organic carbon module, organic pollutants module and coupling module. In order to calibrate and validate our model, the datasets from 12 different waste mixtures and 2 different types of pollutants with different initial conditions were applied. On the other hand, for applying the composting technique in the field of bioremediation of contaminated soil, an in-vessel composting experiment was designed in which the organic urban wastes mixed with soil contaminated by PAHs were used as materials. We studied the dynamics of organic matter, organic micro-pollutants and the microbial populations. The conclusion showed that the concentration of PAHs could be decrease by 50-60% with the effects of organic matters and the accelerated microbial activities compared to bare soil. Furthermore, the successive microbial populations have been observed during the composting process. These experimental results could be well simulated by our model which indicates its capacity in the soil-composting system.

However, we still came across some questions during my research. The simulations for soluble organic substrates were not accurate enough, due to the limits of the biochemical characterization of organic fractions. In our model, only the function of temperature has been considered as the environmental factor, more limiting factors such as moisture, oxygen, … need to be investigated in the further studies. The microbial diversity of each decomposition phase has been investigated in the experiment but was not added in the model because its impact on PAHs degradation is not clear enough. In order to answer all these questions, further researches needs to be done, although the study in the field of microbial flora has begun to be carried out.

RESUME

Avec l'augmentation de niveau de vie des populations, de plus en plus déchets urbains sont produits chaque jour en grande quantité. Ces déchets non seulement occupent une place importante mais dégradent l'environnement en particulier parce qu'ils contiennent divers polluants, qui peuvent porter atteinte à la santé humaine. Le compostage permet aux déchets urbains d'être recyclés en transformant la matière organique en engrais pour les sols agricoles. Par ailleurs, ce procédé peut aussi être utilisé comme méthode de biorestauration pour les sols pollués. Les modèles mathématiques sont des outils qui permettent de comprendre et éventuellement de modifier le processus de compostage. Ils pourraient également prédire la stabilité des produits issus du compostage et quantifier la nocivité des polluants qu'ils contiennent.

L'objectif dans cette étude était de construire un modèle décrivant la dynamique des micropolluants organiques au cours du compostage et paramétrer le modèle sous l'interface de MATLAB. Ce modèle peut être utilisé selon les besoins des usagers avec 3 modules: le module de carbone organique, le module de polluants organiques et le module de couplage. Afin de calibrer et valider notre modèle, un ensemble de données de 12 différents mélanges de déchets et 4 différents types de polluants ont été utilisés. Pour l'application de la technique de compostage dans le domaine de la bioremédiation des sols contaminés, une expérience de compostage en laboratoire a été conçue dans lequel les déchets urbains organiques ont été mélangés avec un sol contaminé par des HAP. Nous avons étudié la dynamique des matières organiques, des micropolluants organiques et des populations microbiennes. Les résultats ont montré que la quantité des HAP dégradée a été de 50-60% lorsque le sol est composté avec des déchets organiques. En outre, des populations microbiennes successives ont été observées pendant le processus de compostage. Ces résultats expérimentaux ont été simulés par notre modèle afin de tester sa capacité dans un système sol-compostage.

Cependant, quelques questions de recherches se posent encore: en ce qui concerne la modélisation, la simulation des substrats organiques solubles n'est pas assez bonne, ce qui est probablement dû à des limites sur l'étude des caractéristiques biochimiques des fractions organiques soluble; par ailleurs, seule la fonction température a été considérée comme facteur de l'environnement dans notre modèle, des limitations dues à l'l'humidité ou à l'oxygène, par exemple, doivent être étudiées dans des études ultérieures. L'activité microbienne pendant chaque phase de dégradation des HAPs n'a pas encore été assez clairement établie pour être incorporée dans notre modèle.

GENERAL INTRODUCTION

Municipal solid waste (MSW) refers to waste generated from householders. Due to vast population growth and urbanization, the volume of MSW produced in China has dramatically increased. For instance, about 1.1 x 10^8 and 1.6 x 10^8 ton of the MSW produced in China had been reported in 1995 and 2004, respectively (Ministry of Construction of China, 2005), corresponding to an increase of 45% in just a span of 10 years. By the end of 2004, a total of 661 cities had 559 MSW disposal systems in China (Ministry of Construction of China, 2005). MSW treatment is mainly carried out using three processes corresponding to three different treatment technologies: landfill (86.5%), composting (6.4%) and incineration (7.1%) (Ministry of Construction of China, 2005). However, in 2005, only 35% of landfill sites are considered safe (Fang, 2007). The rest of landfill sites are simply filled in order to dispose waste. In response, the China government has recently turned its attention to the construction of MSW treatment plants in order to address the growing problem on MSW.

In France, everyday, more and more wastes are produced along with the evolution of life style and daily consummation. On 40 years, the quantity of wastes has been doubled with an average of 360 kg per year and per person.

In the million tons of waste collected each year (Source ADEME - ITOMA 2004):

- 47% were stored in discharge

- 28% incinerated with a recovery d' energy (1% without recovery of energy)

- 10% sent to a biological treatment (methanisation or composting)

- 14% sorted to be recycled

On the other hand, in Europe and France, the composting of organic urban origin waste of constitutes a field of valorization largely. The household refuse recycled by composting each year in European Union countries is estimated at 32 x 10^6 tons (T) (European Commission, 2005) and the whole organic urban origin waste treated by composting accounts for 5 x 10^6 T in France (ADEME, 2006). The European policy of management of waste (Directive 1999/31/CE) as well as the commitments concerning the French level within the framework of Grenelle of the Environment

(2007) underlines the needs for reducing the tonnage of produced waste and the part of waste which can be recycled hidden or incinerated. The valorization of waste by composting is thus thought to play an important role in the French and European strategies of waste management.

Composting is indeed a widely used biological process accepted as a bio-treatment It is a "controlled" procedure of organic components degradation (from vegetables and animals origin), due to the activity of successive microbial communities evolving in aerobic conditions (i.e. in the presence of oxygen), and leading to the development of humified and stabilized organic matter (Francou, 2008). The product is called compost and can be used as amendment in agriculture.

The composting of organic fraction of urban wastes make possible to recycle it into cultivated soils to improve soil structure and fertility. The composting process has received much attention in recent years because of pollution concerns. Since composting has been demonstrated to have an important role in processing much of the biodegradable waste and therefore is effective in biodegrading micro-pollutants like PAHs using both conventional either windrow composting systems (Amir et al., 2005; McFarland and Qiu, 1995; Atagana, 2004) or in-vessel composting system (Antizar-Ladislao et al., 2006; Sasek et al., 2003).

Soil pollution by petroleum products (organic micro-pollutants) is a widespread problem. The past decade, bioremediation techniques have been developed and improved to clean up soils polluted with hazardous chemicals (Skladany and Metting, 1992; Alexander, 1994; Romantschuk et al., 2000). Contaminated soil can be bioremediated by addition of nutrients (biostimulation), addition of microbial inocula (bioaugmentation), aeration and turning, or by a combination of these practices (Alexander, 1994). Also, the addition of organic matter to the hydrocarbon contaminated soil can be beneficial, as it is a source of co-substrates, nutrients and microorganisms, and ameliorates the structure and water-retaining capacity of the soil (Alexander, 1994). Therefore, an increasing number of studies have considered the composting technique as a bioremediation method for contaminated soil.

Due to the great diversity of the organic wastes recycled by composting and organic pollutants (OPs) detected in the composts, modeling is a privileged method to

highlight the generic processes interacting in the fate of OPs. However, no model describing the fate of OPs in the course of composting was proposed in the literature.

Moreover, it's necessary to describe the availability of OPs during composting and in the final composts by taking into account of the mechanisms of interaction between OPs and the organic matter. While great majority of the composting models were developed to simulate the production of heat and the mass loss during the composting process (Mason, 2006). Few models were proposed to describe their transformations of the organic matter and the evolution of its degradability (Kaiser, 1996; Sole-Mauri et al., 2007). These models however have the advantages: on one hand, they propose the description of the biochemical properties of the organic matter in the course of composting, whose evolution is likely to condition the sorption of OPs, and on the other hand, they can simulate the dynamics of the microbial biomass, which likely influence the fate of OPs. No model simulating the dynamics of OPs during composting was found in the literature. However, many models with compartments were developed to simulate the processes of evolution of the pesticides by explicitly taking into account the mechanisms of stabilization and the formation of bound residues. These models are necessary to evaluate the risks in long-term associated with the use of composts in agriculture (Saffih-Hdadi et al., 2003).

Therefore, the objective of my PHD was to build a new dynamic model for composting process to simulate the interactions between organic matters evolution and organic micro-pollutants behaviour taking into account the microbial activities, to evaluate the model with existing data (from French lab) of organic wastes composting and the in-vessel composting experiment results that I have got. The finally objective was to apply our constructed model to the bioremediation of polluted soils in China.

Initiated in September 2008, this French-Chinese cotutelle thesis was financed by Egide (the Foreign Affairs of French Ministry) and by the Department Environment and Agronomy of the INRA (National institute of the Agronomic research) for the part in France. The part in China was financed by the Institut of Urban Environment (Chinese Academy of Sciences) for the Chinese part. The experimental part of the thesis was financed by the CRPE (Research centre on the Cleanliness and the Energy of the Veolia Environnement group). My thesis was directed by Patricia GARNIER and Yong-Guan ZHU, co-advisor was Sabine HOUOT.

This memory comprises a literature review (Chapter I) with a first part describing the process of composting and the transformations of the organic matter which take place during this mode of biological treatment. It also gives an overall picture of the accessible informations in the literature on the contents of OPs of the independent groups detected in the composts and to become to them during composting. The state of the art concerning the modeling of becoming of OPs during composting is also presented. This synthesis leads to the presentation of the specific objectives of this thesis and the presentation of the steps adopted for this work. The manuscript is then composed of 5 chapters (chapters II to VI) presenting the manuscripts of the scientific publications resulting from this work of thesis. A general conclusion and the prospects are given at the end for the report.

CHAPTER 1 LITERATURE REVIEW

1.1 Presentation of composting

Composting is defined basically as biological processes occurring in favourable conditions (good aeration, moisture, etc.) and allowed to transform the raw initial material probably unsanitary or with phytotoxic properties to stable and mature end product(Liang et al., 2003). Thus considerable effort has been directed toward determining the impact of various environmental variables on composting (Schulze, 1961; Suler and Finstein, 1977; Rao et al., 1996). These variables include temperature, moisture content, aeration, nutrient balance, bulking agents, and substrate.

1.1.1 Temperature

The aerobic degradation of organic substrates leads to the increase of temperature that can reach 70-80ºC maximum. On the function of temperature, the composting process follows mesophilic, thermophilic, cooling and maturation phases with a succession of microbial populations (see Fig.1.1).

The distribution of active microorganisms is dictated by the temperature of compost. The rise of temperature permits partial cleansing by the destruction of pathogenic germs, animal parasites, the seeds and bodies of propagation of the plants. If the temperature is too high, it can involve an excessive drying of compost and cause a deceleration of activity of the micro-organisms.

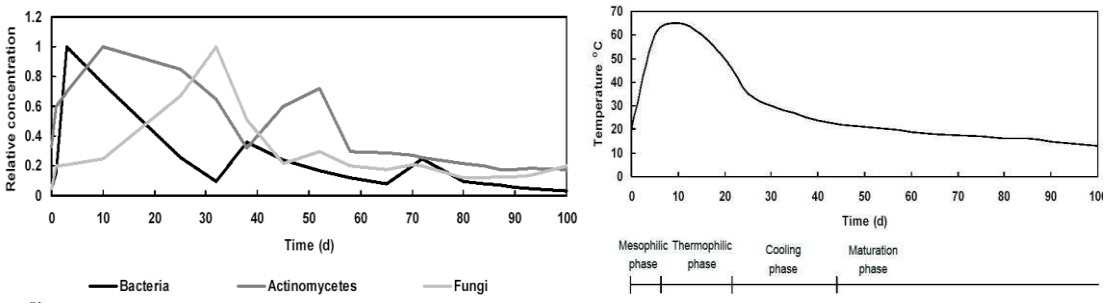


Figure 1.1_A): Microbial succession during the composting process (Epstein, 1997)
1.1_B): Idealized temperature variation in the compost during the composting process

1.1.2 Areation (ventilation)

The matrix of compost is a network constituted of solid particles and interstices of sizes variable which can be filled with water, air or both. The aeration permits to

import oxygen essential to the metabolism of the micro-organisms, however, while the interstices are filled with water, the diffusion of oxygen is not possible. The balance between moisture and ventilation is necessary for the progress of composting. Hamelers (1992) analysed the influence of oxygen content and oxygen intake on the degradation of four different organic matters. Haug (1993) also introduced the model which simulated organic matter degradation with a variable of gas discharge rate.

$$k_{O_2} = \left(\frac{\text{Vol \% } O_2}{K_0 + \text{Vol \% } O_2} \right) \cdot k_{particle} \quad \text{(Xi et al., 2005)} \qquad [1]$$

Where $Vol\%O_2$ represents the percentage of oxygen volume, $k_{particle}$ is a constant (its value varies from 0 to 1), the value of $k_{particle}$ will ajust according to the compost particlesize.

1.1.3 Free Air Space (FAS)

Free Air Space (FAS，%) place an important role during the composting process, because of its transportation with oxygen. The correct function about FAS is as below：

$$k_{FAS} = \frac{1}{1 + e^{[-23.675 \times FAS + 3.4945]}} \quad \text{(Haug, 1993)} \qquad [2]$$

Water can take the pore space among the composting materials, and then influence the structure so as to reduce the porosity. Therefore, the change of moisture will transform the porosity, air exchange rate and the capacity of oxygen supply (Miller et al., 1986) to a great extent. The compost humidity has a close relationship with the porosity and FAS, Golueke et al. (1953) have established the relationship between humidity and porosity. Generally, the higher the humidity is, the bigger FAS the composts need. But when the humidity is larger than 60%, FAS will limit compost processing. Moreover, according to the oxygen consumption rate in the composting process, when FAS is 30%~36%, the organic matter degradation ability of microorganisms is the strongest and when FAS is smaller than 28%, compost ventilation performance drop (Jeris, 1973):. Therefore, to reduce the restriction of composting process, FAS in piles must be bigger than 28%.

1.1.4 Moisture content

The moisture in the matrix of compost is necessary for microbial activities. The optimal moisture for composting is generally located between 50% - 80% of the total gross mass (Richard et al., 2002). During composting, there is production of water at the time of degradation of OM and drainage under the combined action of ventilation and rise of temperature. To compensate for an excessive water loss which limits the microbial activities, a watering of composts is usually realised.

The moisture and oxygen contents are two important environmental factors, that needs to be controlled during management of the composting process. Controlling the moisture content in compost on one hand is to strengthen the microbial activity, on the other hand is to the permit sufficient oxygen supply. The moisture content is very important for the degradation process, and the water pressure is one of the most common limiting factors for the microbial activities in the solid dielectric (Smith, 1978; Griffin, 1981). Low moisture content will limit the microbial activity, so as to stop the physical proliferation. While too high moisture content will cause the anaerobic composting occurs. The oversized humidity will increase the molecular film thickness and cause the interspaces to be much smaller among molecules, thus influence oxygen transportation (Hamelers, 1992; Tseng et al., 1995) An excess humidity will affect the oxygen distribution and the proliferation in the compost piles, the hydrodynamic force function as well as the change of microbial growth rate and then influence biodegradation rate. The insufficient oxygen will reduce degradation of organic matter (Richard and Walker, 1999) and will increase the anaerobic gas emissions (Haug, 1993; Epstein, 1997).

In the field of composting, the humidity revision function is paid attention by many researchers, for example, Haug discovered that the following equation which adapts in the biological solid composting process:

$$k_{H_2O} = \frac{1}{e^{[-17.64 \times (1 - \text{moisturefr} \quad \text{action}) + 7.062]} + 1} \quad \text{(Haug, 1993)} \qquad [3]$$

Moreover, Stombaugh and Nokes (1996) also proposed a set of equations to describe the moisture evolution during the composting process:

$$k_{H_2O} = 0.0 \qquad m_1 < m < m_2$$
$$k_{H_2O} = \frac{m}{m_2} - 1.0 \qquad m_2 < m \leq m_3 \qquad m_1 = 0 \quad kg / kg\ (wet - wt.)$$
$$k_{H_2O} = 1.0 \qquad m_3 < m \qquad m_2 = 0.2 \quad kg / kg\ (wet - wt.)$$
$$m_3 = 0.4 \quad kg / kg\ (wet - wt.) \qquad [4]$$

1.1.5 C/N ratio

The composting substrate is the source of nutrients for the micro-organisms. According to its composition in nutrients, microbial activities adjust on the limiting factors. The balance is particularly important for the major elements: C, N, P, K, S. It seems that C/N between 25 and 40 satisfies composting. The C/N decreases during composting to reach at the final value between 8 and 25. If C/N is too low, the microbiological degradation leads to the formation of excessive ammonia, which will increase the pH and the volatilisation of ammonia. On the contrary, if it is too high, the procedure is limited in nitrogen, which can lead to the formation of acid and make the pH drop, thus stop the microbial activities.

1.1.6 pH value

Generally the pH of green wastes is between 5 and 9 (Morel et al., 1986). According to the literatures, the acidity of wastes appears to have no limit for the procedure of composting.

All in all, initial wastes have acidity slightly stronger than the finished composts. But many work highlighted a phase of acidification at the beginning of composting. This phase of acidification is mainly due to the anaerobic production of organic acids and the immobilization of ammonium in the microbial biomass during the mesophilic phase. Then, during the thermophilic phase, the organic acids are degraded involving an alkalisation of the compost, phenomenon accentuated by the mineralisation of nitrogen.

1.1.7 The fate of microorganisms during the composting process

Actinomycetes are a group of filamentous organisms that are often found in blue-grey

powder-like colonies. Both actinomycetes and fungi are relatively slow growing organisms that are less tolerant of low oxygen concentrations and high temperatures compared to the bacteria. The microbial populations and the temperature in the compost often follow a specific pattern dictated by the degradation of compounds in the organic matter. The composting process can be divided into four phases.

1.2 Evolution of organic matter (OM) during composting

The theoretical evolution of the temperature within the compost during composting makes it possible to define four successive phases, related to the activity of the various microbial populations.

1.2.1 The mesophilic phase

Easily biodegradable OM involves a strong microbial activity generating a strong production of heat and a fast rise of the temperature in the middle of the compost. The present micro-organisms are primarily bacteria, no-actinomycetes, as well as fungi (Vergé-Leviel, 2001).

1.2.2 The thermophilic phase

Very quickly the temperature reaches values 60°C even 75°C. Only the heat-resisting micro-organisms can survive these high temperatures. This phase is characterized by the presence of actinomycetes and thermophilous nonfilamentous bacteria. The mushrooms disappear beyond 60°C or survive in the form of spores. During this phase, a big part of OM is lost under the form of carbon dioxide CO_2 and a draining of the compost related to the evaporation of water occurs. The phase of fermentation corresponds primarily to the degradation of the easily biodegradable molecules: glucides, proteins, lipids (Vergé-Leviel, 2001).

1.2.3 The cooling phase

The reduction in the quantity of easily degradable OM causes a deceleration of the microbial activity involving a cooling of compost. The mesophilic micro-organisms colonize the composting system again.

1.2.4 The maturation phase

During this last phase, the processes of humification dominate, as well as the slow degradation of the resistant compounds. This phase is characterized by the colonization of the compost by mushrooms when lignin and the cellulose become the dominant substrates. Among colonizing fungi, the filamentous fungi of the white, brown and soft rots are known for their role in the degradation of lignin and another xenobiotic related molecules (PAHs, chlorophenols…) (Vergé-Leviel, 2001). During this phase, the diversity of the metabolic micro-organisms augments. This phase lasts until the use of the composts.

1.3 Bioremediation of contaminated soil by composting

1.3.1 Contaminated soil by PAHs

Soil pollution by petroleum products which contain high concentration of PAHs is a widespread problem. Polycyclic aromatic hydrocarbons (PAHs) are hydrocarbons that contain at least two fused benzene rings in linear, angular, or cluster arrangements. PAHs in the molecular weight range between naphthalene (128.16) and coronene (300.36) are of environmental concern (Ashok and Saxena, 1995). Many PAHs are stable and persistent in the environment and toxic. PAHs are common by products formed either by thermal alteration of buried organic matter (petrogenic) or by incomplete combustion of organic matter (pyrogenic) (Suess, 1976; Sims and Overcash, 1983; Nikolaou et al., 1984).

PAHs also exhibit extraordinary structural diversity. The number of possible PAH isomer is large and it expands rapidly as the number of rings and alkylations increase. However, not all the possible PAHs exist because of the low conformational stability of larger ring numbers, especially for linearly fused PAHs (Harvey, 1997).

Polycyclic aromatic hydrocarbons (PAHs) are ubiquitous contaminants found in most of the processes of incomplete combustion of wood and fossil fuels (Jones and Voogt, 1999). Major sources of petrogenic PAHs also include crude oil and its refined products, coal, and oil shale (Harvey, 1997; Page et al., 1999).

During pyrolysis and pyrosynthesis, cracking of complex organic molecules into

smaller and unstable fragments (pyrolysis) results in the formation of free radicals with short average lifetimes. The highly reactive free radicals produce more stable and highly condensed aromatic ring systems through recombination reactions (pyrosynthesis) (Ballentine et al., 1996; Mastral and Callen, 2000).

1.3.2. Potential bioremediation of PAH-contaminated soils by composting

The Earlier studies showed that higher molecular weight PAHs remained in the soil after 16 weeks and 11 months of pilot-scale and full-scale land farming, respectively (Atagana, 2003; Atagana, 2004a). The past decade, bioremediation techniques have been developed and improved to clean up soils polluted with hazardous chemicals (Skladany and Metting, 1992; Alexander, 1994; Romantschuk et al., 2000). A promising approach to reduce PAH pollution is the utilization of the natural potential of microorganisms to utilize hydrocarbons since the bioremediation techniques are cheaper than the other alternatives (soil washing, solidification and stabilization, incineration, thermal treatment or advanced oxidation processes) used for cleaning up of contaminated sites (Clarinet, 2007).

Contaminated soil can be bioremediated by addition of nutrients (bio-stimulation), addition of microbial inocula (bioaugmentation), aeration and turning, or by a combination of these practices (Alexander, 1994). Also, the addition of organic matter to the hydrocarbon contaminated soil can be beneficial, as it is a source of co-substrates, nutrients and microorganisms, and ameliorates the structure and water-retention capacity of the soil (Alexander, 1994). When fresh organic substrates are incubated with a contaminated soil, a thermophilic phase is likely to occur and the process is called composting. Earlier composting experiments using hydrocarbon-contaminated soil co-composted with cow manure and mixed vegetable waste showed that more than 90% of the hydrocarbons including some of the recalcitrant components were removed (Atagana et al., 2003). Co-composting hydrocarbon-contaminated soil with poultry manure showed that PAHs could be removed from the soil by composting (Atagana, 2004b).

The composting process used to stabilise organic materials can be considered as a bioremediation process (Bollag & Bollag 1995). Numerous studies have shown that composting has an enormous potential for bioremediation through sustaining

microbial populations of a wide range of microorganisms, which are able to degrade a variety of organic contaminants at the laboratory and/or field scales (Antizar-Ladislao et al., 2005; Moretto et al., 2005; Semples et al., 2001; Lau et al., 2003). Composting has been proven to degrade PAHs, in rates that exceed 80% in some cases and require treatment time shorter than land-farming (Amir et al., 2005).

Composting strategies for soils contaminated with organic pollutants in general has been recently reviewed by Semple et al. (2001). The number of studies on composting of petroleum- contaminated soil and petroleum-based oil wastes is increasing (e.g. Beaudin et al., 1996, 1999; Al-Daher et al., 1998; Kirchmann and Ewnetu, 1998; Milne et al., 1998; Jørgensen et al., 2000; Chaw and Stoklas, 2001; Namkoong et al., 2002). Elevated temperatures stimulate hydrocarbon degradation (Atlas, 1975), and enhance the contaminant availability by increased solubility and mass transfer (Pignatello and Xing, 1996).

1.3.3 Evolution of PAHs during composting

Compost is a pool of considerable microbial diversity that can potentially serve as a source for the biological treatment of wastes by degradation, including PAHs, pesticides, and other contaminants. The PAHs are the contaminants whose evolutions during the composting were studied the most. The PAHs will be degraded partially during decomposition of OM. The term of degradation includes the PAHs mineralised, transformed in metabolites, volatilised or adsorbed on the OM of composts. The principal transformation could take place during the thermophile phase, but some studies showed that the degradation would be probably most important during the maturation phase of composting (Verge-Leviel, 2001).

Low-molecular-weight PAHs are readily degraded. However, high-molecular-weight PAHs (four and more rings) are more persistent, because of their low bioavaibility, due to their strong adsorption onto the soil organic matter (Manilal and Alexander, 1991; Weissenfiels et al., 1992). Oleszczuk (2007) indicated that the changes in the PAH content were less visible for three and four-ring but more visible for high weight molecular compounds of PAHs, this conclusion was similar to the study of Amir et al. (2005).

Therefore, many investigations have focused attention on the degradation of high-molecular-weight PAHs for cleaning up contaminated sites. The ability to predict the rate of PAHs degradation in soils of different properties is one of the most important challenges for soil remediation technologies (Harmsen, 2004). Soil is the main, ultimate sink for most organic contaminants.

1.4 Modelling the dynamics of OM and OP during the composting

Mathematical modelling can be employed as a useful tool in order to understand and to improve the composting process.

1.4.1 Summary of environmental conditions

Most modeler have focused on the composting system with large scales, and the mass and energy balance were considered as the foundation when they investigate the dynamics of substrates in composting system (Mason, 2006; Sole-Mauri et al., 2007; Lin et al., 2008; Vlyssides et al., 2009). Furthermore, most models were used to describe the environmental factors which were thought to be the elementary factors influencing the composting process. These factors are: temperature (Gray et al., 1971; Suler and Finstein, 1977; Finstein, 1980; Nakasaki K et al., 1985; Golueke, 1987; Richard and Walker, 1998), microbial biomass(Nakasaki et al., 1985; Nakasaki and Akiyama, 1988), moisture (Suler and Finstein, 1977; Schulze, 1961; Jeris and Regan, 1973; Bakshi, 1987), oxygen content (Suler and Finstein, 1977; Richard et al., 1999), porosity(Jeris and Regan, 1973), particular size (Gray et al., 1971) and C/N ratio (Morisaki et al., 1989). Among these factors, the microbial biomass, temperature, moisture and oxygen content were usually considered as the correction coefficients.

In recent years，a number of researchers have proposed a kinetic model to describe the composting efficiency on the function of these environmental factors (Finstein, 1980; Miller et al., 1986; Ndegwa et al., 2000; Xi et al., 2005). One of the common one belongs to Haug (1993) who showed a form as below containing 4 environmental factors: temperature (T, °C), oxygen content (O_2, volume %), moisture content (kg H2O / kg wet-wt.) and FAS (m^3 air/ m^3 bulk agent).

$$k(x_1, x_2, ..., x_n) = k_S \cdot f_1(x_1) \cdot f(x_2) \cdot ... f_n(x_n) \quad [5]$$

Where, k^S ($hour^{-1}$) represents the reaction rate under the standard conditions of

composting; n refers to the number of environmental factors; f_1, f_2…f_n are the functions corresponding to the environmental factors, under the special conditions, these factors will affect the reaction rate, while under the standard condition, the value of these function equal to 1.

The function of temperature in these models is a multiplicative function of the constant of potential biodegradation. This constant is increased when the temperature is higher and the microbial activity is enhanced, on the other hand, it is decreased when the temperature is too low. In the case of composting, when the temperature is too high (around 60°C) the function of temperature will decrease, because the microbial activities are limited. The functions of temperature are different for soil and compost. There are several propositions of functions (see Table 1.1).

Mason in 2006 has realized a summary about composting models and especially the functions of temperature. He found that the function of Rosso et al. (1993) described better the influence of temperature than the others.

Table 1.1: The different functions of temperature

Temperature correction	**Reference**
$f_{T(1)} = \frac{T(80-T)}{1600} \ldots 0 < 80°C$ $f_{T(2\ldots4)} = \frac{T(60-T)}{20(80-T)} \ldots 0 < 60°C$	Kaiser (1996) (For composting)
$f_T = \frac{T}{T_2 - T_1}$ $(T_1<T<T_2)$ $f_T = 1.0$ $(T_2<T<T_3)$ $f_T = 3.75 - \frac{T}{T_2 - 10}$ $(T_3<T)$	Stombaugh et Nokes (1996) $T_1 = 0℃$, $T_2 = 30℃$, $T_3 = 55℃$ (For composting)
$f_T = (a + b * e^{C*(T/T_{ref})})^d$ $(T_{ref}=15℃)$ a = -0.566 ; b = 0.620 ; c = 0.9125 ; d = 1.026	Recous et al. (1995) (For soil)
$f_T = \frac{(T-T_{max})(T-T_{min})^2}{(T_{opt}-T_{min})[(T_{opt}-T_{min})(T-T_{opt})-(T_{opt}-T_{max})(T_{opt}-T_{min}-2T)]}$	Rosso et al. (1993) (For composting)

1.4.2 Summary of OM models

The multi-component compositions of OM largely determines the degree of involvement of different microorganisms in the degradation process, regulates the spectrum of microbial enzymes excreted (the soil called induction effect), specifies the effect of enzymes on the decomposed molecules, thus influencing the total rate of organic matter degradation, which can be evaluated, for example, by the decrease in organic carbon concentration. The degradation rates of individual components can vary widely. The modelling of Composting process is based on the organic matter degradation and biotransformation.

There exist several models in the literature which describe the processes of decomposition of OM. The OM models in which we were interested can be divided in two groups: the simple models and the models with more details on the biochemical characteristics.

1) The simple models describing the decomposition of OM (see Fig.1.2): the organic compounds of OM are accessible to the microbial biomasses and a part of OM is mineralized into by the form of CO_2. Generally, in the field of soil, the limitation of the decomposition comes only from the capacity of OM which is degraded by microbial biomass.

2) The Models describing the decomposition of OM on considering the biochemical characteristics of organic substances (see Fig.1.3 and 1.4): the organic compounds of OM are hydrolyzed and assimilated by microbial biomass. The limitation of the decomposition comes not only from OM but also from the microbial biomass which can be limiting.

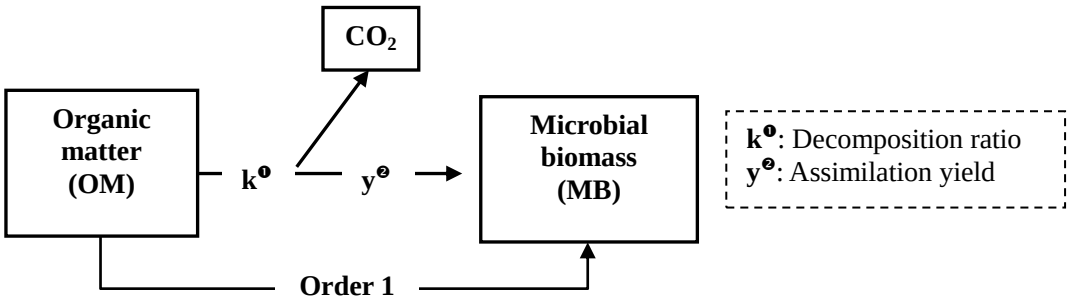


Figure 1.2: Model describing the flux of C and N in the course OM decompositionin the field of soil: Model STICS (Nicolardot et al., 2001)

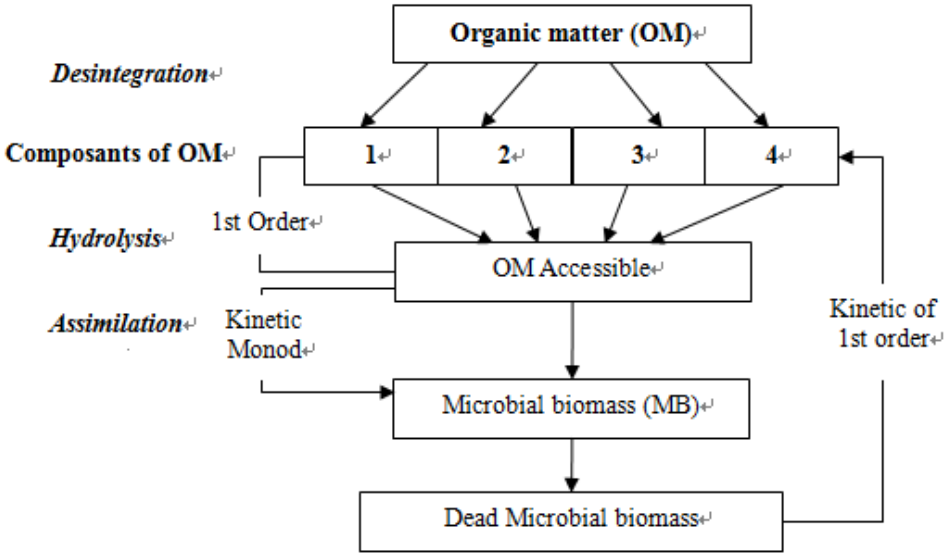


Figure 1.3: Schematic Representation of ADM1 model: conversion of a process of the anaerobic digestion (Batstone et al., 2002)

The model ADM1 is used to simulate the anaerobic digestion. This model distinguishes the disintegration and the hydrolysis which are extracellular mechanisms. All the dynamics follow a kinetic of 1st order. The phase of disintegration is a nonbiological stage which transforms the components of the substrate into proteins and lipids. The phase of hydrolysis is enzymatic. It converts proteins and lipids into monosaccharide, amino acids and fatty-acid with long chains at the same time. The kinetics of Monod was used to represent the microbial growth. The decays of microbial biomasses evolve following the 1st order kinetic (Delgadillo-Mirquez et al., 2007).

In the literature of OM model during the composting, we are also interested in the model of Kaiser (1996). It distinguishes the OM compartments into three big parts: easily-biodegradable fraction (MB), slowly-biodegradable fraction (MH) and inert or non-biodegradable fraction (MI) according to their decomposition rates under the various microbial activities. These various micro-organisms are activated according to the temperature (See Figure 1.4). Where, MB refers to the organic fraction which may be dissolved immediately and assimilated by the microorganism; MH is composed of the dissolved macro-molecules and this kind of material needs to be hydrolyzed before the microbial assimilation; MI refers to the organic fraction which has almost no biological reactions. In 2007, Sole-Mauri et al. proposed a method to identify the

organic matter in more details: Carbohydrate (X_C), protein (X_P), liquids (X_L), hemicellulose (X_H), cellulose (X_{CE}), lignin (X_{LG}) and inert organic fraction (X_I). Table 1.2 concludes some models describing the dynamics of organic matters in recent literatures. The principal differences between the models "soil" and "composting" are as follows (see details in Table 1.3).

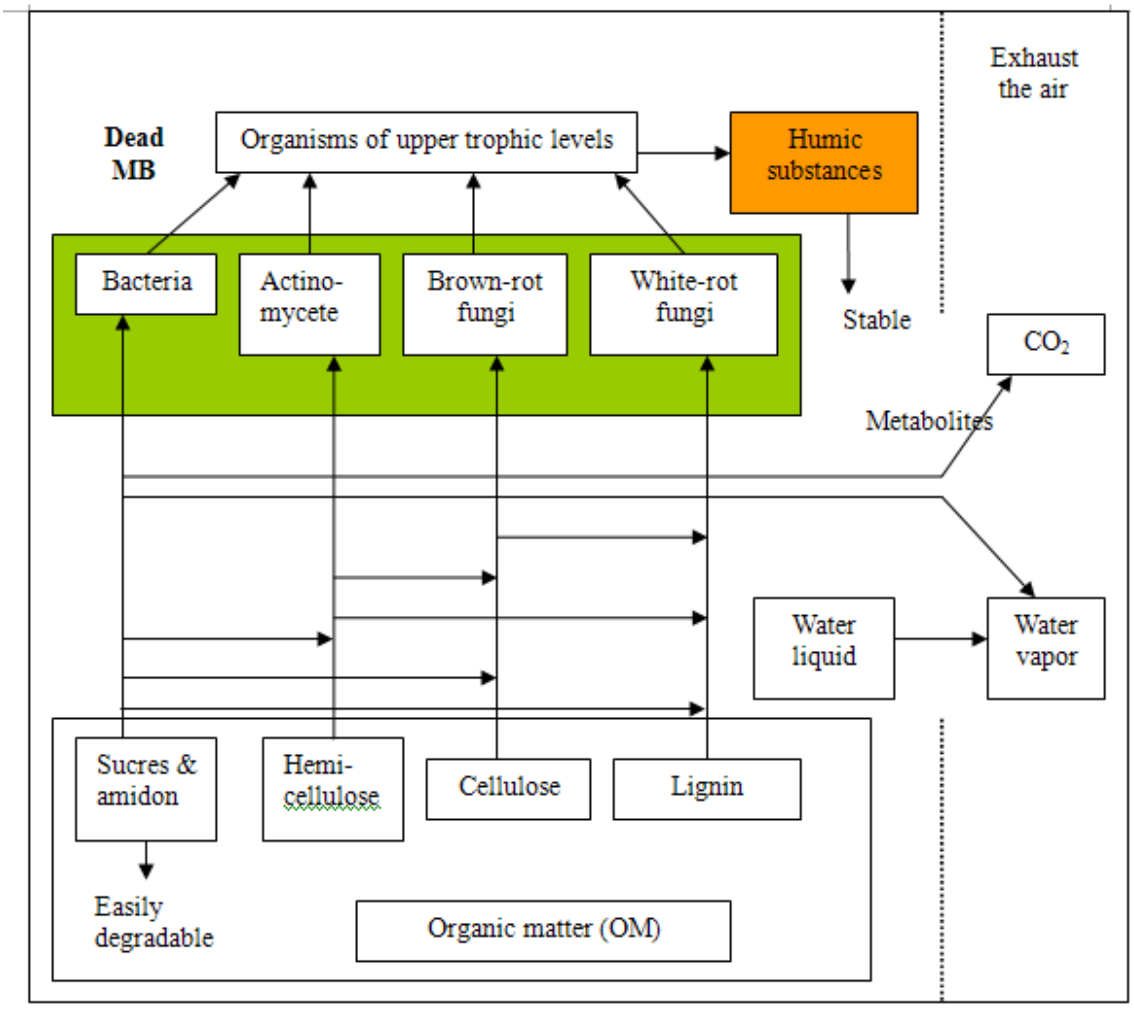


Figure 1.4: Schema of the model of Kasier (1996)

Table 1.2: Organic matter modelling in the field of soil and composting

Models	Field	Aerobic	Number of compartments	Hydrolysis	Kinetic of microbial growth	Microbial decay to the system
Kaiser, 1996	composting	Aerobic	5	No	Monod	Return to Humic OM
Batstone et al., 2002	digestion	Anaerobic	3	Yes	Monod	Return to the initial OM
Garnier et al., 2003	soil	Aerobic	4	No	First order	Return to Humic OM
Tremier et al., 2005	composting	Aerobic	3	No	Monod	Return to the initial OM
Sole-Mauri et al., 2007	composting	Aerobic	7	Yes	Monod	Return to the initial OM

To summarize, the principal differences between the models "soil" and "composting" are as follows (see details in Table 1.3).

The growth of microbial biomass μ can be described in three types of kinetics according to the literature (see Table 1.4). Generally, the studies prefer the 2nd order (Monod), for example Stombaugh (1996), Mason (2006) and Kaiser (1996).

Table 1.3: Comparisons between the OM model in soil and during composting

Model	Limitation	General expression of OM decomposition
In soil	Comes especially from OM	$\frac{dC}{dt} = -kC$
During composting	Comes from OM and MB	$\frac{dC}{dt} = -\mu X$ « μ » can be calculated by different kinetic of order (see details in Table x)

Table 1.4: Three orders of the microbial growth μ

Croissance de BM	Equation	Description
Ordre 0	$\mu = \mu_{max}\, f_T\, f_W$	The microbial growth varies only on the function of temperature (T) and moisture content (W)
Ordre 1	$\mu = \mu_{max} C\, f_T\, f_W$ (C : la concentration du substrat)	The microbial growth varies on the concentration of substrate and the site environment
Ordre 2(Monod)	$\mu = \mu_{max}\, f_T\, f_W \frac{C}{K_S + C}$ (Ks : demi-saturation)	The microbial growth varies on the concentration of substrate and the site environment but there is a limit for the microbial growth

1.4.3 Summary of OP models

In the literature, the models of organic pollutants (OPs) exist especially in the field of the soil but they can also be adapted to the composting. We found several types of models (showed in Table 1.5): A) The models with two compartments which describe the phenomenon of degradation, adsorption and desorption; B) The multi-compartment models (i.e. Fig.1.5) which distinguish the fraction weakly adsorbed and strongly adsorbed; C) The models which separate the molecular parent and their metabolites (i.e. Fig.1.6).

Table 1.5: Summary of OP models

Reference	Compartiments	Equations
Barriuso et al. (1991)	- Soluble Sw - Adsorbed Ss	Ss = Kd * Sw Kd: coefficient de distribution
Xue et Selim, 1995 & Shelton et Doherty, 1997 **(see figure 8)**	- Soluble Sw - Easily accessible Ss1 - diffuse dans MO Ss2	$\frac{\partial S_w}{\partial t}$ = - K1 * Sw + K-1*Ss1 $\frac{\partial S_{s1}}{\partial t}$ = K1 * Sw – (K -1 + K2) *Ss1 +K-2*Ss2 $\frac{\partial S_{s2}}{\partial t}$ = K2*Ss1 - K-2*Ss2
Saffih-Hdadi (2003) **(see figure 9)**	- Pesticide - Metabolite	See Table 1.6

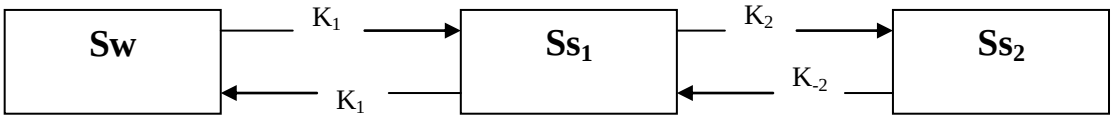


Figure 1.5: Multi-compartiment model *

(*: Xue and Selim, 1995; Shelton and Doherty, 1997)

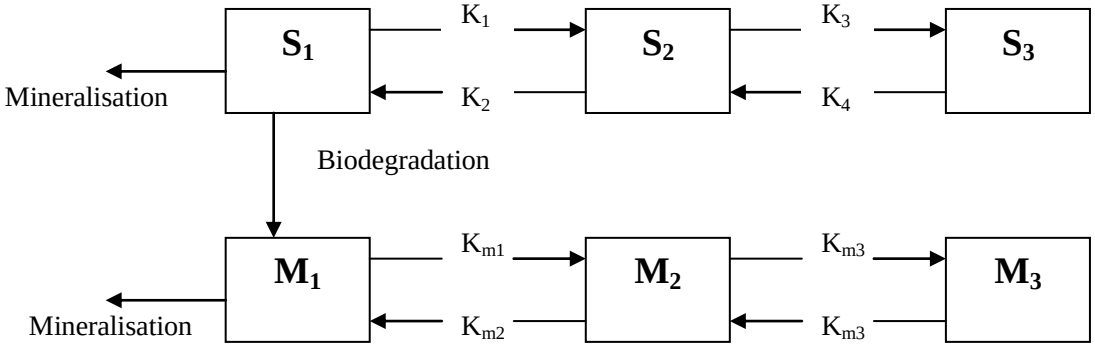


Figure 1.6: Model of Saffih-Hdadi (2003)

*Ki, $K_{mi:}$ Kinetic coefficients of sorption for molecular parent and their metabolites

*S: pesticide / M: metabolite

Table 1.6: The equations for model of Saffih-Hdadi (2003)

Composant phase	Sorption	Biodegradation		Metaboliste production	
		Cometabolisme❶	Specific❷	Cometab-	Specific
$[\frac{dS_1}{dt}]$	$= - K_1S_1 + K_2S_2$	$-\alpha_1\{\frac{B(t)}{B_0}\}.S_1$	$-\left\{\frac{\mu S_1.B_{S1}}{(K_{S1}+S_1).Y_{S1}}\right\}.S_1$		
$[\frac{dS_2}{dt}]$	$= K_1S_1 - K_2S_2 - K_3S_2 + K_4S_3$				
$[\frac{dS_3}{dt}]$	$= K_3S_2 - K_4S_3$				
$[\frac{dM_1}{dt}]$	$= -K_{m1}M_1 + K_{m2}M_2$	$-\alpha_{m1}\{\frac{B(t)}{B_0}\}.M_1$	$-\left\{\frac{\mu_{m1}S_1.B_{M1}}{(K_{M1}+M_1).Y_{M1}}\right\}.M_1$	$f_{pc}\alpha_1\{\frac{B(t)}{B_0}\}S_1$	
$[\frac{dM_2}{dt}]$	$= K_{m1}M_1 - K_{m2}M_2 - K_{m3}M_2 + K_{m4}M_3$				
$[\frac{dM_3}{dt}]$	$= K_{m3}M_2 - K_{m4}M_3$				

S_1: variation of the concentration in soluble phase of pesticide

S_2: variation of the concentration of pesticide easily adsorbed

S_3: variation of the concentration of pesticide strongly adsorbed on the function of time

K_1: for **sorption** between the soluble phase and easily adsorbed phase

K_2: for **desorption** between the soluble phase and easily adsorbed phase

K_3: for **sorption** between the easily adsorbed phase and the difficult adsorbed phase

K_4: for **desorption** between the easily adsorbed phase and the difficult adsorbed phase

B (t): the total biomass

B_0: the initial biomass at the beginning of experiment

The model distingue the degradation by cometabolisme and by specific metabolisme:

❶ Biodegradation by **cometabolisme**, where the total biomass B(t) of soil dissipate the present pesticide in the soluble phase like the other organic components.

❷ Biodegradation by specific metabolisme, assuring that a part of the total biomass $B_{S1}(t)$ contribute to the biodegradation of pesticide and the growth of microbial population.

This description of the biodegradation is very difficult to reveal in experiments and thus to parameterize in the model.

1.5 Objectives of the thesis

our work is sought to i) build a new dynamic model for composting process to simulate the interactions between organic matters (OM) evolution and organic micro-pollutants (OP) behaviour; ii) Evaluate the model with existing data (from French lab) of organic wastes composting; iii) Apply it to the bioremediation of polluted soils in China. In order to complete our objective, two parts of work will be done during my PHD: modelling and experiments.

- For modelling, we'll construct and then validate the model of OM coupling with OMP. The model will be programmed and implemented in Matlab (Mathwork, USA). For the OM model, experimental results by Francou (2008) and Doublet (2008) have been applied, who used the method of Van Soest to determined soluble organic matter, hemicelluloses-like, cellulose-like, and lignin-like contents in composts. They concluded the most general types of composts and then offered us a good data-base for calibrating our model and validating it. For OP model, the experimental results by Lashermes (2011) and Hartlieb (2003) have been applied, who used the method of ^{14}C-labelled to identify the different phases of OP. After the evaluation of our composting model, its structure, kinetics foundations, simulation abilities and validation performance, we'll develop our model to utilize in the soil composting system. The experiments during my PHD aim to be applied on the evaluation of our model for the bioremediation in soil composting system.
- For experimentation, I will use contaminated soil to study the dynamics of organic micro-pollutants, especially 16 PAHs during the soil-waste composting system. The soil is taken from Chaoyang District in Beijing which is highly polluted by the coal industry (coke plants). The texture of soil is loam-sandy soil concerning 10% of clay. In the experiments, I will focus on the characterization of OM by the method of Van Soest (Van Soest and Wine, 1967), analysis of 16 PAHs by the extraction of Soxhlet and GC-MS method,

as well as the qualification and quantification of micro-organisms by the method of PLFA. The experimental results will provide us a data base to calibrate our model for soil-waste composting system.

1.6 References

ADEME. http://portail.bu.univ-artois.fr/webcontent/viewer/viewer.asp?INSTANCE=INCIPIO&EXTERNALID=WBCTDOC_1257. 2004.

Al-Daher, R., Al-Awadhi, N., El-Nawawy, A., 1998. Bioremediation of damaged desert environment using windrow soil pile system inKuwait. Environment International 24: 175–180.

Alexander, M., 1994. Biodegradation and Bioremediation. Academic Press, New York.

Amir, S., Hafidi M, Merlina G, Hamdi H, Revel JC, 2005. Fate of polycyclic aromatic hydrocarbons during composting of lagooning sewage sludge, Chemosphere 58: 449–458.

Antizar-Ladislao, B., Lopez-Real, J., Beck, A.J., 2005. Laboratory studies of the remediation of polycyclic aromatic hydrocarbon contaminated soil by in-vessel composting, Waste Manage. 25: 281–289.

Antizar-Ladislao, B., Lopez-Real, J., Beck, A.J., 2006. Degradation of polycyclic aromatic hydrocarbons (PAHs) in an aged coal-tar contaminated soil under in-vessel composting conditions, Environ. Pollut. 141: 459–468.

Atagana, H.I., 2003. Bioremediation of creosote contaminated soil: a pilot-scale landfarming evaluation. World J. Microbiol. Biotechnol. 19: 571-581.

Atagana, H.I., 2004. Bioremediation of creosote-contaminated soil in South Africa by landfarming. J. Appl. Microbiol. 96: 510-520.

Atagana, H.I., 2004. Co-composting of PAH-contaminated soil with poultry manure. Lett. Appl. Microbiol. 39: 163-168.

Atagana, H.I., Haynes RJ, Wallis FM, 2003. Co-composting of soil heavily contaminated with creosote with cattle manure and mixed vegetable waste. Soil and Sediment Contamination: An Int. J. 12(6): 889-899.

Atlas, R.M., 1975. Effects of temperature and crude oil composition on petroleum biodegradation. Applied Microbiology 30: 396–403.

Bakshi, M.P.S., Gupta, K., Langar, P.N., 1987. Effect of moisture level on the chemical composition and nutritive value of fermented straw. Biological Wastes, 21(4): 283-289.

Ballentine, D.C., Macko, S.A., Turekian, V.C., Gilhooly, W.P., Martincigh B., 1996. Compound specific isotope analysis of fatty acids and polycyclic aromatic hydrocarbons in aerosols: implications for biomass burning. Organic Geochemistry, 25(1-2): 97-104.

Barriuso, E., Schiavon, M., Andreux, F., Portal J, 1991. Localization of atrazine non-extractable (bound) residues in soil size fractions. Chemosphere, 22(12): 1131-1140.

Batstone, D.J., Keller, J., Angelidaki, I., Kalyuzhnyi, S.V., Pavlostathis, S.G., Rozzi, A., Sanders, W.T.M., Siegrist, H., Vavilin, V.A., 2002. The IWA Anaerobic Digestion Model No 1(ADM 1). Water Science & Technology, 45(10): 65-73.

Beaudin, N., Caron, R.F., Legros, R., Ramsay, J., Lawlor, L., Ramsay, B., 1996. Cocomposting of weathered hydrocarbon-contaminated soil. Compost Science and Utilization, 4; 37–45.

Beaudin, N., Caron, R.F., Legros, R., Ramsay, J., Ramsay, B., 1999. Identification of the key factors affecting composting of a weathered hydrocarbon-contaminated soil. Biodegradation, 10; 127–133.

Bollag, J.M., Bollag, W.B., 1995. Soil contamination and the feasibility of biological remediation. In: Skipper HD and Turco RF (eds) Bioremediation: Science and Application, (pp 1–13). SSSA Special Publication, 13. Madison, Wisconsin.

Clarinet. Remediation of Contaminated Land. Technology Implementation in Europe, http://www.clarinet.at/library/WG7 Final Report.pdf (accessed 17 October 2007).

Corbeels, M., Hofman, G., Van Cleemput, O, 1999. Simulation of net N immobilisation and mineralisation in substrate-amended soils by the NCSOIL computer model. Biology and fertility of Soils, 28(4): 422-430.

Delgadillo-Mirquez, L., Lardon, L., Steyer, J.P., Patureau, D, 2011. A new dynamic model for bioavailability and cometabolism of micropollutants during anaerobic digestion. Water Research, 45: 4511-4521.

Doublet, J, INFLUENCE DU CO-SUBSTRAT CARBONE SUR LA NATURE DES MATIERES ORGANIQUES ET LES FORMES DE L'AZOTE DES COMPOSTS DE BOUES; CONSEQUENCE SUR SA DISPONIBILITE, in Les Matières Organiques en France. 2008. p. 280.

Doublet, J., Francou, C., Poitrenaud, M., Houot S., 2010. Sewage sludge composting: Influence of initial mixtures on organic matter evolution and N availability in the final composts. Waste Manage, 30: 1922–1930.

Epstein, E. The Science of Composting. Technomic Publishing Co., Inc. Basel, Switzerland, 1997.

European Communities, Waste Generated and Treated in Europe 1995-2003. Office of Official Publications of European Communities. 2005: Luxembourg.

Fang, J.D., 2007. Site selection for sanitary landfill of municipal solid waste. Channel Science 6, 58–59 (in Chinese).

Finstein, M.S., 1980. Composting microbial ecosystem: implications for process design and control. Compost Sci./Land Util., 21: 25–27.

Francou, C., Lineres, M., Derenne, S., Villio-Poitrenaud, M.L., Houot, S., 2008. Influence of green waste, biowaste and paper-cardboard initial ratios on organic matter transformations during composting. Bioresour Technol, 99: 8926–8934.

Garnier, P., Néel, C., Aita, C., Recous, S., Lafolie, F., Mary, B., 2003. Modelling carbon and nitrogen dynamics in a bare soil with and without straw incorporation. European Journal of Soil Science, 54(3): 555-568.

Gray, K.R., Sherman, K., Biddlestone, A.J., 1971. A review of composting. Part 1. Process Biochemistry, 6(6): 32-36.

Golueke, C.G., McGauhey, P.H. Reclamation of Municipal Refuse by Composting. In: Technical Bulletin No. 9 Sanitary Engineering. Research Laboratory, University of California, Berkeley, CA, U SA, 1953.

Golueke, C.G., Diaz, L.F., 1987. Composting and the limiting factor principle. Biocycle, 28: 22–25.

Griffin, D.M. Water and microbial stress. In: M. Alexander (ed.). Advances in microbial ecology. Plenum Press, 1981, New York/London. pp. 91-136.

Hamelers, H.V.M. A theoretical model of composting kinetics. In: H.A.J. Hoitink and H. Keener (eds.). Science and Engineering of Composting. Columbus Ohio, Renaissance Publications, 1992, pp. 36-58.

Hartlieb, N., Ertunc, T., Schaeffer, A., Klein, W., 2003. Mineralization, metabolism and formation of non-extractable residues of 14C-labelled organic contaminants during pilot-scale composting of municipal biowaste. Environmental Pollution, 126(1): 83-91.

Harvey RG, Polycyclic Aromatic Hydrocarbons. 1997, Wiley-VCH, Inc.: New York. p. 667.

Haug, R.T. The Practical Handbook of Compost Engineering. Lewis Publishers, Boca

Raton, FL, USA, 1993.

Jeris, J.S., Regan, R.W.,1973. Controlling environmental parameters for optimal composting II: moisture, free air space and recycle. Compost Science, 1: 14.

Jones, K. C. and de Voogt, P., 1999. 'Persistent organic pollutants (POPs): state of the science', Environ. Pollution 100, 209–221.

Jørgensen, K.S., Puustinen, J., Suortti, A.-M., 2000. Bioremediation of petroleum hydrocarbon-contaminated soil by composting in bio-piles. Environmental Pollution 107, 245–254.

Kaiser, J., 1996. Modelling composting as a microbial ecosystem: A simulation approach[J]. Ecological Modelling, 91 (1–3), 25–37.

Kirchmann, H., Ewnetu, W., 1998. Biodegradation of petroleum-based oil wastes through composting. Biodegradation 9, 151–156.

Kishimoto, M., Preechaphan, C., Yoshida, T, Taguchi, H.. 1987. Simulation of an aerobic composting of activated sludge using a statistical procedure. MIRCEN Journal, 3, 113–124.

Lashermes, G., Houot, S., Barriuso, E., 2010. Sorption and mineralization of organic pollutants during different stages of composting. Chemosphere, 79, 455-462.

Lau K.L., Tsang Y.Y., Chiu S.W., 2003. Use of spent mushroom compost to bioremediate PAH-contaminated samples. Chemosphere, 52: 1539–1546.

Liang, C., Das, K.C., McClendon, R.W.. The influence of temperature and moisture contents regimes on the aerobic microbial activity of a biosolids composting blend. Bioresource Technology 86, 131–137.

Lin, Y.P., Huang. G.H., Lu, H.W., He, L., 2008. Modeling of substrate degradation and oxygen consumption in waste composting processes. Waste management, 28(8): 1375-1385.

Manilal, V.B., Alexander, M., 1991. Factors affecting the microbial degradation of phenanthrene in soil. Applied and Microbiology and Biotechnology 35, 401–405.

Mason, I.G., 2006. Mathematical modelling of the composting process: A review. Waste management, 26(1): 3-21.

Mastral, A.M., Callen, M.S., 2000. A review on polycyclic aromatic hydrocarbon (PAH) emissions from energy generation. Environmental science & technology, 34(15): 3051-3057.

Morel, J.L., Guckert, A., Nicolardot, B., Denistant, D., Catroux, G., Germon, J.G., 1986. Etude de l'évolution des caractéristiques physico-chimiques et de la stabilité biologique des ordures ménagères au cours du compostage. Agronomie, 6(8): 693-701.

Morisaki, N., 1989. Nitrogen transformation during thermophilic composting. Journal of Fermentation and Bioengineering, 67(1): 57-61.

McFarland, M.J., Qiu, X.J., 1995. Removal of benzo(a)pyrene in soil composting systems amended with the white-rot fungus phanerochaete-chrysosporium, J. Hazard. Mater. 42, 61–70.

Miller, F.C., Finstein, M.L., Strom, P.F., 1986. Waste treatment composting as a controlled system. Biotechnology, 8: 363-398.

Milne, B.J., Baheri, H.R., Hill, G.A., 1998. Composting of a heavy oil refinery sludge. Environmental Progress 17, 24–27.

Ministry of Construction of China, 2005. China Urban Construction Statistics Yearbook (2004). China Architecture and Building Press, Beijing.

Moretto, L.M., Silvestri, S., Ugo, P., Zorzi, G., Abbondanzi F., Baiocchi C., Iacondini A., 2005. Polycyclic aromatic hydrocarbons degradation by composting in a soot-contaminated alkaline soil, J. Hazard.Mater. B126: 141–148.

Nakasaki, K., Shoda, M., Kubota, H., 1985. Effect of temperature on composting of sewage sludge. Appl. Environ. Microbiol., 50(6): 1526–1530.

Namkoong, W., Hwang, E.-Y., Park, J.-S., Choi, J.-Y., 2002. Bioremediation of diesel-contaminated soil with composting. Environmental Pollution 119, 23–31.

Ndegwa, P.M., Thompson, S.A., Merka, W.C., 2000. A dynamic simulation model of in-situ composting of caged layer manure. Compost Science & Utilisation, 8(3), 190–202.

Nicolardot, B., Recous, S., Mary, B., 2001. Simulation of C and N mineralisation during crop residue decomposition: A simple dynamic model based on the C:N ratio of the residues. Plant & Soil 228, 83-103

Oleszczuk, P., 2007. Changes of polycyclic aromatic hydrocarbons during composting of sewage sludges with chosen physico-chemical properties and PAHs content. Chemosphere, 67(3): 582-591.

Page, D.S., Boehm, P.D., Douglas, G.S., Bence, A.E., Burns, W.A., 1999. Mankiewicz

PJ. Pyrogenic polycyclic aromatic hydrocarbons in sediments record past human activity: a case study in Prince William Sound, Alaska. Mar. Pollut. Bull., 38: 247-260.

Pignatello, J.J., Xing, B., 1996. Mechanisms of slow sorption of organic chemicals to natural particles. Environmental Science and Technology, 30, 1–11.

Rao, N., Grethlein, H.E., Reddy, C.A., 1996. Effect of temperature on composting of atrazine-amended lignocellulosic substrates. Compost science and utilization (USA): 83-88.

Recous, S., Effet de la temperature sur la mineralisation d'un residu vegetal (mais) et de la matiere organique d'un sol. In Ecosystemes naturels et cultives et changements globaux. 1995, Les Dossiers de I'Environnement. INRA. p. 81-85.

Richard, T.L., Walker, L.P.. Temperature kinetics of aerobic solid-state biodegradation. 1998.

Richard, T.L., Walker, L.P., 1999. Oxygen and temperature kinetics of aerobic solid-state biodegradation. W. Bidlingmaier et al. (ed.) Proc. of Organic Recovery and Biological Treatment, Part 1. ORBIT99, Weimar, Germany. 2–4 Sept., pp. 85–91.

Richard, T.L., Hamelers, H.V.M., Veeken, A., Silva, T., 2002. Moisture relationships in composting processes. Compost Science and Utilization, 10(4): 286-302.

Romantschuk, M, Sarand, I, Petanen, T., Peltola, R., Jonsson-Vihanne, M., Koivula, T., Yrjala, K., Haahtela, K., 2000. Means to improve the effect of in situ bioremediation of contaminated soil: an overview of novel approaches. Environmental Pollution, 107: 179–185.

Rosso, L., Lobry, J.R., Flandrois, J.P. 1993. An unexpected correlation between cardinal temperatures of microbial growth highlighted by a new model. Journal of theoretical biology, 162(4): 447-463.

Saffih-Hdadi, K., Bruckler, L., Barriuso, E., 2003. Modeling of sorption and biodegradation of parathion and its metabolite paraoxon in soil. J. Environ. Qual, 32(6): 2207-2215.

Sasek, V., Bhatt, M., Cajthaml, T., Malachova, K., Lednicka, D., 2003. Compost-mediated removal of polycyclic aromatic hydrocarbons fromcontaminated soil, Arc. Environ. Contam. Toxicol., 44: 336–342.

Schulze, K.L., 1961. Aerobic decomposition of organic waste materials. Final Report, Project RG-4180 (C5R4), National Institute of Health, Washington, DC.

Semples, K.T., Reid, B.J., Fermor, T.R., 2001. Review of composting strategies to treat organic pollutants in contamined soil, Environ. Pollut., 112: 269–283.

Skladany, G.J., Metting Jr, F.B., 1992. Bioremediation of contaminated soil. In: Metting Jr., F.B. (Ed.), Soil Microbial Ecology: Applications in Agricultural and Environmental Management. Marcel Dekker, New York, pp. 483–513.

Shelton, D.R., Doherty, M.A., 1997. A model describing pesticide bioavailability and biodegradation in soil. Soil Science Society of America Journal, 61(4): 1078-1084.

Sims, R.C., Overcash, M.R., 1983. Fate of polynuclear aromatic compounds (PNAs) in soil-plant systems. Residue Reviews (Germany, FR), 88: 1-68.

Sole-Mauri, F., Illa, J., Magrí, A., Prenafeta-Boldú, F.X., Flotats, X. 2007. An integrated biochemical and physical model for the composting process. Bioresource technology, 98(17): 3278-3293.

Smith, D.W.. Water relations of microorganisms in nature [N]. In: Microbial Life in Extreme Environments. D.J. Kushner (Ed.). Academic Press, 1978, New York. pp. 369-380.

Stombaugh, D.P., Nokes, S.E., 1996. Development of a biologically based aerobic composting simulation model[J]. Transactions of ASAE, 39 (1): 239–250.

Suess, M.J., 1976. The environmental load and cycle of polycyclic aromatic hydrocarbons. Science of the total environment, 6(3): 239-250.

Suler, D.J., Finstein, M.S., 1977. Effect of temperature, aeration, and moisture on CO_2 formation in bench-scale, continuously thermophilic composting of solid waste. Appl. Environ. Microbiol., 33: 345–350.

Tremier, A., De Guardia, A., Massiani, C., Paul, E., Martel, J.L., 2005. A respirometric method for characterising the organic composition and biodegradation kinetics and the temperature influence on the biodegradation kinetics, for a mixture of sludge and bulking agent to be co-composted. Bioresource technology, 96(2): 169-180.

Tseng, D.Y., Chalmers, J.J., Tuovinen, O.H., Hoitink, H.A.J., 1995. Characterization of a bench-scale system for studying the biodegradation of organic solid wastes. Biotechnol. Progr., 11: 443-451.

Van Soest, P.J., Wine, R.H.. Use of detergents in the analysis of fibrous feeds. IV. Determination of permanganate[N]. Journal of A. O. A. C.,1967, 50, 1: 50-55.

Verge-Leviel, C.. Les micropolluants organiques dans les composts d'origine urbaine : étude de leur devenir au cours du compostage pour l'évaluation des risques de contaminants des sols après épandage des composts. Thèse de Doctorat de l'INA P-G, 144p. 2001.

Vlyssides, A., Mai, S., Barampouti, E.M., 2009. An integrated mathematical model for co-composting of agricultural solid wastes with industrial wastewater. Bioresource technology, 100(20): 4797-4806.

Weissentiels, W.D., Klewer, H.J., Langhoff, J., 1992. Adsorption of polycyclic aromatic hydrocarbons (PAHs) by soil particles: in Kuence on biodegradability and biotoxicity. Applied Microbiology and Biotechnology, 36: 689–696.

Xi, B.D., Wei, Z.M., Liu, H.L., 2005. Dynamic Simulation for Domestic Solid Waste Composting Processes. The Journal of American Science, 1(1): 34-45.

Xue, S.K., Chen, S., Selim, H.M., 1997. Modeling alachlor transport in saturated soils from no-till and conventional tillage systems. Journal of environmental quality, 26(5): 1300-1307.

PART I: MODELING ORGANIC CARBON AND ORGANIC POLLUTANT DYNAMICS DURING COMPOSTING OF ORGANIC WASTES

CHAPTER 2: MODELLING OF ORGANIC MATTER DYNAMIC DURING THE COMPOSTING PROCESS

Authors: Y. Zhang[1, 2], G. Lashermes[2,3], S. Houot[2], J. Doublet[4], JP. Steyer[5], YG. Zhu[1], E. Barriuso[2], P. Garnier[2, *]

1 –*Chinese Academy of Sciences, Institute of Urban Environment, Xiamen, People's Republic of China*

2 –INRA, UMR 1091 Environnement et Grandes Cultures, F-78850 Thiverval-Grignon, France

3 - INRA, UMR 614, Fractionnement des AgroRessources et Environnement (INRA-URCA), 2 Esplanade Roland Garros, F-51100 Reims, France

4 – VEOLIA Environment – Research and Innovation, F-78520 Limay, France

5 - *INRA, UR 50, Laboratoire Biotechnologie de l'Environnement, Avenue des Etangs,* F-11100 Narbonne, France

***Corresponding author:** INRA-AgroParisTech, UMR1091 Environnement et Grandes Cultures, 78850 Thiverval-Grignon, France. Tel: +33 1 30 81 53 14; Fax: +33 1 30 81 53 96.

E-mail address: pgarnier@grignon.inra.fr (Patricia Garnier)

Accepted by **Waste Management**

2.1 Abstract

The composting of urban organic wastes enables the recycling of their organic fraction in agriculture. The objective of this new composting model was to gain a clearer understanding of the dynamics of organic fractions during composting and to predict the final quality of composts. Organic matters were split into different compartments according to their degradability. The nature and size of these compartments were studied using a biochemical fractionation method. The evolution of each compartment and the microbial biomass were simulated, as was the total organic carbon loss corresponding to organic carbon mineralization into CO_2. Twelve composting experiments on different feedstocks were used to calibrate and validate our model. We obtained anunique set of estimated parameters. A good agreement was achieved between simulated and experimental results describing the evolution of different organic fractions, except for some composts because of a poor simulation of the cellulosic and soluble pools. The degradation rate of the cellulosic fraction appeared to be highly variable, depending on the origin of the feedstocks. The initial soluble fraction could contain some degradable and recalcitrant elements that are not easily accessible experimentally.

2.2 Introduction

The organic fraction of urban wastes can be recycled into cultivated soils after composting. The composting process converts biodegradable wastes into sanitised and stable organic matter that is valuable for agriculture. The biodegradability of composts after their application on soil as amendments is correlated to their stability and depends on the biochemical characteristics of their organic matter. A high ratio between the lignin and cellulosic pools ensures greater stability (Bernal et al., 1998) that is also associated with a large loss of carbon through mineralization during composting.

Mathematical models are useful tools for understanding and improving the composting process and for predicting the stability of the final product. Hence, most composting models generally predict the evolution of dry mass, temperature, moisture, oxygen and carbon dioxide (see the review by Mason, 2006). However, to our knowledge, very few of these models have described the evolution of the biochemical composition of organic matter (OM) that reflects its potential degradability in soil after application. Some models have recently been proposed to better describe the quality of organic matter. These models divide organic matter into several pools with specific biodegradability features, ranging from two, for the model proposed by Tremier et al. (2005a), to six, for the model proposed by Sole-Mauri et al. (2007). However, these models have not been tested using experimental data of the evolution of the organic matter fractions during composting.

On the other hand, some experimental work has been published on the degradability of different organic mixtures as a function of their respective initial composition and biochemical properties (Francou et al., 2008 and Doublet et al., 2011). These studies have shown that the evolution of degradability is directly correlated to the initial biochemical properties of the feedstock. A simulation of this organic fraction evolution during composting would help to assess the quality of the final product and to predict its subsequent behaviour in soil after application.

The objectives of the present study were to propose and test a new composting model that could predict the decomposition of organic matter from its initial biochemical properties. The model was compared with experimental laboratory data on

composting using different initial feedstocks (Francou et al., 2008; Doublet et al., 2011). The model was first calibrated to obtain a unique set of input parameters and was then tested using these parameters with a second set of data for validation purposes only. Finally, the sensitivity of the model to variations in input parameters and initial conditions was analysed.

2.3 Materials and Methods

2.3.1 The model

2.3.1.1 General presentation

Figure 1 shows the general structure of the proposed model. Organic matter was broken down into compartments corresponding to the biochemical fractions described using the Van Soest fractionation method (Van Soest and Wine, 1967; AFNOR, 2009). This method is based on successive solubilisations of the organic fractions: H2O (soluble in hot water), SOL (soluble in neutral detergent), HEM (hemicelluloses-like), CEL (cellulose-like) and LIC (lignin-like). These compartments have been shown to be useful to simulate organic matter decomposition in soil models (Corbeels et al., 1999; Henriksen & Breland, 1999; Garnier et al., 2003).

Heterogeneities and different evolutions of the SOL fraction characteristics during decomposition have been illustrated in several studies (Lichtfouse et al., 1998; Pascual et al., 1999; Francou et al., 2008; Peltre et al., 2010), which detected changes to the chemical characteristics of the SOL fractions and the simultaneous presence of easily degradable substrates and humic substances in the soluble fractions. Thus, this fraction was divided into two pools, one with rapid degradability (SOL-F) and the other with slow degradability (SOL-S) (Fig.2.1).

All organic pools were hydrolysed into substrates available for microbial growth using a first order kinetic model, depending on their specific hydrolysis constants. The initial fraction of available substrate corresponds to the H2O fraction in the initial mixture before composting. Several compartments corresponding to different microbial populations could be included in the model to account for different physiologic parameters for bacteria and fungi or for mesophilic and thermophilic populations. In this first version of the model, a single microbial population was considered (biomass compartment in Fig.1), and its growth from the hydrolysed

substrates was modelled using Monod kinetics modulated with the temperature-limiting function proposed by Rosso et al. (1993). The hydrolysis of organic substances by extracellular enzymes has been described as a process that is separated from assimilation by micro-organisms, such as in the models of Bastone et al., 2002, Garnier et al., 2003 and Sole-Mauri et al., 2007. This biomass compartment decomposes at a specific rate that was assimilated to the death rate of the microorganisms and the dead cells are recycled into either the SOL-S compartment (characterised by a slow degradation rate) or directly into the H2O compartment (characterized by a rapid degradation rate). The recycling of the dead biomass back into the initial system has already been described in other models, such as composting or digestion models (Bastone et al., 2002; Sole- Mauri et al., 2007).

In this first version of the model, we assumed that moisture, oxygen and nitrogen were not limiting factors of decomposition. The experimental data used to evaluate the model were obtained under the same conditions. However, as the model develops in the future, limiting factors should be included.

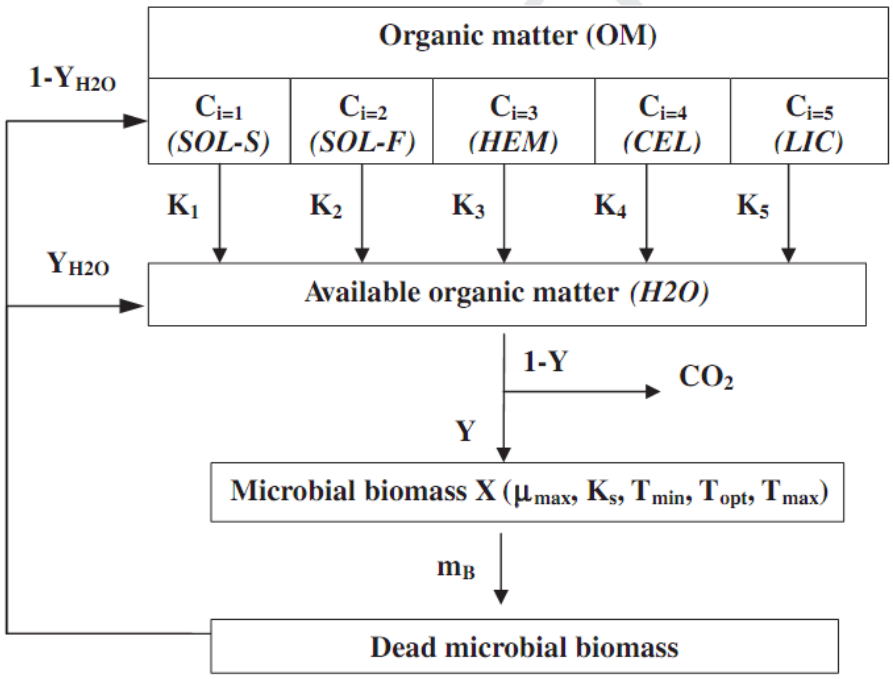


Figure 2.1: General schema of the composting model of organic matter

2.3.1.2 Model equations

Using existing numerical models constructed for various composting systems, a series of general equations with daily time steps is proposed to describe the dynamics of organic matter during composting on the basis of mass balance (Table 1). This model describes the organic matter dynamics expressed as a percentage of initial total organic carbon (TOC). In the following equations, all C variables are represented as g of organic carbon per 100 g of initial TOC.

Only one microbial population was applied during these initial simulations because of the lack of experimental data to describe other populations. The dynamics of microbial biomass X are described using the following equation:

$$\frac{dX}{dt} = \mu X - m_B X \qquad [1]$$

Where X (g C $100g^{-1}$ initial TOC) corresponds to the content of microbial biomass with a specific microbial growth rate μ (d^{-1}) and a decay rate m_B (d^{-1}). The growth rate of microbial population μ follows a Monod kinetic:

$$\mu = \mu_{max} \frac{C_S}{K_S + C_S} f_T \qquad [2]$$

Table 2.1: Used Petersen's matrix (1965) for composting model

Process	Variables							Ratio * concentration
	SOL	HEM	CEL	LIC	H2O	X	CO_2	
Consumption of SOL	-1				1			K1 * SOL-S + K2 * SOL-F
Consumption of HEM		-1			1			K3 * HEM
Consumption of CEL			-1		1			K4 * CEL
Consumption of LIC				-1	1			K5 * LIC
Mortality of X	$1-Y_{mcs}$				Y_{mcs}	-1		m_B * X
Growth of X					-1 / Y	1	(1- Y) / Y	μ * X
	Concentration of SOL	Concentration of HEM	Concentration of CEL	Concentration of LIC	Concentration of H2O	Concentration of X	Evolution of CO_2	$r_i = \sum_j r_{ij} = \sum_j \nu_{ij}\sigma_{ij}$

Where μ_{max} (d^{-1}) is the specific maximum growth rate of the microbial biomass; H2O (g C $100g^{-1}$ initial TOC) represents the content of available substrate for microbial biomass (H2O fraction); K_S (g C $100g^{-1}$ initial TOC) is a constant of half-saturation of the available substrate by microbial biomass. The function of temperature f_T used was the function of Rosso et al. (1993):

$$f_T = \frac{(T - T_{max})(T - T_{min})^2}{(T_{opt} - T_{min})[(T_{opt} - T_{min})(T - T_{opt}) - (T_{opt} - T_{max})(T_{opt} + T_{min} - 2T)]} \quad [3]$$

The temperature function (f_T) is the multiplicative coefficient used to correct the growth of the microbial biomass. The function proposed by Rosso et al. (1993) uses three cardinal points: minimum (T_{min}), optimum (T_{opt}) and maximum (T_{max}) temperatures (°C). Each of these points is specific to a particular microbial biomass and determines the evolution of its growth. Our temperature function characterises a global biomass that includes all successive groups of micro-organisms: psychrophilic micro-organisms for minimum temperatures, mesophilic micro-organisms for optimum temperatures and thermophilic micro-organisms for maximum temperature (Bailey and Ollis, 1986).

The $C_{i=3}$ (HEM), $C_{i=4}$ (CEL) and $C_{i=5}$ (LIC) organic compartments (g C 100 g^{-1} initial TOC) degrade according to the following equation [4], with a corresponding rate coefficient of K_i (d^{-1}) (i =3, 4, 5). The hydrolysis of all organic fractions produces the available soluble substrate H2O:

$$\frac{dC_i}{dt} = -K_i C_i \qquad (i = 3,4,5) \quad [4]$$

The soluble fraction (SOL) is separated into two pools (Fig. 1): $C_{i=1}$, corresponding to the soluble OM with slow degradability (SOL-S), and $C_{i=2}$, corresponding to the soluble OM with rapid degradability (SOL-F). The two pools of the soluble fractions (SOL) are degraded into available substrate (H2O) as for the other organic pools. Additionally, a fraction Y_{H2O} of dead microbial biomass returns to the H2O compartment, and the remaining part is incorporated in $C_{i=1}$, which is the slowly degradable fraction SOL-S. Francou et al. (2008) and Doublet et al. (2011) found an increase in the proportion of the SOL fraction in the total organic matter during their composting experiments. They concluded that there was a carbon transfer from the HEM, CEL and LIC fractions into more soluble pools, with a chemical modification

of the SOL fraction as shown by Peltre et al. (2010). Therefore, the equations for $C_{i=1}$ and $C_{i=2}$ are proposed as follows:

$$\frac{dC_1}{dt} = -K_1 C_1 + (1 - Y_{H2O}) m_B X$$
$$\frac{dC_2}{dt} = -K_2 C_2 \quad [5]$$

where $C_{i=1}$ (g C 100 g^{-1} initial TOC) is the content of the SOL-S; $C_{i=2}$ is the content of the SOL-F; $K_{i=1}$ (d^{-1}) is the degradation rate for the SOL-S; and $K_{i=2}$ is the degradation rate for the SOL-F. During the entire process, $C_{i=1}$ + $C_{i=2}$ corresponds to the concentration of the SOL fraction determined experimentally. At the beginning of composting, $C_{i=1}$ was fixed at 0, and $C_{i=2}$ corresponded to the initial quantity of the SOL fraction. The increase in the SOL-S fraction during composting simulates the ongoing progressive humification of the organic matter.

The evolution of the available organic fraction H2O over time is the difference between inputs corresponding to the degradation of organic compartments ($C_{i = 1\text{-}5}$), and outputs due to microbial growth, balanced by the assimilation yield Y of available organic matter, and at a proportion Y_{H2O} of dead microbial biomass returning to this compartment:

$$\frac{dH2O}{dt} = \sum_{i=1}^{5} K_i C_i - \frac{\mu X}{Y} + Y_{H2O}\, m_B X \quad [6]$$

The formation of CO_2 corresponds to the mineralisation of organic matter due to microbial biomass growth:

$$\frac{dCO_2}{dt} = (1 - Y)\frac{\mu X}{Y} \quad [7]$$

The model has been programmed in Matlab (Mathwork, USA).

2.3.2 Data acquisition for the model calibration

2.3.2.1 Initial mixtures

To evaluate the model, we used the results of controlled composting experiments in pilot-scale reactors using different mixtures of wastes as follows: mixtures R1 to R6,

including green wastes, biowastes and paper-cardboard (Francou, 2003; Francou et al., 2008), and mixtures P1 to P6, made with digested sewage sludge and various bulking agents for composting, such as screening refuse from green waste compost, grass clippings, a mixture of crushed hardwood materials mixed with dried ground leaves, crushed pallets, barks and corn stalks (Doublet et al., 2011). Because of the different dry matter (DM) contents of the bulking agents, the final mixing ratios of sludge and bulking agents ranged from 1:4 to 1:7.5, expressed in DM.

2.3.2.2 Composting procedure

Mixtures R1 to R6 (Francou, 2003, Francou et al., 2008) and P1 to P6 (Doublet et al., 2011) were composted for 12 weeks with regular turning, under very similar conditions in both cases. All mixtures were composted in 170 L reactors with forced aeration. Temperatures were measured automatically by sensors installed vertically from the top to a depth of 50 cm in the composting mixture. Figure 3 gave two examples of temperature recorded for P1 and R1 composting experiments.

The evolution of compost mass was measured during composting. After 2, 4 and 12 weeks, following Francou et al. (2008) and after 2, 6 and 12 weeks, following Doublet et al. (2011), each compost was sampled for biochemical analyses. All initial mixtures were weighed before being placed in the reactors, before each turning and just after replacement. Mass losses related to sampling were corrected in the global mass balance for composting.

The TOC was measured in each sample and determined on dried and 200 µm ground samples by elementary analysis according to the French NF ISO 10694 standard (AFNOR, 1999). The amount of CO_2 evolving during composting was calculated from periodical TOC measurements and dry mass losses.

2.3.2.3 Biochemical analyses

The chemical extraction procedure developed for fibrous feed characterisation (Van Soest and Wine, 1967) is described in the French XPU 44162 standard (AFNOR, 2009) and was used to determine the soluble organic matter, cellulose, hemicelluloses and lignin content in the compost (Fancou et al., 2008).

All fractionations were performed on one gram samples using glass crucibles with a coarse porosity (40-100 μm). The distribution of carbon within the different fractions was expressed as a percentage of total organic carbon. Four successive extractions for soluble substances were performed as follows: 30 min with 100 ml of boiling water at 100°C (H2O) and 60 min with 100 ml of hot neutral detergent (SOL). Then, the hemicellulose-like (HEM) fraction was extracted for 60 min with hot acid detergent, and the cellulose-like (CEL) fraction was extracted for 180 min in cold concentrated acid. The residues remaining corresponded to the lignin-like (LIC) fraction. Fig.2.2 shows the biochemical fractions of each initial mixture.

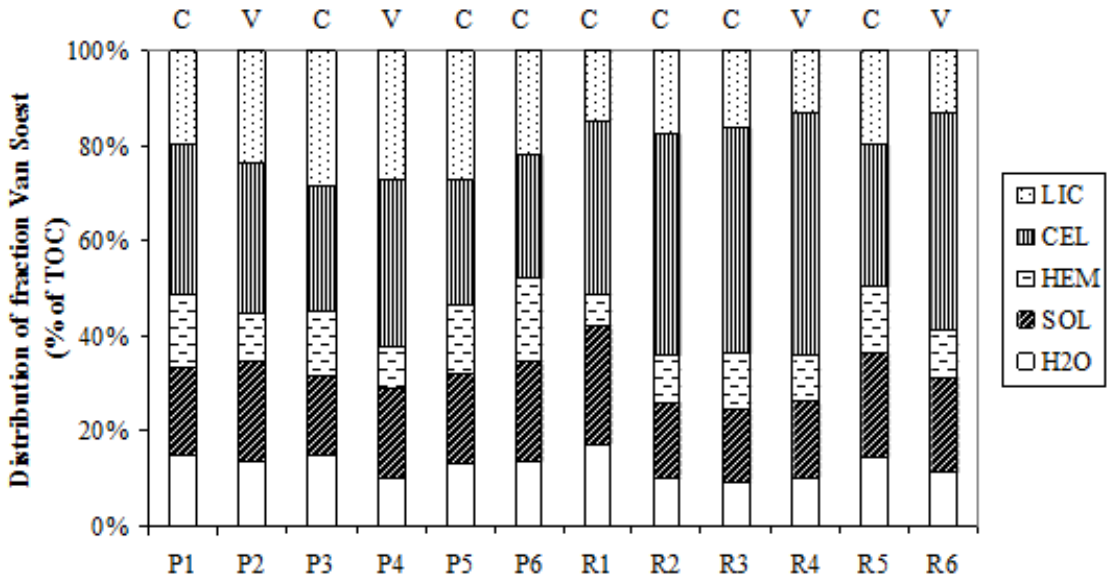


Figure 2.2: Van Soest biochemical fractions of the initial composting mixtures used for model calibration and validation (Francou et al., 2008; Doublet et al., 2011). R1 to R6 are mixtures based on green waste (Francou et al., 2008); P1 to P6 mixtures are based on sewage sludge (Doublet et al., 2011). Mixtures marked with a "C" constituted the calibration dataset, and those marked with a "V" were randomly selected to constitute the validation dataset.

2.3.3 Calibration and evaluation of the model

The model requires inputs of the initial carbon quantity in each fraction of organic matter, the microbial biomass (X), the kinetic parameters for the organic fractions ($K_{i=1\sim5}$) and the microbial biomass X (μ_{max}, T_{min}, T_{opt}, T_{max} and m_B) and the limiting factors (K_S, Y_{H2O}, Y). Overall, the model consists of 13 parameters. The experimental

temperatures of each composting experiment were used in the model (Fig.2.3 gave temperature for P1 and R1 composts). The initial quantity of microbial biomass was supposed to be small enough and similar for all simulations (with the value of 0.05 g C 100 g_{-1} initial TOC).

From the total of 12 mixtures (R1 to R6 and P1 to P6), eight were randomly selected (four feedstock mixtures from R1-R6 and four from P1-P6) to constitute the calibration dataset. These mixtures were used to estimate the parameters of the model. The calibration dataset consisted of mixtures R1, R3, R5, R6, P1, P2, P3 and P5. The four remaining mixtures, R2, R4, P4 and P6, constituted the validation dataset. They were not used for model calibration but were kept for validation.

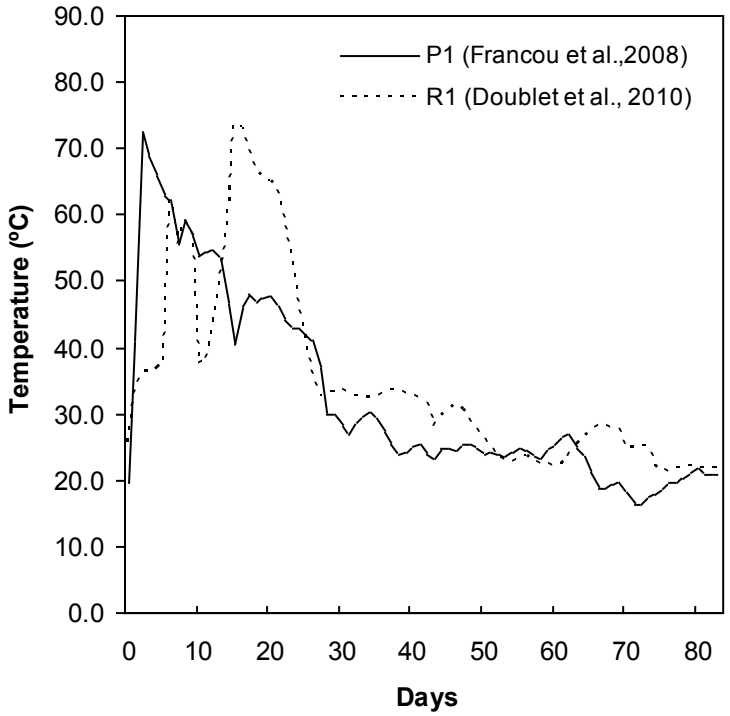


Figure 2.3: The evolution of the temperature during the composting process for P1 (Doublet, 2008) and R1 (Francou, 2003).

2.3.3.1 Calibration

The three coefficients T_{min}, T_{opt} and T_{max} were chosen on the basis of our experimental data and those in the literature. The experimental temperatures ranged from 20°C to 80°C. The reference values were determined according to Tremier et al. (2005b): T_{min} = 0°C; T_{opt} = 49.3°C and T_{max} = 82.7°C. These values were used to define Rosso's function (1993). For the Y value, 0.5 was adopted for our model. This value was

within the range of 0.4-0.6 proposed by William and Payne (1970) to describe the ratio between the carbon assimilated and mineralised by micro-organisms. The hydrolysis constants of HEM (K_3), CEL (K_4) and LIC (K_5) were estimated by fitting a first order kinetic to the median of each corresponding pool evolution (Doublet et al., 2011; Francou, 2003; Francou et al., 2008). The other six parameters (K_1, K_2, μ_{max}, m_B, Y_{H2O} and K_S) were estimated for each mixture (R1, R3, R5, R6, P1, P2, P3 and P5) by model inversion using the calibration dataset.

The total root mean squared error ($RRMSE_{tot}$) was defined as the sum of the RRMSE calculated for each compartment; i.e., H2O, SOL, HEM, CEL, LIC and the mineralised CO_2:

$$\text{RRMSE} \quad (\%) \quad = \frac{100}{\overline{O}} - \sqrt{\sum_{i=1}^{N} (S_i - O_i)^2 / N} \qquad [8]$$

Where N is the number of samples; O_i, S_i, and $\bar{O}$ correspond to the values measured and simulated by the model, and the average of the measured values. Parameter optimization was performed using the "fmincon" procedure in MATLAB, including $RRMSE_{tot}$ as the objective function.

The mean difference $\overline{D}$ and the modelling efficiency E_f were also implemented for all compartments:

$$\overline{D} = \sum_{i=1}^{N} (S_i - O_i) / N \qquad [9]$$

$$E_f = 1 - \frac{\sum_{i=1}^{N} (O_i - S_i)^2}{\sum_{i=1}^{N} (O_i - \overline{O})^2} \qquad [10]$$

2.3.3.2 Evaluation

The RRMSE of each compartment (H2O, SOL, HEM, CEL, LIC, and CO_2), $RRMSE_{tot}$, the mean difference $\overline{D}$ and the modelling efficiency EF were also used to evaluate the model. These statistics were calculated using the simulations obtained with the calibrated model (all parameters being fixed) for both the eight composting

experiments of the calibration dataset and the four remaining composting experiments of the validation dataset.

2.3.3.3 Sensitivity analysis

To assess the relative effects of individual parameters on the model performance, a sensitivity analysis was performed. The values of the unique set of parameters proposed for the calibrated model (P_0) were considered the default values around which each parameter was successively modified to ±20%. The effect of these individual changes was investigated on the cumulative flux of mineralised CO_2.

The sensitivity coefficient S to parameter P was calculated as follows:

$$\sigma_{20\%(x)} = \frac{1}{t_f}\int_0^{t_f} \frac{S(P + 20\%, P_0, t) - S(P, P_0, t)}{S(P, P_0, t)}dt \qquad [11]$$

where time t ranged from 0 to t_f; and S (P, P_0, t) denotes the simulated value of variable S at time t associated with parameter P equal to its estimated value P_0 (Bernard et al., 2001). The sensitivity of CO_2 mineralization dynamics to the biochemical characteristics of the initial mixture was studied. We supposed five different mixtures (see Fig.9): OM1 to OM5, which corresponded to organic mixtures with higher fractions of SOL, H2O, HEM, CEL and LIC, respectively. These five mixtures were considered as representative of our samples.

The model sensitivity of the initial quantity of microbial biomass to mineralisation (CO_2) behaviour was determined. Values of 0.005, 0.05, 0.5, and 5 g C/100 g initial total organic carbon (TOC) were tested using our model. These values were comparable to those reported in the review by Eiland et al. (2001), who found a range from 1.4 to 8.6 mg microbial carbon per g of organic matter (approximately 0.056 to 0.430 g C 100 g^{-1} dry mass).

2.4 Results and Discussion

2.4.1 Estimation of model parameters

The three hydrolysis rates, K_3 (for HEM), K_4 (for CEL) and K_5 (for LIC), were calculated directly from the eight composting experiments by fitting the median with

a first order kinetic (Fig.4). The simulation was close to the median kinetic but tended to underestimate the HEM at the final date. The highest rate was found for the HEM (K_3=0.0190 d^{-1}) and the lowest for the LIC (K_5=0.0001 d^{-1}). The CEL compartment had an intermediate value of K_4=0.009 d^{-1}. The hydrolysis rates were lower for the LIC and the HEM than for the CEL (see Fig.2.4), probably because the experimental data displayed large variations for the HEM and the LIC. Francou et al. (2008) found a marked increase in the LIC at days 7 and 14. The hydrolysis rate K_5 for the LIC was very low because the LIC displayed almost no decrease during the 83 days of these experiments. These values were slightly lower than those found for organic matter decomposition in soil. For example, Corbeels et al. (1999) found values of 0.02 and 0.002 d^{-1} for the HEM+CEL and the LIC, respectively.

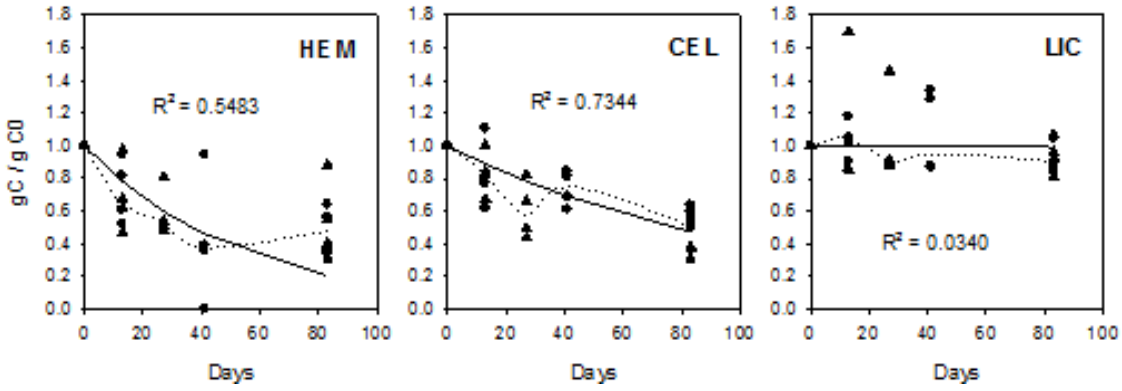


Figure 2.4: Experimental evolutions of the HEM, CEL and LIC fractions during the eight composting experiments of the calibration dataset. Symbols represent experimental values; dotted lines represent experimental medians. Solid lines represent the simulated evolutions obtained with first order kinetics, including the hydrolysis constants K_3, K_4 and K_5 for the HEM, CEL and LIC, respectively. The symbols ● represents the mixtures based on green waste (Francou, 2003; Francou et al., 2008); the symbols ▲ represents the mixtures based on sewage sludge (Doublet et al., 2011).

Table 2.2 shows the modelling efficiency (EF) for the parameter estimation using the eight mixtures of the calibration dataset (P1, P2, P3, P5, R1, R3, R5 and R6). The highest E_f was obtained for the CO_2, CEL and H2O compartments. By comparison, the LIC compartment always had negative values for the EF, which means that the

average of the experimental data was better than the model. The LIC content changed very little during composting (see Fig.6), and a small range of variation induced low E_f values. Francou et al. (2008) found an increase in the LIC values for sample R1 at days 7 and 14 probably due to compost heterogeneity. Moreover, we found that the RRMSE (%) for the LIC was no higher than for the other compartments, suggesting that the quality of the LIC simulations was similar to that of the others. The simulation of the HEM fractions produced a low E_f and a high RRMSE (%), which was indicative of poor prediction of this compartment by the model because of a high degree of variability in the experimental degradation kinetics (see Fig.2.4).

Table 2.2: Modelling Efficiency during the calibration stage using the eight data set of composting P1, P2, P3, P5, R1, R3, R5 and R6

		Pilot mixtures							
		P1	P2	P3	P5	R1	R3	R5	R6
RRMSE (%)	SOL	11	1	23	19	13	2	18	11
	HEM	33	32	36	52	40	37	19	18
	CEL	21	11	16	13	23	11	9	36
	LIC	11	15	9	12	32	14	7	5
	H2O	24	25	40	17	16	13	31	21
	CO2	31	40	4	25	37	37	14	50
	RRMSE $_{tot}$ [a]	131	125	128	139	161	114	99	142
$\overline{D}$ [b]	SOL	-0.3	0.2	1.1	-1.5	0.3	0.1	-0.2	0.0
	HEM	-2.5	-1.3	-0.1	1.7	-2.1	0.1	0.7	0.0
	CEL	2.4	-0.7	-2.5	-0.9	3.0	3.4	-2.2	9.4
	LIC	1.2	-3.0	1.3	2.5	-5.6	1.9	0.8	0.3
	H2O	-1.3	-1.3	-0.7	-0.8	-1.0	-0.1	-0.8	-0.8
	CO2	-3.1	3.5	0.1	-3.7	2.6	-8.2	-0.5	-13.7
E_f [c]	SOL	0.48	1.00	0.30	-1.12	0.80	0.99	0.34	0.84
	HEM	0.00	0.15	0.07	0.52	-22.35	-0.25	0.79	0.72
	CEL	0.39	0.76	0.54	0.45	0.68	0.88	0.81	0.30
	LIC	-0.59	-1.34	-0.29	-2.31	-1.16	-2.05	-0.21	-0.16
	H2O	0.61	-0.11	-1.09	0.79	0.85	0.95	0.86	0.86
	CO2	0.75	0.66	1.00	0.83	0.86	0.68	0.96	0.35

[a] Total mean square error of the OC module, RRMSEtot

[b] Mean difference (as a % of initial TOC)

[c] Efficiency coefficient

[d] Mean statistics of the six composting replicates

Table 2.3 shows the parameters estimated during the calibration procedure, together with their mean values and standard deviations calculated using the calibration dataset. The highest variability was obtained for K_1 (the hydrolysis rate of SOL-S), while the half-saturation parameter K_S presented the smallest variability. The mean optimised value of microbial mortality m_B was found to be 0.229 d^{-1} and was in the same range of the values found previously by Sole-Mauri et al. (2007), who calculated m_B values of 0.24 d^{-1} for fungi, 0.24 to 0.36 d^{-1} for actinomycetes and 0.48 to 0.72 d^{-1} for bacteria. An optimised growth rate (μ_{max}) of 5.99 d^{-1} was observed under our conditions, while Tremier et al. (2005b) had found values ranging from 3.12 to 8.16 d^{-1} for composting temperatures between 19.6°C and 56.9°C. The average Y_{H2O} value of 0.4096 suggested that almost 60% of the dead microbial biomass had returned to the slow degradable compartment that could be considered a "humified" pool of organic matter. For exogenous organic matters added to soil, such humification coefficients estimated in the soil had previously displayed lower values between 0.1 and 0.6 (Nicolardot et al.; 2001). The C decay rate of humified microbial debris products found in the soil model of Corbeels et al. (1999) (0.0065 d^{-1}), was in the range values of estimated K_1 of table 3 (0.0001-0.06 d^{-1}). The average hydrolysis constant for the SOL-F (K_2) of 0.0612 d^{-1} was lower than 0.25-0.8 d^{-1} found in soil by Corbeels et al. (1999) and Garnier et al. (2003). For this compartment, as for the HEM, CEL and LIC, we found that the kinetics were slower during composting than in the soil.

Using these estimated parameters, the dynamics of mixture P1, which presented a median quality of fit in the calibration dataset, was correctly simulated when compared with the observed data (Fig.2.5). The SOL fraction initially decreased as a result of the decomposition of the initial soluble degradable fraction, which corresponded to the most labile part of the organic matter (SOL-F) and therefore the most likely to mineralise (Cook and Allan, 1992). This first phase was followed by a rise in SOL values, driven by the formation of a soluble, slowly degradable fraction (SOL-S), which was fed by the dead microbial biomass. The SOL was correctly simulated despite a low E_f of 0.48 (Table 2.3) because of its limited changes during composting. These results confirmed that both graphics and statistics are necessary to evaluate a model. The amount of CO_2 was not satisfactorily simulated at day 14. The

underestimation of total CO_2 mineralised at day 14 may have resulted from a simulated growth of micro-organisms that was too slow, but no data were available to validate the evolutions affecting the microbial compartment.

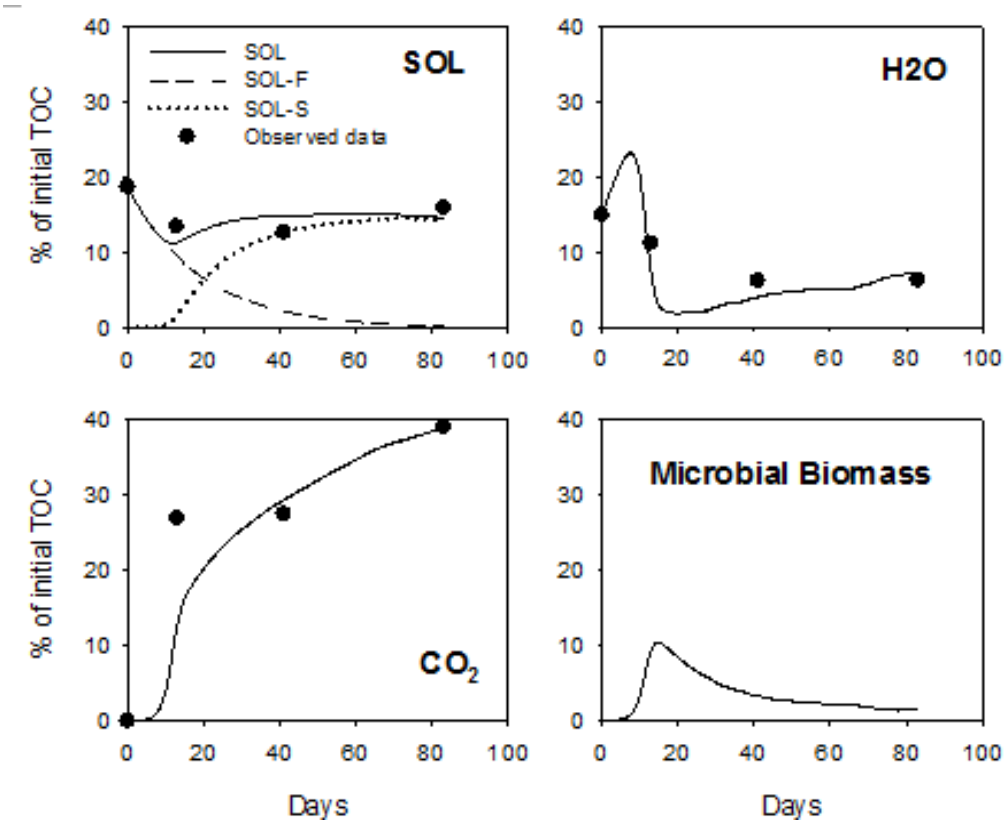


Figure 2.5: Example of the experimental (points) and simulated (lines) evolutions of the SOL and H2O fractions, and the CO_2 and microbial biomass during composting obtained with the calibration procedure of the model (seven parameters being fixed and six optimised for each composting experiment). In this case, the P1 mixture displayed a median quality of fitting to the calibration dataset. Regarding SOL, the heavy black curve represents the total SOL fraction composed of SOL-S and SOL-F.

2.4.2 Evaluation of calibrated model

For this step, the eight composting mixtures used for the model calibration were again simulated using mean parameter values (highlighted in Table 2.3). The statistics on the modelling efficiency of the simulations obtained with the calibrated model are shown in Table 2.4 for the calibration dataset: The E_f values were lower than in Table 2.3, and RRMSE (%) values were higher, indicating a degraded prediction by the model in this second step. The use of a unique set of parameters mainly affected the

SOL and H2O compartments, which displayed much lower E_f and higher RRMSE values in Table 4 than in Table 3 (particularly for P2, P3, P5, R3). The P1, P2, P3 and P4 mixtures, which contained digested sewage sludge, exhibited a negative $\overline{D}$ for the SOL data, indicating that the model underestimated this fraction. We made the assumption that the SOL-S was equal to zero in the initial mixture of wastes, although some recalcitrant compounds may have been present at the beginning of the composting of mixtures containing digested sewage sludge (Dignac et al., 2000). Accounting for this could have improved the quality of the SOL simulations, but we were not able to quantify this fraction with the available experimental data, and more research is required to access its chemical quality. The R6 sample was poorly simulated, with a very high for the CEL. This underestimation of the CEL degradability also led to a poor simulation of CO_2.

Table 2.3: Parameter values taken from the literature, estimated with the calibration procedure and used in the calibrated model. The parameter values used in the calibrated model are highlighted.

Mixtures	Parameters												
	K_1[a]	K_2[a]	mB[a]	μmax[a]	Ks[a]	Y_{H2O}[a]	Tmin[b]	Topt[b]	Tmax[b]	Y[b]	K_3[c]	K_4[c]	K_5[c]
	d^{-1}				g C		°C				d^{-1}		
P1	0.0083	0.0521	0.1272	4.1136	101.21	0.3824	0	49.3	82.7	0.5	0.019	0.009	0.0001
P2	0.0036	0.0592	0.1950	4.7193	100.95	0.4562	-	-	-	-	-	-	-
P3	0.0001	0.0528	0.6267	7.6466	94.55	0.4773	-	-	-	-	-	-	-
P5	0.0025	0.0499	0.1628	4.8981	101.43	0.3941	-	-	-	-	-	-	-
R1	0.0207	0.0651	0.2324	4.2149	101.27	0.4330	-	-	-	-	-	-	-
R3	0.0600	0.0555	0.1816	7.2344	112.99	0.4087	-	-	-	-	-	-	-
R5	0.0092	0.0749	0.2011	10.0000	94.34	0.1349	-	-	-	-	-	-	-
R6	0.0390	0.0710	0.1051	5.1398	101.80	0.3153	-	-	-	-	-	-	-
Mean[d]	**0.0179**	**0.0612**	**0.2290**	**5.9958**	**101.07**	**0.4096**	**0**	**49.3**	**82.7**	**0.5**	**0.019**	**0.009**	**0.0001**
sd	*0.0212*	*0.0093*	*0.1658*	*2.0899*	*5.7396*	*0.1090*							

[a]Parameters estimated using the calibration procedure of the model

[b]Parameters taken directly from the literature

[c]Parameters estimated by fitting the median of the experimental data with first order kinetics

[d]Mean of parameters used in the calibration procedure calculated from the eight composting experiments of the calibration dataset

Table 2.4: Statistics to evaluate the calibrated model. The eight composting experiments (P1, P2, P3, P5, R1, R3, R5 and R6) of the calibration dataset were used.

		Pilot mixtures							
		P1	P2	P3	P5	R1	R3	R5	R6
RRMSE (%)	SOL	19	21	41	33	28	65	31	30
	HEM	33	32	36	52	40	37	19	18
	CEL	21	11	16	13	23	11	9	36
	LIC	11	15	9	12	32	14	7	5
	H2O	48	43	57	28	38	24	53	51
	CO2	24	59	78	20	49	47	18	55
	$RRMSE_{tot}$ [a]	156	181	237	158	210	198	137	195
$\overline{D}$ [b]	SOL	-1.2	-1.7	-3.5	-5.0	1.4	2.3	-1.2	1.9
	HEM	-2.5	-1.3	-0.1	1.7	-2.1	0.1	0.7	0.0
	CEL	2.4	-0.7	-2.5	-0.9	3.0	3.4	-2.2	9.4
	LIC	1.2	-3.0	1.3	2.5	-5.6	1.9	0.8	0.3
	H2O	-1.3	-2.3	-5.1	-0.3	-3.6	1.1	1.4	1.4
	CO2	-1.1	6.5	7.6	-0.4	4.4	-10.9	-2.0	-15.6
E_f [c]	SOL	-0.44	-0.20	-1.28	-5.27	0.02	-9.36	-0.85	-0.21
	HEM	0.00	0.15	0.07	0.52	-22.35	-0.25	0.79	0.72
	CEL	0.39	0.76	0.54	0.45	0.68	0.88	0.81	0.30
	LIC	-0.59	-1.34	-0.29	-2.31	-1.16	-2.05	-0.21	-0.16
	H2O	-0.60	-2.39	-3.22	0.42	0.15	0.84	0.59	0.19
	CO2	0.85	0.29	-0.55	0.89	0.76	0.50	0.93	0.22

[a] Total mean square error of the OC module, RRMSE-OCtot

[b] Mean difference (as a % of initial TOC)

[c] Efficiency coefficient

[d] Mean statistics of the six composting replicates

After the first test based on the results of the eight mixtures used for model calibration, the four other mixtures in the validation dataset (R2, R4, P4 and P6) were used to complete the model evaluation. The statistics on the modelling efficiency of the simulations obtained with the calibrated model on the validation dataset are shown in Table 2.5. The highest E_f value was found for CO2, and the lowest E_f value was found for the LIC and the SOL; these results are consistent with the calibration dataset in Table 2.4. The low E_f value for the LIC could still be explained by the minor changes affecting this fraction during composting. The R2 sample was not well simulated and produced the highest RRMSE and a low E_f. This result was mainly due to a poor prediction of the CEL, which was markedly overestimated during composting, leading to an underestimation of CO2 (see the $\overline{D}$ of R2 in Table 2.5) similar to the R6

mixture of the calibration dataset (Table 2.4). Doublet et al. (2011) and Eklind and Kirchmann (2000) also found that the degradation rate of the CEL and the HEM varied according to the substrate origin because of the different bonds between the cellulosic and lignin compartments. Bertrand et al. (2006) found that the cellulose from crop residues containing a similar amount of lignin decomposed at different rates in soil because of differing lignin qualities (condensed or uncondensed-like lignins). Corbeels et al. (1999) introduced a retardation coefficient for the degradation rates of the CEL and the HEM calculated from the value of the LIC fraction. A similar retardation factor could be included in our model to describe the bioaccessibility of the CEL and the HEM depending on the quality of the LIC.

Table 2.5: Statistics to evaluate the model. The four independent composting experiments P4, P6, R2 and R4 of the validation dataset were used.

		Pilot mixtures			
		P4	P6	R2	R4
RRMSE [a] (%)	SOL	49	36	27	45
	HEM	46	11	21	32
	CEL	14	15	55	9
	LIC	21	6	14	14
	H2O	27	34	23	27
	CO_2	25	25	59	26
	$RRMSE_{tot}$ [d]	182	127	199	153
$\overline{D}$ [b]	SOL	-1.7	-0.4	1.2	2.0
	HEM	-3.5	0.4	-0.1	-0.8
	CEL	0.5	-2.1	13.0	-3.3
	LIC	3.8	1.0	1.3	-0.8
	H2O	0.0	-1.3	-0.7	0.7
	CO_2	-1.3	0.0	-16.8	-0.1
EF [c]	SOL	0.05	0.05	-1.11	-1.84
	HEM	-1.89	0.96	0.60	-0.87
	CEL	0.70	0.41	0.15	0.74
	LIC	-1.39	-1.22	-0.36	-0.20
	H2O	-0.30	-0.26	0.67	0.30
	CO_2	0.83	0.83	0.20	0.86

[a] Relative root mean square error (RRMSE)

[b] Mean difference (in % of initial TOC)

[c] Efficiency coefficient

[d] Total RRMSE of the model, $RRMSE_{tot}$

Figure 2.6 shows an example of model validation using R4, which presented a median quality of fittings among the validation dataset. In this figure, the dynamics of the different compartments were correctly simulated for the different organic fractions, although the E_f values were low for the SOL, HEM, LIC and H2O (Table 2.5).

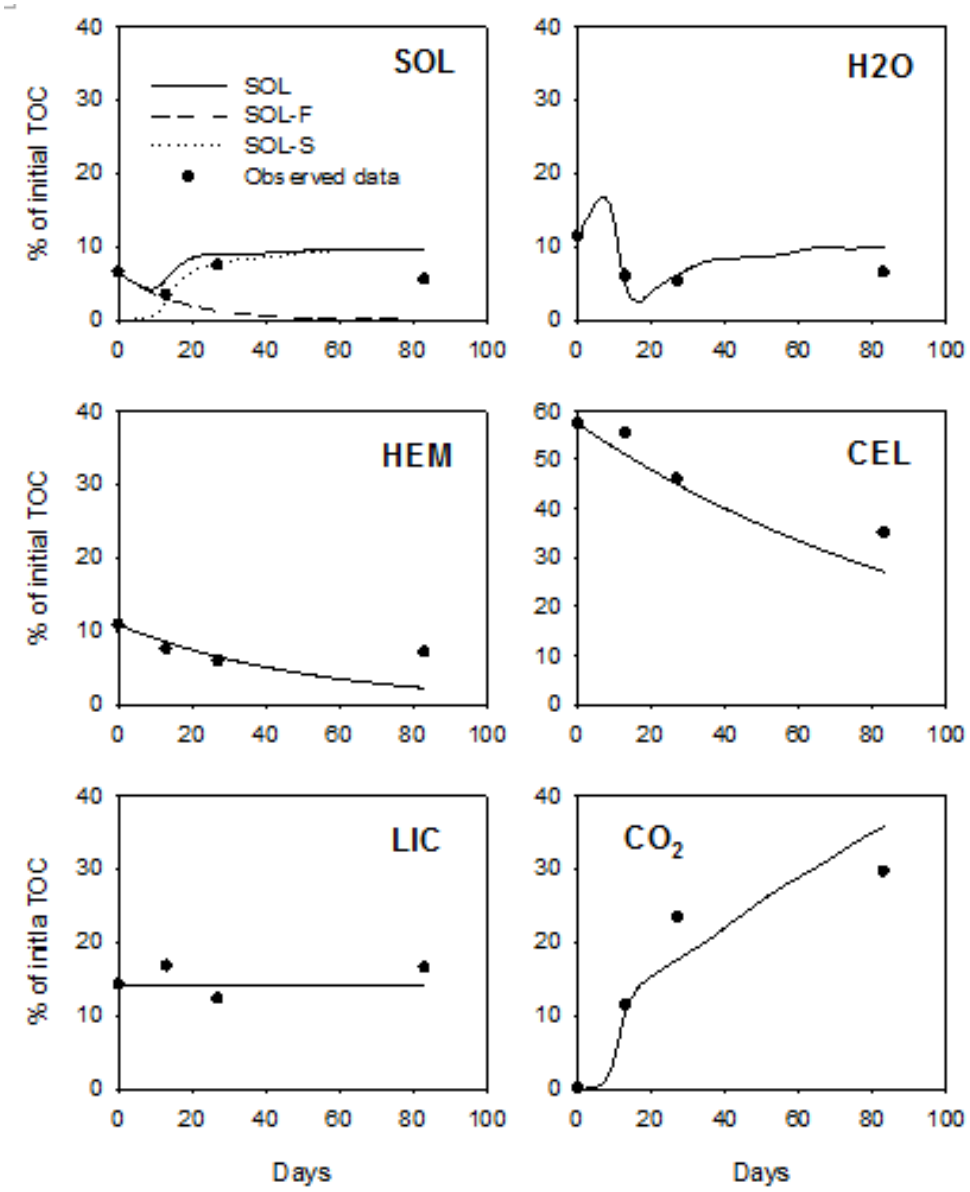


Figure 2.6: Example of the experimental (points) and simulated (lines) evolutions of the biochemical fractions and CO_2 during composting and obtained using the calibrated model (all parameters being fixed and described in Table 2.3; for the six parameters previously optimised, the mean of the optimised values was taken). In this case, the R4 mixture displayed a median quality of fitting to the validation dataset.

Figure 2.7 compares the simulated and measured final compositions of the four composts and their initial compositions. For each of these composts, the final HEM fraction was always very small when the CEL remained quite large and when the LIC changed very slightly. The model was able to correctly predict the final composts of P4, P6 and R4, but not R2. This compost, made up mainly of paper-cardboard and green waste, displayed a higher degradation of the CEL than that found in P4 or P6, which were made from sludge, screening refuse and branches.

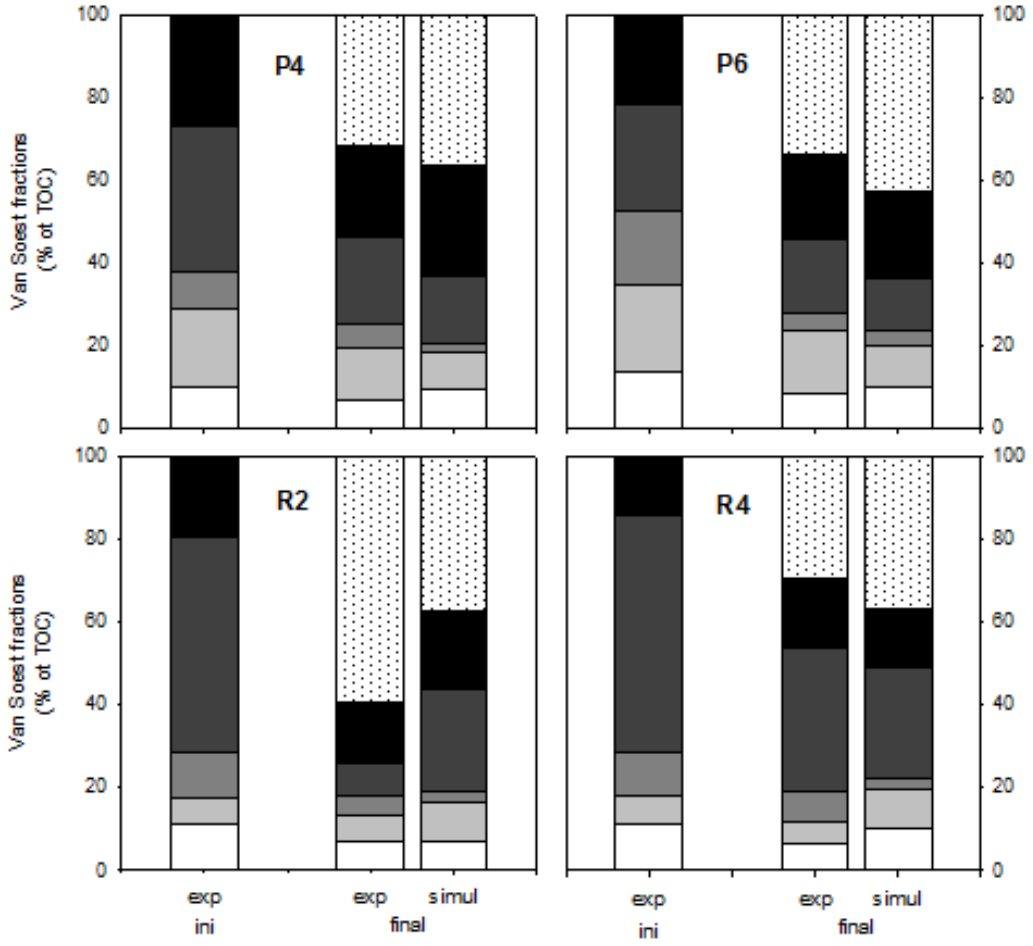


Figure 2.7: Comparison of observed and simulated, initial and final, biochemical composition of the composting experiments in the validation dataset. “exp_ini” expresses initial observed data of Van Soest fractions (% of TOM); “exp_final” expresses final observed data of Van Soest fractions; “simul_final” expresses final simulated data of Van Soest fractions.

2.4.3 Sensitivity analysis

Sensitivity analyses were performed on the ten input parameters ($K_{i=1-5}$, Y, m_B, μ_{max}, K_S and Y_{H2O}) of the model and tested against the mineralized carbon curves (from R5). Figure 2.8 shows that the evolution of CO_2 was more sensitive to the parameters linked to microbial functioning, such as the assimilation rate (Y), specific maximum microbial growth rate (μ_{max}), saturation constant (Ks) and death rate (m), than to the kinetic parameters attached to the biochemical fractions. The degradation rate of the CEL had more impact than the others because the CEL is always a large compartment (see Fig.2.2). This result could explain the discrepancy between the simulation and experimental data for CO_2 in R4 (Fig.2.6) and R6 (Table 2.4), which may have been due to a poor estimation of K4 (degradation rate of CEL) in this compost.

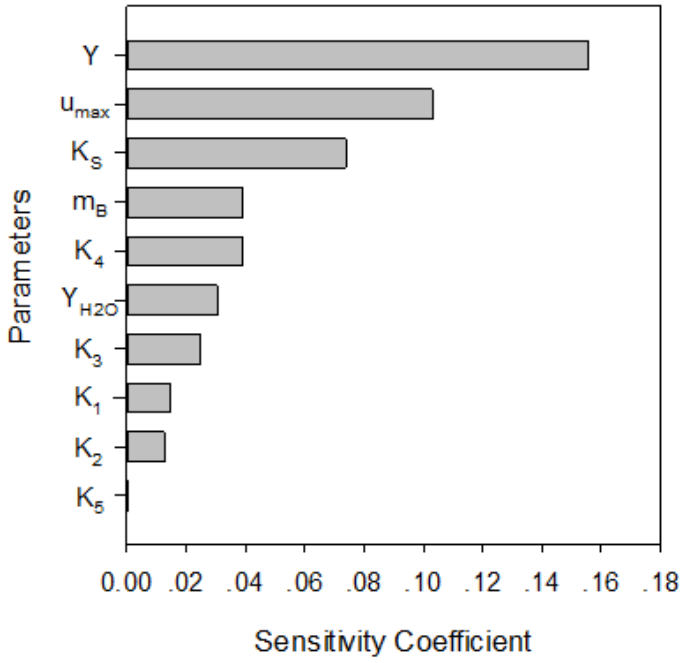


Figure 2.8: Analysis of model sensitivity to the CO_2 fraction for 10 model parameters (Y, u_{max}, K_S, m_B, K_3, Y_{H2O}, K_2, K_1, K_5, K_4).

A sensitivity analysis of our model to the initial quality of the OC (relative fraction of each biochemical component) was also performed using different realistic qualities of organic feedstocks (shown in Fig.2.9). The microbial biomass displayed different growth dynamics which led to different evolutions of CO_2 emission. At day 83, the maximum difference between the CO_2 emissions of 10% was quite small, suggesting that the model was not very sensitive to the biochemical composition of the initial

mixtures. The OM5 mixture with the largest LIC fraction led to the lowest CO_2 emissions, and the OM2 with the largest SOL fraction produced the largest amounts of CO_2. The experimental data exhibited a higher sensitivity of CO_2 emission to initial mixtures, with a maximum difference of 35% between samples at day 83. The use of a unique set of parameters in the model could explain the loss of sensitivity to the initial mixtures.

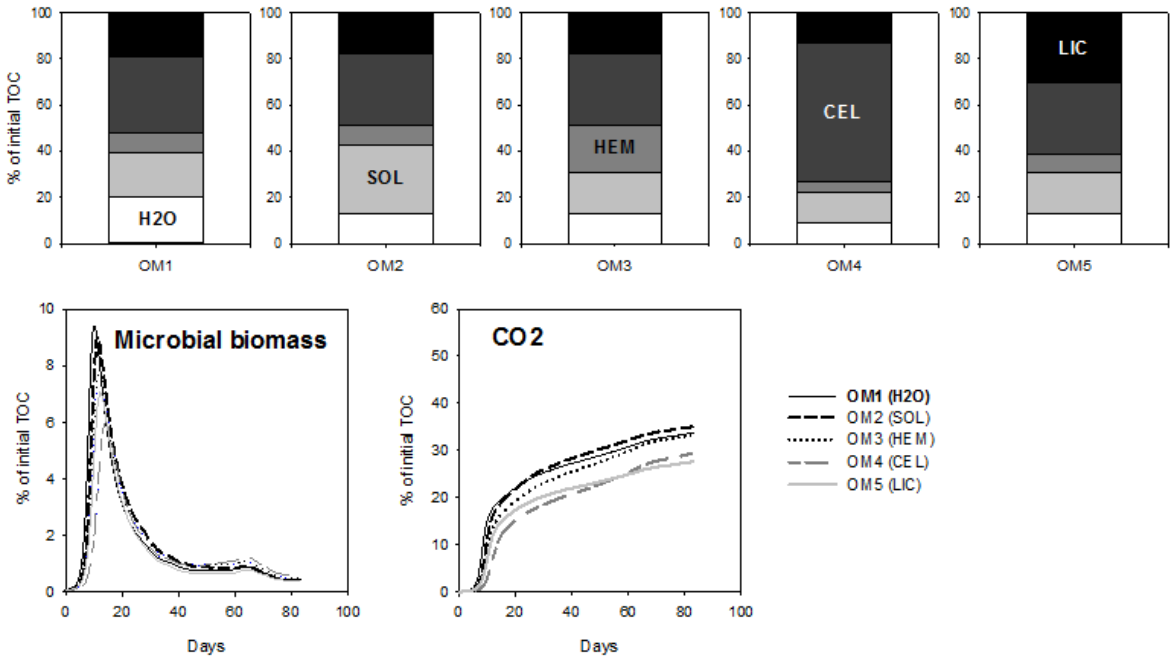


Figure 2.9: Model sensitivity to the biochemical composition of the initial organic mixture (OM). We took a standard sample containing 15, 20, 10, 35 and 20% of H2O, SOL, HEM, CEL and LIC, respectively. From this standard sample, we calculated a new sample with the highest fraction of each compartment. All the other compartments were decreased proportionally. OM1, OM2, OM3, OM4, OM5 contained the highest proportion of H2O, SOL, HEM, CEL and LIC, respectively. Figures show the initial biochemical compositions of the OM, the evolution of the microbial biomass and the evolution of carbon mineralisation.

The sensitivity to the initial microbial biomass quantity, shown in Fig.2.10, indicated that the influence of the initial biomass quantity on mineralisation was only observed at the beginning of composting. The CO_2 emission rate increased with an increase in the initial microbial biomass. After day 18, all the curves merged. This result may explain the underestimation of experimental CO_2 observed by the model at day 14 in P1 (see Fig.2.5).

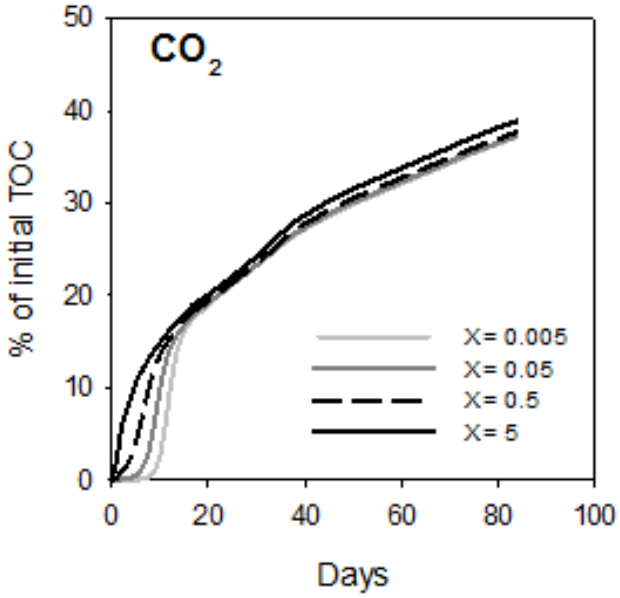


Figure 2.10: The effects of the initial quantity of microbial biomass on the evolution of C mineralisation. Initial values of 0.005, 0.05, 0.5 and 5 (% of initial TOC) were tested for microbial biomass.

2.5 Conclusion

The novelty of our approach was to propose a simulation of the organic matter quality based on its biochemical fractions and to calibrate this model using measurable pools. We assumed that each simulated biochemical fraction was characterized by a unique and specific degradation rate, whatever the organic waste mixture. From 12 composting experiments performed under similar experimental conditions and varying in terms of the initial organic matter characteristics, we were able to obtain a unique set of parameters that could simulate the evolution of organic matter characteristics during experimental composting. The evolutions over time of the different fractions were correctly simulated, except for some compost. The final characteristics were not always well predicted. In some cases, when the model failed,

the cellulose displayed different degradation kinetics. This result suggests that the degradation rate of cellulose is not an intrinsic property but that it should be expressed by accounting for its accessibility in the materials. In some other cases, the soluble fraction was not well simulated because its initial chemical characteristics could not be assessed. Further research is required to clarify these two important points. By improving the modelling of these two compartments, it should be possible to improve the model's sensitivity to the initial quality of the OM.

In this study, we focused only on simulating organic matter decomposition, and we imposed the temperatures. In the future, our biological model needs to be included in existing composting models so that evolutions in temperature, water and oxygen, as well as their feedback on organic matter degradation, can be simulated at the same time.

2.6 Acknowledgements

We would like to thank Dr. C. Francou from Veolia Environment, Research and Development, for allowing us to use his data and for supplying additional information. We also thank M. Le Villo-Poitrenaud, from Veolia, for her constructive contribution to this manuscript.

2.7 References

AFNOR, 1999. Norme française NF ISO 10694. Qualité du sol - Dosage du carbone organique et du carbone total après combustion sèche (analyse élémentaire). AFNOR, Paris, France.

AFNOR. 2009. Norme française NFU 44-162. Amendements organiques et supports de culture – Fractionnements biochimiques et estimation de la stabilité biologique. AFNOR, Paris, France. Bernal, MP., Sanchez-Monedero, MA., Paredes, C., Roig, A., 1998. Carbon mineralization from organic wastes at different composting stages during their incubation with soil. Agriculture Ecosystems & Environment 69, 175-189.

Bailey, J., Ollis, D., 1986. Biochemical Engineering Fundamentals. McGraw-Hill Book Co, Singapore.

Batstone, D.J., Keller, J., Angelidaki, I., Kalyuzhnyi, S.V., Pavlostathis, S.G., Rozzi, A., Sanders,

Bernard, O., Zakaria, H.S., Dochain, D., Genovesi, A., Steyer, J.P., 2001. Dynamical model developpement and parameter identification for an anaerobic wastewater treatment process. Biotechnology and Bioengineering 75, 424-438.

Bertrand, I., Chabbert, B., Kurek, B., Recous, S., 2006. Can the biochemical features and histology of wheat residues explain their decomposition in soil? Plant and Soil 281, 291-307.

Cook, B.D., Allan, D.L., 1992. Dissolved organic matter in old field soils: total amounts as a measure of available resources for soil mineralization. Soil Biology and Biochemistry 24, 585-594. Corbeels, M., Hofman, G., Van Cleemput, O., 1999. Simulation of net N immobilisation and mineralisation in substrate-amended soils by the NCSOIL computer model. Biology and Fertility of Soils 28, 422-430.

Corbeels, M., Hofman, G., 1999. Van Cleemput O. Simulation of net N immobilisation and mineralisation in substrate-amended soils by the NCSOIL computer model. Biology and fertility of Soils 28, 422-430.

Dignac, M.F., Ginestet, P., Rybacki, D., Bruchet, A., Urbain, V., Scribe, P., 2000. Fate of wastewater organic pollution during activated sludge treatment: Nature of residual organic matter. Water Research 34, 4185-4194.

Doublet, J., 2008. Influence du co-substrat carboné sur la nature des matières organiques et les formes d‟azote des composts de boue ; conséquences sur la disponibilité de cet azote. Thesis of doctorat AgroParisTech, Paris, France. 280p.

Doublet, J., Francou, C., Poitrenaud, M., Houot, S., 2011. Influence of bulking agents on organic matter evolution during sewage sludge composting; consequences on compost organic matter stability and N availability. Bioresource Technology 102, 1298-1307.

Eiland, F., Klamer, M., Lind, A.M., Leth, M., Baath, E., 2001. Influence of initial C/N Ratio on chemical and microbial composition during long term composting of straw. Microbial Ecology 41, 272–280.

Eklind, Y., Kirchmann, H., 2000. Composting and storage of organic household waste with different litter amendments. I: carbon turnover. Bioresource technology 74, 115-124.

Francou, C., 2003. Stabilisation de la matière organique au cours du compostage de déchets urbains: Influence de la nature des déchets et du procédé de compostage – Recherche d‟indicateurs pertinents. Thesis of doctorat INA P-G, 388p.

Francou, C., Linères, M., Derenne, S., Le Villio-Poitrenaud, M., Houot, S., 2008. Influence of green waste, biowaste and paper-cardboard initial ratios on organic matter transformations during composting. Bioresource Technology 99, 8926-8934.

Garnier, P., Néel, C., Aita, C., Recous, S., Lafolie, F., Mary, B., 2003. Modelling carbon and nitrogen dynamics in soil with and without straw incorporation. European Journal of Soil Science 54, 555–568.

Henriksen, T.M., Breland, T.A., 1999. Evaluation of criteria for describing crop residue degradability in a model of carbon and nitrogen turnover in soil. Soil Biology & Biochemistry. 31, 1135-1149.

Kaiser, J., 1996. Modelling composting as a microbial ecosystem: A simulation approach. Ecological Modelling 91, 25-37.

Lichtfouse, E., Chenu, C., Baudin, F., Leblond, C., Da Silva, M., Behar, F., Derenne, S., Largeau, C., Wehrung, P., and Albrecht, P., 1998. A novel pathway of soil organic matter formation by selective preservation of resistant straight-chain biopolymers: chemical and isotope evidence. Organic Geochemistry 28, 411-415.

Lin, YP., Huang, GH., Lu, HW., He, L., 2008. Modeling of substrate degradation and oxygen consumption in waste composting processes. Waste Management 28, 1375-1385.

Mason, I.G., 2006. Mathematical modelling of the composting process: A review. Waste Management 26, 3-21.

Nicolardot, B., Recous, S., Mary, B., 2001. Simulation of C and N mineralisation during crop residue decomposition: A simple dynamic model based on the C:N ratio of the residues. Plant & Soil 228, 83-103.

Pascual, J.A., Garcia, C., Hernandez, T., 1999. Comparison of fresh and composted organic waste in their efficacy for the improvement of arid soil quality. Bioresource Technology 68, 255-264.

Payne, W.J., 1970. Energy yields and growth of heterotrophs. Annual Review of Microbiology 24, 17-52.

Peltre, C., Dignac, M.F., Derenne, S., Houot, S., 2010. Change of the chemical composition and biodegradability of the Van Soest soluble fraction during composting: a study using a novel extraction method. Waste Management 30, 2448–2460.

Petersen, E.E., 1965. Chemical reaction analysis. Prentice-Hall, Englewood Cliffs, NJ.

Rosso, L., Lobry, J.R., Flandrois, J.P., 1993. An unexpected correlation between cardinal temperatures of microbial growth highlighted by a new model. Journal of Theorical Biology 162, 447-463.

Sole-Mauri, F., Illa, J., Magry, A., Prenafeta-Boldu, F.X., Flotats, X., 2007. An integrated biochemical and physical model for the composting process. Bioresource Technology 98, 3278–3293.

Tremier, A., de Guardia, A., Massiani, C., Paul, E., Martel, J.L., 2005 a. A respirometric method for characterising the organic composition and biodegradation kinetics and the temperature influence on the biodegradation kinetics, for a mixture of sludge and bulking agent to be co-composted. Bioresource Technology 96, 169–180.

Tremier, A., De Guardia, A., Martel, J.L., 2005 b. Evaluating the biodegradability of an organic waste thanks to a respirometric characterization. 1st International conference on engineering for waste treatment, beneficial waste and by-products, Albi, 17-19 May 2005.

Vlyssides, A., Mai, S., Barampouti, EM., 2009. Source: An integrated mathematical model for co-composting of agricultural solid wastes with industrial wastewater. Bioresource Technology 100, 4797-4806.

Van Soest, P. J., Wine, R.H., 1967. Use of detergents in the analysis of fibrous feeds. IV. Determination of permanganate. Journal of A. O. A. C., 50, 1:50-55.

W.T.M., Siegrist, H., Vavilin, V.A., 2002. The IWA Anaerobic Digestion Model N°1 (ADM1). Water Science and Technology 45, 65-73.

CHAPTER 3: A MODEL COUPLING ORGANIC CARBON AND ORGANIC POLLUTANT DYNAMICS DURING COMPOSTING

G. Lashermes[1], Y. Zhang[1,3], S. Houot[1], E. Barriuso[1], J.P. Steyer[2], D. Patureau[2], P. Garnier[1,*]

1 - INRA (French National Institute for Agricultural Research)–AgroParisTech, UMR1091, Environment and Arable Corps, 78850 Thiverval-Grignon, France.

2 - INRA, UR50, *Laboratoire de Biotechnologie de l'Environnement* , Avenue des Etangs, 11100 Narbonne, France.

***Corresponding author:** INRA-AgroParisTech, UMR1091 Environnement et Grandes Cultures, 78850 Thiverval-Grignon, France. Tel: +33 1 30 81 53 14; Fax: +33 1 30 81 53 96.

E-mail address: pgarnier@grignon.inra.fr (Patricia Garnier)

Submitted by **Journal of Environmental Quality, 2011**

3.1 Abstract

The new COP-Compost model has been developed to simulate the evolution of organic pollutants (OP) availability during composting in interaction with organic matter. It comprises one module for the evolution of organic carbon (OC) and one module for the dynamics of OP. The OC module simulates OC degradation based on the biochemical composition of the initial waste mixture. The OP module simulates OP mineralization and its speciation. The OC module was first calibrated and evaluated using experimental data from the literature obtained using 170-L pilots. The coupled OC-OPs model was evaluated from composting experiments performed in 4-L pilots using either ^{14}C-labeled fluoranthene, 4-n-nonylphenol, linear alkylbenzene sulfonate or glyphosate. The distribution of organic pollutants between soluble, sorbed and non-extractable fractions was measured by extraction procedures. We propose a calibration of the model and have demonstrated that coupling the OC and OP modules can improves the simulation of OP speciation during composting.

3.2 Introduction

There has been a considerable Europe-wide increase in recent years in the treatment of organic waste by composting (European Communities, 2005). However, composts may contain organic pollutants (OPs) (Brändli et al., 2005). Characterization of their content and their availability in the final composts are of paramount importance to estimating the environmental impact of recycling practices on agricultural soils (Bright and Healey, 2003).

Organic pollutants can be either degraded through the microbial activity that occurs during composting or be stabilized through the formation of associations with waste organic matter. The level of OP degradation reached during composting depends on both OP degradability related to its chemical structure, and structural and functional microbial diversity. The characteristics of waste organic matter and its degradability influence the growth of microbial populations which may develop contrasting abilities to degrade OPs (Haderlein et al., 2006). Organic pollutant degradation seems mainly to be achieved by microorganisms through co-metabolism (Barker et al., 2002; Kocamemi and Çeçen, 2009). In parallel, OP stabilization during composting starts via the sorption process and can become irreversible, resulting in the formation of non-extractable (bound) residues (NER) (Barriuso et al., 2008). The OP will be more or less available, depending on its extractability in water (freely available) or another solvent (potentially available), the NER being considered as unavailable (Gevao et al., 2000). The sorption of OPs depends on their chemical/structural properties (Sabljić et al., 1995) and on the characteristics of the organic matter in terms of polarity (Xing et al., 1994) and aromaticity (Benoit et al., 2008).

Thus, the sorption of OPs on organic matter may reduce their availability to compost microflora and potentially limit their biodegradation (Wauchope et al., 2002). On the other hand, the formation of NER has been found to be influenced by both the degree of the sorption phenomenon (Kästner et al., 1999) and total microbial activity (Benoit and Barriuso, 1997). Composting is therefore a complex environment in which the processes of sorption, biodegradation and NER formation interact and condition OP behavior. Tools such as mathematical models can help to formalize generic hypotheses concerning the evolution of organic matter and the simultaneous transformations of OPs during composting.

To our knowledge, no model describing both the evolution of organic matter and OP behaviour during composting has been reported in the literature. Most composting models have been based on the heat and mass balance (Mason, 2006). Few models have described the transformation of organic matter during composting (Kaiser, 1996; Sole-Mauri et al., 2007). These models simulate both changes to the biochemical properties of organic matter and to successive microbial populations during composting. No models simulating OP behavior during composting are available in the literature, but models have been proposed to describe the sorption-desorption and biodegradation of OPs in soil (Shelton and Doherty, 1997; Saffih-Hdadi et al., 2003).

The aim of this work was to propose a new model called COP-Compost (simulation of Carbon of organic matter and Organic Pollutant evolutions during Composting). This model comprises two modules: one describing evolutions in organic carbon (OC) and the other OP behavior. The second objective was to calibrate and evaluate the OC module using data from the literature (Doublet, 2008; Francou et al., 2008; Lashermes et al., 2010) and then to calibrate the OP module for four OPs: a polycyclic aromatic hydrocarbon (fluoranthene), two surfactants (4-n-nonylphenol – NP, and a linear alkylbenzene sulfonate – LAS) and a herbicide (glyphosate). This last calibration was performed using data from composting experiments performed with ^{14}C-labeled OP.

3.3 Description of the COP_Compost model

The two modules (OC and OP) of the COP-Compost model can be used separately or coupled (Fig.3.1, Table 3.1). The model has been programmed in Matlab® language (The Mathwork, USA). All equations in the two modules are described in Appendix 1.

3.3.1 Organic C module

Briefly, OC is divided into five pools ($C_{i,\ i=1-5}$) with decreasing degradability. Following first order kinetics with specific hydrolysis constants, these organic pools were hydrolyzed into one organic pool, CS, defined as the substrate available for microbial growth. These five pools could be determined using the Van Soest fractionation method (AFNOR, 2005): OC soluble in neutral detergent (SOL) and the hemicellulose-like (HEM), the cellulose-like (CEL) and lignin-like (LIC) fractions. The SOL fraction was further divided into two pools with fast (SOL-F) and slow

(SOL-S) degradability (Francou et al., 2008). The available substrate (C_S) was defined as being the hot water soluble fraction of total OC (H2O). Microbial biomass growth and its assimilation of the available substrate were modeled using Monod kinetics, modulated by the temperature growth-limiting function proposed by Rosso et al. (1993). The microbial biomass gradually died off, and the dead cells were recycled into either the SOL-S pool (characterized by a slow hydrolysis rate) or the H2O pool of available substrate.

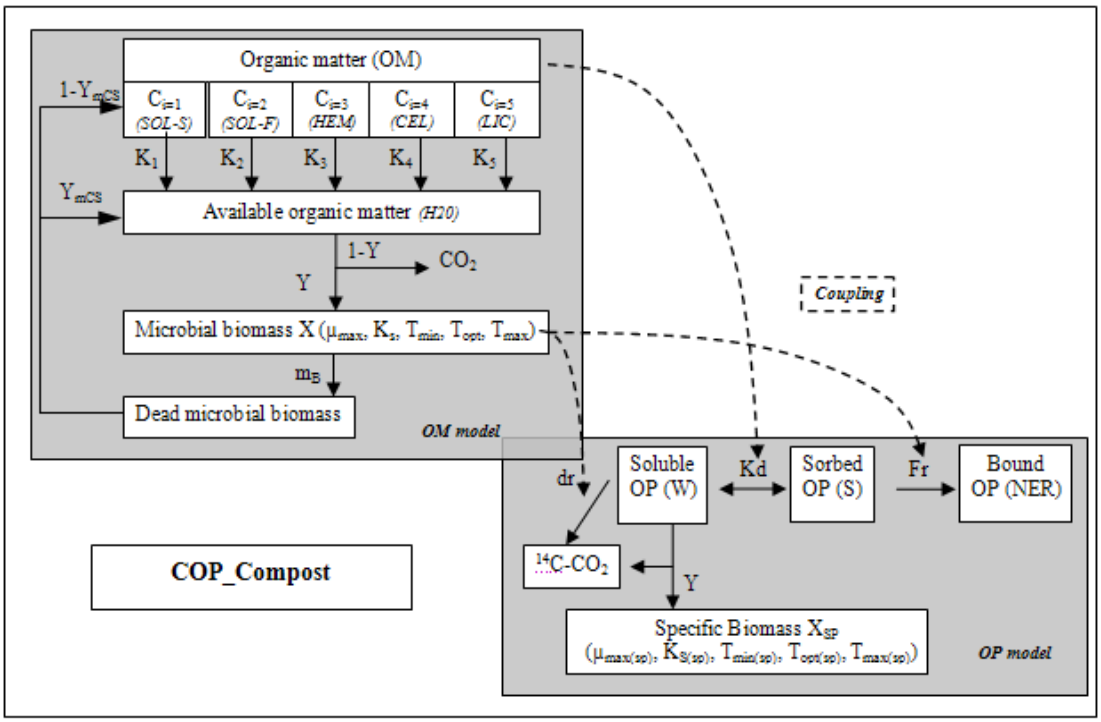


Figure 3.1: Schematic representation of the COP-Compost model. The total OC is divided into six pools based on biochemical fractionation. Parameters and variables are described in Table 3.1.

Table 3.1: Variables and parameters in the COP-Compost model

	Symbol	Description	Value proposed*	Unit
Variables of the model				
OM model	C_{i-1}	Proportion of OM in the SOL fraction with slow degradation (SOL-S)		% of initial TOC
	C_{i-2}	Proportion of OM in the SOL fraction with fast degradation (SOL-F)		% of initial TOC
	C_{i-3}	Hemicellulose (HEM)		% of initial TOC
	C_{i-4}	Cellulose (CEL)		% of initial TOC
	C_{i-5}	Lignin (LIC)		% of initial TOC
	C_s	OM soluble in hot water (H20)		% of initial TOC
	X	Microbial biomass		% of initial TOC
	CO_2	Carbon dioxide gas		% of initial TOC
OP model	W	soluble OP in which is water extractable		% of initial ^{14}C
	S	Sorbed OP which is solvent extractable		% of initial ^{14}C
	NER	Bound residues non extractible		% of initial ^{14}C
	^{14}C-CO_2	^{14}C-labeled carbon dioxide gas		% of initial ^{14}C
Parameters of the model				
OM model	K_1	Rate of transformation in available C_{i-1} (SOL-S)	0.018	day^{-1}
	K_2	Rate of transformation in available C_{i-2} (SOL-F)	0.061	day^{-1}
	K_3	Rate of transformation in available C_{i-3} (HEM)	0.019	day^{-1}
	K_4	Rate of transformation in available C_{i-4} (CEL)	0.009	day^{-1}
	K_5	Rate of transformation in available C_{i-5} (LIC)	0.001	day^{-1}
	Y	Assimilation rate of the available OM for X	0.5	
	μ_{max}	Maximal specific growth rate for microbial biomass	5.996	day^{-1}
	K_s	Saturation constant for Monod kinetic	101.1	% of initial TOC
	T_{min}	Minimum temperature for microbial growth	0	°C
	T_{max}	Maximum temperature for microbial growth	49	°C
	T_{opt}	Optimum temperature for microbial gorwth	83	°C
	m_B	Death constant for microbial biomass	0.2290	day^{-1}
	Y_{mort}	Availability rate for dead microbial biomass	0.4	
OP model	Kd	Adsorption coefficient of OM		g C ads g^{-1} C sol
	Kd_1	Adsorption coefficient of C_{i-1} (SOL-S)		g C ads g^{-1} C sol
	Kd_2	Adsorption coefficient of C_{i-2} (HEM)		g C ads g^{-1} C sol
	Kd_3	Adsorption coefficient of C_{i-3} (CEL)		g C ads g^{-1} C sol
	Kd_4	Adsorption coefficient of C_{i-4} (LIC)		g C ads g^{-1} C sol
	Fr_B	NER formation rate related to biological activity		day^{-1}
	Fr_C	NER formation rate related to chemical reactivity of the compost organic matter		day^{-1}
	dr	OP degradation rate		day^{-1}

3.3.2 Organic pollutant module

The model proposed by Saffih-Hdadi et al. (2003) to describe pesticide behavior in soil was simplified and adapted to compost. The composting OP module considered three pools of OPs: soluble, sorbed and bound to organic matter. The model also considered a compartment of CO_2 arising from OP mineralization. The OP compartments were characterized by means of successive extractions with water (soluble fraction), then with another solvent adapted to the properties of OP (sorbed fraction). Finally, non-extractable residues (NER) were measured after the extractions and represented the OP bound to organic matter. The model assumed that: i) NER were produced from sorbed OPs, and ii) OP biodegradation only occurred in the soluble phase. The NER formation and OP biodegradation rates were represented by Fr and dr, respectively. Moreover, the distribution of OP between the soluble and sorbed pools was an instantaneous equilibrium described using a sorption coefficient (Kd).

3.3.3 Model coupling OC and OP modules

Three coupling hypotheses to describe the interactions between OC and OP modules were proposed:

Hypothesis 1: The overall OP sorption coefficient Kd was assumed to be the sum of the sorption coefficients (Kd_i) in the different OC pools ($C_{i,\ i=1\text{-}5}$), balanced with the proportions of OC in the pools. This hypothesis was used successfully to evaluate the sorption capacity of plant residues with respect to herbicides, based on their biochemical fractions such as cellulose, hydrosoluble and lipid compounds (Gaillardon et al., 1983). Moreover, the biochemical nature of an organic substrate strongly influenced the degree of OP sorption (Benoit et al., 1996) and the OP sorption capacities of lignin were found to be markedly higher than those of cellulose (Xing et al., 1994).

Hypothesis 2: Most OPs were assumed to be degraded by microorganisms through co-metabolism during composting, the microorganisms using compost organic matter as a primary energy source (Barker et al., 2002). The level of OP degradation was therefore supposed to depend on the potential degradability of the chemicals and on

the overall microbial activity driven by organic matter decomposition (Laine et al., 1997).

Hypothesis 3: The formation of NER from sorbed OPs was assumed to depend on the chemical reactivity of the OPs and overall microbial activity. Indeed, the influence of microbial activity on NER formation has long been reported (Benoit and Barriuso, 1997; Kästner et al., 1999). The parent chemicals, and the metabolites formed from their degradation, may be incorporated into growing biomass (Barriuso et al., 2008) or linked to organic matter after oxidation reactions catalyzed by extracellular enzymes (Gevao et al., 2000).

3.4 Data acquisition for model calibration and evaluation

3.4.1 Data acquisition for calibration and evaluation of the OC module

3.4.1.1 Composting experiments in 170-L pilots

In order to calibrate and perform an initial evaluation of the OC module, we used the results of composting experiments carried out in 170-L pilots using different mixtures of wastes: mixtures R1 to R6 included green waste and biowaste (Francou, 2003; Francou et al., 2008), and mixtures P1 to P6 consisted of sewage sludge and green waste (Doublet, 2008). The composts were sampled after 2, 4, 6 or 12 weeks of composting. At each sampling date, the mass losses were measured.

Total organic C (TOC) contents were determined on dried and 200 μm ground samples of the initial mixture and compost samples using elementary analysis by dry combustion according to the French standard NF ISO 10694 (AFNOR, 1999). The amount of mineralized OC was calculated as the difference between the TOC in the initial mixture and the TOC remaining in the reactor at the sampling date, taking account of mass and OC losses related to sampling. The Van Soest biochemical fractionation was then performed on all samples: the H2O fraction was extracted with distilled water at 100°C for 30 min, the SOL fraction was extracted with neutral detergent for 1 h, and the HEM, CEL and LIC fractions (expressed as a % of initial TOC) were obtained sequentially in accordance with French standard XPU 44-162 (AFNOR, 2005).

3.4.1.2 Composting experiments in 4-L pilots

The OC module was also evaluated a second time, at a different composting scale, using a series of experiments performed in 4-L pilots on one mixture (L) of sewage sludge and green waste composted in six replicates (Lashermes et al., 2010). The composts were sampled after 2, 6 and 12 weeks of composting. The TOC contents and biochemical fractionation of the initial mixture and compost samples were analyzed and the mineralized fraction was calculated as previously described.

3.4.2 Data acquisition for OP module calibration

The 4-L pilots were then used for a further set of experiments, during which the initial mixture (L) artificially contaminated with ^{14}C-OP was placed in each reactor in order to measure the evolution of OP speciation during composting and to calibrate the OP module. Composting experiments were carried out in triplicate for each ^{14}C-OP. The solutions of ^{14}C-labeled OPs were prepared with either [3C-ring-^{14}C] fluoranthene (specific activity: 1665 MBq mmol-1, 98.3% purity), [methyl-^{14}C] N-(phosphonomethyl) glycine (glyphosate) (specific activity: 81.4 MBq mmol^{-1}, 93.8% purity), [U-ring-^{14}C] 4-n-nonylphenol (specific activity: 1924 MBq mmol^{-1}, 99% purity), or [U-ring-^{14}C] sodium linear dodecylbenzene sulfonate (specific activity: 230.9 MBq mmol^{-1}, 92.7% purity) by isotopic dilution with non-labeled OPs. The initial contents of OPs in the waste mixture (expressed in mg kg^{-1} DM) were: 3, 2860, 1.5 and 34 for glyphosate, LAS, fluoranthene and NP, respectively. The ^{14}C-CO_2 and the volatile organic compounds produced were trapped respectively in NaOH and methanol plugs and analyzed by liquid scintillation counting (LSC). Lixiviated ^{14}C was also quantified using LSC.

A sequential extraction was performed in triplicate on fresh samples equivalent to 5 g DM of the spiked initial waste mixture and compost samples in order to determine the amount of ^{14}C-activity in water and the solvent extractable fractions, as well as NER. Water extracts with 75 mL of MilliQ water (Millipore, Molsheim, France) were recovered by centrifugation (2400 g, 20 min) after 24 h shaking. Three successive extractions were then performed with 3*75 mL methanol (or ammonium hydroxide solution for glyphosate). After the extractions, the compost samples were dried and

ground. The ^{14}C-OP concentrations in supernatants were measured by LSC, and the non-extracted radioactivity, corresponding to the NER, was determined by LSC of the ^{14}C-CO_2 obtained after combustion. At each sampling date, the percentages of ^{14}C-activity in the different fractions (mineralized, volatilized, leached, water and solvent extractable, NER) were calculated based on the total ^{14}C-activity recovered at the sampling date (sum of ^{14}C in the different fractions).

3.4.3 Data acquisition for the coupling between OC and OP modules

The sorption coefficients (Kd) of each OP were determined on mature composts sampled after 12 weeks of composting in the 4L reactors, using compost samples from the experiments performed without any artificial contamination with ^{14}C-OP at the beginning of composting (Lashermes et al., 2010). Fresh compost samples were shaken for 24h with ^{14}C-OP solutions. Water extracts were then recovered by centrifugation (5500 g, 10 min). The concentrations of ^{14}C-OP in the supernatant were determined by LSC. The Kd (g sorbed C g^{-1} soluble C) was determined as where was the amount of sorbed ^{14}C-CO_2 and was the proportion of initial ^{14}C-OP in solution after equilibration.

3.5 Model calibration and evaluation

3.5.1 Calibration and evaluation of the OC module

From the total of 12 initial mixtures composted in 170-L pilots (R1 to R6 and P1 to P6), eight were selected at random (R1, R3, R5, R6, P1, P2, P3 and P5) to estimate the parameters of the OC module while the four remaining mixtures (R2, R4, P4 and P6) were used for the initial evaluation of the OC module. A second evaluation of the OC module was performed using the organic mixture L composted in the 4-L pilot.

To run the OC module, 13 parameters were necessary. Seven fixed parameters were obtained from the literature or calculated directly from the measurements, while six were estimated by inverse modeling of the OC module. Table 1 shows the parameters of the equations presented in Appendix 1. The minimum (T_{min}), optimum (T_{opt}) and maximum (T_{max}) temperatures for microbial growth necessary for the temperature

function used in Rosso et al. (1993) were chosen based on the findings of Tremier et al. (2005), with T_{min} = 0°C; T_{opt} = 49.3°C and T_{max} = 82.7°C. The assimilation yield of the OC available for microbial biomass Y was fixed at 0.5 within the value range of 0.4-0.6 proposed by William and Payne (1970). The hydrolysis constants of the HEM (K_3), CEL (K_4) and LIC (K_5) fractions were calibrated directly, based on the median kinetics of the experimental evolutions of the HEM, CEL and LIC fractions, respectively (Doublet, 2008; Francou et al., 2008). Once these seven parameters had been fixed, the remaining six parameters (K_1, K_2, μ_{max}, m_B, Y_{mcs} and K_S) were optimized for each of the eight mixtures (R1, R3, R5, R6, P1, P2, P3 and P5) in the calibration data set. For subsequent procedures, the parameters used (K_1, K_2, μ_{max}, m_B, Y_{mcs} and K_S) were calculated as the mean of the optimized values obtained during model calibration.

Parameter optimization was performed using the fmincon function of the Matlab Optimization Toolbox (Mathwork, USA) which applies a sequential quadratic programming algorithm. The objective function was the total root mean square error ($RRMSE\text{-}OC_{tot}$) defined as the sum of all the RMSE-OC(j) values calculated between the experimental and simulated values of the j variables of the OC module (j=1-6 for the SOL, HEM, CEL, LIC, H2O fractions and for CO_2 production) (Smith et al., 1997), as follows:

$$RRMSE - OC(j) = \frac{100}{E(j)} \sqrt{\sum_{i=1}^{n} \frac{(S(j)_i - E(j)_i)^2}{n}} \quad [1]$$

where n is the number of measurement dates, S(j)i and E(j)i are respectively the simulated and experimental values of variable j, and $\bar{E}(j)$ is the average of n experimental values. The best simulation was that producing the lowest $RRMSE\text{-}OC_{tot}$.

The efficiency coefficient, E_f, and the mean difference, $\overline{D}$, of the model were used in addition to evaluate the simulations (Smith et al., 1997):

$$E_f = \frac{\sum_{i=1}^{n} (E_i - \overline{E})^2 - \sum_{i=1}^{n} (S_i - \overline{E})^2}{\sum_{i=1}^{n} (E_i - \overline{E})^2} \quad [2]$$

Where n is the number of measurement dates, Si and Ei are respectively the simulated and experimental values, and $\overline{E}$, is the average of n experimental values.

$$\overline{D} = \frac{\sum_{i=1}^{n} (S_i - E_i)}{n} \qquad [3]$$

3.5.2 Calibration and evaluation of the OP module

The parameters of the OP module were optimized for each of the OP composting experiments. Parameter estimation for the OP module was also performed using the fmincon function of the Matlab. The total root mean square error (RRMSE-OP_{tot}) was defined as the sum of all the RRMSE-OP(j) calculated between the experimental and simulated values of the j variables (j=1-4 for the soluble and sorbed fractions, NER and CO_2, respectively) (equation [1]).

During the four runs, Run A was performed with the OP module only, so that OC evolution would have no influence on the parameters, while Runs B, C and D coupled the OP and OC modules. During all runs, the NER formation rate (Fr) and OP degradation rate (dr) were optimized, while the sorption coefficient (Kd) was treated separately in the different runs:

- In Run A (without coupling) and Run B (with coupling), experimental Kd values were used as fixed values and Kd parameter were not calibrated.

- In Run C, the same Kd was considered for all pool C_i and was optimized for each OP.

- In Run D, the four sorption coefficients Kd_i on OC pool C_i values were optimized for each OP.

The sum of RRMSE-OP_{tot} obtained in a run was multiplied by the number of parameters requiring optimization in order to evaluate the overall performance of the simulations. The best run was that which produced the lowest weighted sum of RRMSE-OP_{tot}. The objective was to limit the number of parameters requiring optimization. The run generating the best simulations was selected and median values of the parameters obtained for the three replicated composting experiments on each

OP were proposed for model calibration.

3.6 Results and discussion

3.6.1 Calibration of the OC module

Table 1 presents the parameters estimated for the OC module using eight mixtures (R1, R3, R5, R6, P1, P2, P3 and P5). The three hydrolysis constants: K_3 (for HEM), K_4 (for CEL) and K_5 (for LIC), were calculated directly from the eight compost experiments by fitting the median evolution of respectively HEM, CEL and LIC, respectively with a first order kinetic. The highest hydrolysis constant was found for HEM and the lowest for LIC. The LIC hydrolysis constant K_5 was very low because LIC displayed almost no decrease during the short duration of these experiments. These values were slightly lower than those found for the decomposition of organic in soil (Corbeels et al., 1999). However, the kinetic parameters were expressed with reference to standard conditions of temperature and humidity that are not the same in this model and in soil models. The mean optimized value of microbial mortality (m_B) was found to be 0.229 d^{-1}, which was within the lower range of the values previously proposed by Sole-Mauri et al. (2007). An optimized growth rate (μ_{max}) of 5.99 d^{-1} was found under our conditions, while Tremier et al. (2005) had determined values ranging from 3.12 to 8.16 d^{-1} for composting temperatures of between 19.6°C and 56.9°C. The average value of 0.4096 for Y_{mcs} indicated that almost 60% of the dead microbial biomass had returned into the slow degradable compartment that could be considered as a "humified" pool of organic matter. For exogenous organic matters added to soil, such humification coefficients estimated in soil have lower values of between 0.1 and 0.6 (Nicolardot et al., 2001). The average hydrolysis constant for SOL-F (K_2) of 0.0612 d^{-1} was lower than that found in soil (0.25-0.8 d^{-1}) by Corbeels et al. (1999) and Garnier et al. (2003). In this compartment, we found that as for HEM, CEL and LIC, the kinetics were slower during composting than in soil. Table 2 shows the modeling efficiency E_f. The highest E_f value was obtained for the CO_2, CEL and H2O compartments. By comparison, the SOL and LIC compartments displayed lower E_f values.

3.6.2 Evaluation of the OC module

The four other sets of experimental data obtained in 170-L pilots (R2, R4, P4, P6), plus that obtained in a 4-L pilot (L) were used to evaluate the model. The average RMSE-OCtot of the validation datasets (155) was lower than that of the calibration datasets (184), thus showing an improvement in the simulations for validation (Table 3.2). The dynamics of the L mixture were well simulated when compared to the observed data (Fig.3.2). The simulations obtained were within the range of variation of the experimental measurements in the six composting replicates. When considering the validation dataset and the two composting scales (170 or 4 L), the highest E_f values were found for CO_2 and CEL, while the lowest E_f were found for LIC and SOL, as in the calibration set. The evolution of SOL may have been affected during composting by processes other than those described in the model. We also made the assumption that SOL-S was equal to zero in the initial mixture of wastes. The initial SOL fraction may have contained more recalcitrant products from some waste, such as digested sewage sludge. This might have improved the quality of SOL simulations but we were not able to quantify this fraction by measurements. E_f depends on the range of variation of the variable, being higher when the range is high and lower when it is low.

This might explain the low E_f value found for LIC (whose content changes very little during composting) and the high E_f for CO_2 (which can vary considerably).

The relationships between simulated and experimental data are presented in Fig.3.3, and included the calibration and validation mixtures. The highest R^2 values were obtained for the CEL, SOL and LIC compartments, attesting to the relevance of the hydrolysis constants proposed for these pools. By comparison, the HEM and H2O compartments displayed the lowest R^2 values. At the 4-L scale, the OC C_S available, corresponding to the H2O pool, was under-estimated, especially at the beginning of composting, while the mineralized fraction (CO_2) tended to be over-estimated during the same period.

Although no data were available to validate the true evolution of the microbial pool, the results suggested that the microbial growth simulated on the available substrate C_S was probably too high. If a lower maximum growth rate for microbial biomass (μ_{max})

and a higher saturation constant for the Monod kinetic (K_S) had been used, the available OC evolution and CO_2 production would have better matched the experimental data. The parameterization of the OC module proposed could nevertheless be validated at the scale of composting (4 L), although this differed from the scale used to acquire the data used for model calibration (170 L).

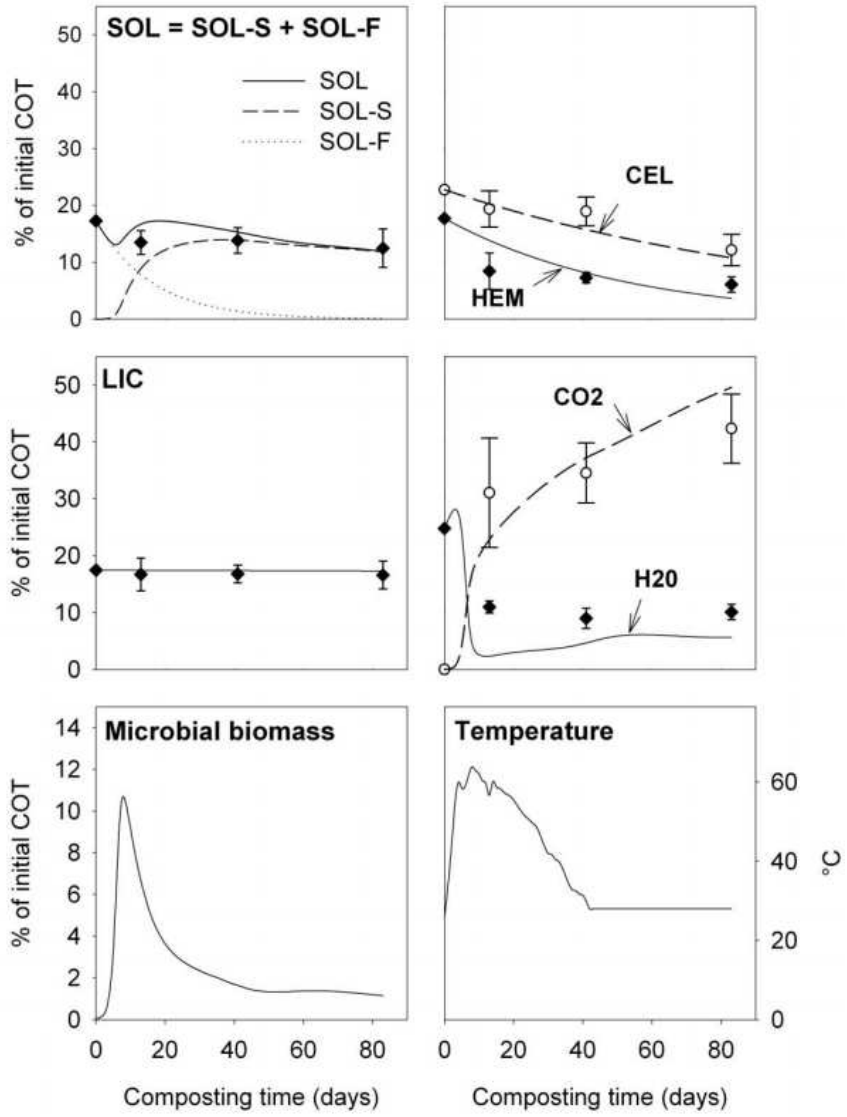


Figure 3.2: Experimental (symbols) and simulated (lines) data on biochemical fractions, carbon dioxide, water, microbial biomass (simulated only), and temperature (experimental only) during composting. The simulations were obtained using the OC module. The symbols represent the mean ± standard errors of experimental values of the six composting replicates.

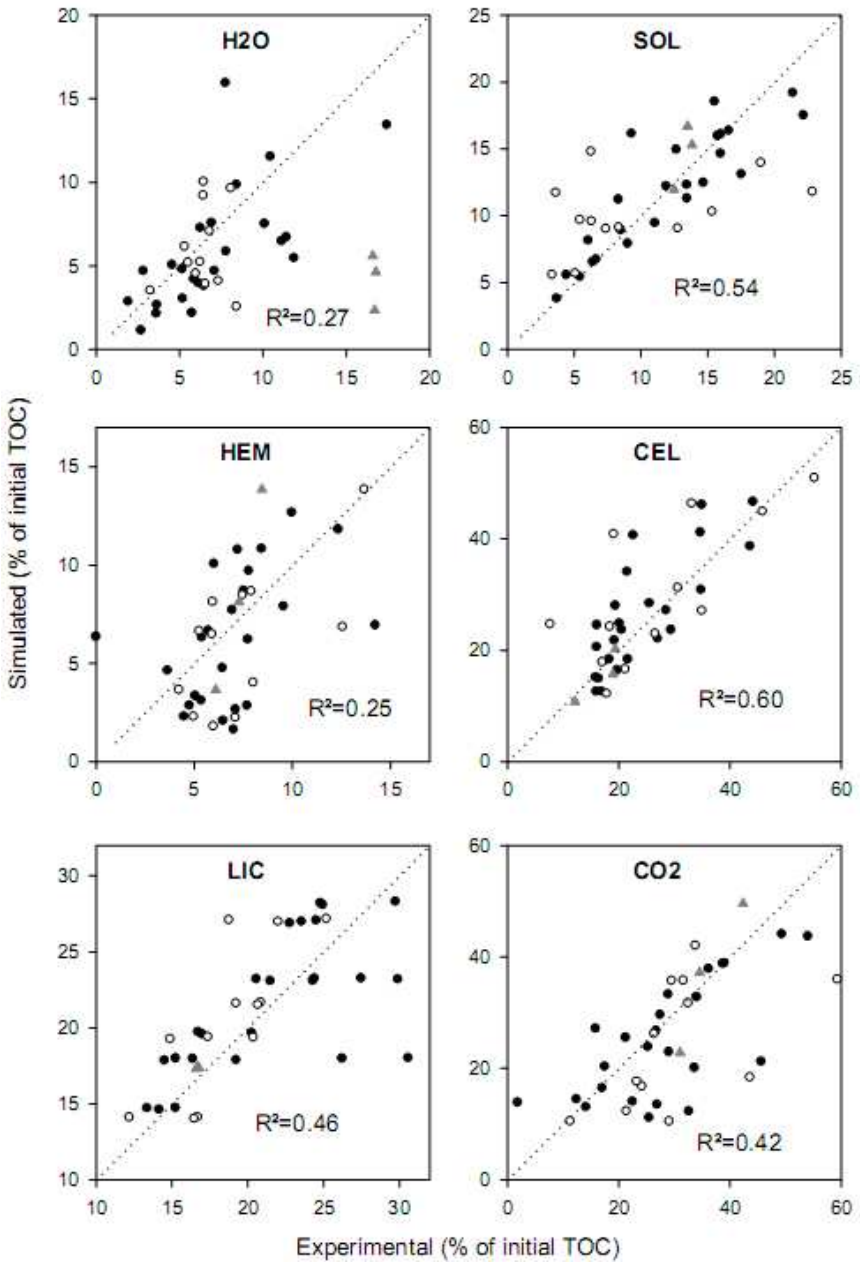


Figure 3.3: Relationships between experimental and simulated values of biochemical fractions, carbon dioxide and water. Full dots: data used for OC module calibration (Mixtures P1, P2, P3, P5, R1, R3, R5, R6), empty dots and grey triangles: data used for validation (P4, P6, R2, R4 and L, respectively). The dotted line is the 1:1 line.

Table 3.2: Statistical evaluation of the goodness-of-fit of the OC module

		Pilot mixtures												
		Calibration								Evaluation				
		P1	P2	P3	P5	R1	R3	R5	R6	P4	P6	R2	R4	L[d]
RMSE-OC	SOL	19	21	41	33	28	65	31	30	49	36	27	45	11
	HEM	33	32	36	52	40	37	19	18	46	11	21	32	30
	CEL	21	11	16	13	23	11	9	36	14	15	55	9	10
	LIC	11	15	9	12	32	14	7	5	21	6	14	14	4
	H2O	48	43	57	28	38	24	53	51	27	34	23	27	38
	CO_2	24	59	78	20	49	47	18	55	25	25	59	26	21
	$RMSE\text{-}OC_{tot}$[a]	156	181	237	158	210	198	137	195	182	127	199	153	114
$\overline{D}$[b]	SOL	-1.2	-1.7	-3.5	-5.0	1.4	2.3	-1.2	1.9	-1.7	-0.4	1.2	2.0	0.9
	HEM	-2.5	-1.3	-0.1	1.7	-2.1	0.1	0.7	0.0	-3.5	0.4	-0.1	-0.8	1.0
	CEL	2.4	-0.7	-2.5	-0.9	3.0	3.4	-2.2	9.4	0.5	-2.1	13.0	-3.3	-0.9
	LIC	1.2	-3.0	1.3	2.5	-5.6	1.9	0.8	0.3	3.8	1.0	1.3	-0.8	0.5
	H2O	-1.3	-2.3	-5.1	-0.3	-3.6	1.1	1.4	1.4	0.0	-1.3	-0.7	0.7	-4.3
	CO_2	-1.1	6.5	7.6	-0.4	4.4	-10.9	-2.0	-15.6	-1.3	0.0	-16.8	-0.1	0.3
E_f[c]	SOL	-0.44	-0.20	-1.28	-5.27	0.02	-9.36	-0.85	-0.21	0.05	0.05	-1.11	-1.84	0.27
	HEM	0.00	0.15	0.07	0.52	-22.35	-0.25	0.79	0.72	-1.89	0.96	0.60	-0.87	0.58
	CEL	0.39	0.76	0.54	0.45	0.68	0.88	0.81	0.30	0.70	0.41	0.15	0.74	0.78
	LIC	-0.59	-1.34	-0.29	-2.31	-1.16	-2.05	-0.21	-0.16	-1.39	-1.22	-0.36	-0.20	-2.12
	H2O	-0.60	-2.39	-3.22	0.42	0.15	0.84	0.59	0.19	-0.30	-0.26	0.67	0.30	0.33
	CO_2	0.85	0.29	-0.55	0.89	0.76	0.50	0.93	0.22	0.83	0.83	0.20	0.86	0.87

[a] Total mean square error of the OC module, $RMSE\text{-}OC_{tot}$
[b] Mean difference (as a % of initial TOC)
[c] Efficiency coefficient
[d] Mean statistics of the six composting replicates

3.6.3 Calibration of the OPs module

3.6.3.1 Comparison of the different simulation hypotheses (Runs A to D)

The simulations generally improved from Run A to Run D, as shown by the decrease in the sum of RRMSE-OPtot (Table 3.3). One example of the different simulation runs with a median goodness of fit is presented in Fig.3.4 for LAS.

Table 3.3: Parameter values and evaluation statistics of OP simulations of Runs A, B, C, and D for the four OPs (units are given in Table 3.1).

Run[a]	Model coupling		Glyphosate			LAS			Fluoranthene			NP			Sum	Weighted Sum[c]
			GLY-1	GLY-2	GLY-3	LAS-1	LAS-2	LAS-3	FLT-1	FLT-2	FLT-3	NP-1	NP-2	NP-3		
A, B, C, D		NER_0		3.9			4.6			5.4			27.4			
A Experimental Kd	no	*Kd*		0.9			4.8			21.9			6.4			
		Fr	0.020	0.028	0.060	0.004	0.006	0.004	0.002	0.005	0.004	0.030	0.030	0.023		
		Dr	0.009	0.019	0.032	0.103	0.208	0.185	0.001	0.002	0.001	0.255	0.380	0.326		
		$RMSE\text{-}OP_{tot}$[b]	103	101	113	86	105	109	70	49	116	105	112	134	1203	2406
B Experimental Kd	yes	*Kd*		0.9			4.8			21.9			6.4			
		Fr	0.0066	0.0065	0.0127	0.0011	0.0014	0.0009	0.0007	0.0016	0.0013	0.0061	0.0043	0.0044		
		Dr	0.0027	0.0044	0.0069	0.0263	0.0335	0.0360	0.0002	0.0005	0.0004	0.0483	0.0500	0.0550		
		$RMSE\text{-}OP_{tot}$	81	51	84	115	68	75	58	45	80	81	75	103	915	1831
C Optimization of Kd (single value)	yes	*Kd*	1.0	1.0	1.5	2.9	2.5	2.7	23.2	21.5	15.0	3.1	3.2	2.5		
		Fr	0.0062	0.0061	0.0090	0.0012	0.0017	0.0011	0.0007	0.0016	0.0014	0.0062	0.0056	0.0047		
		Dr	0.0028	0.0043	0.0087	0.0175	0.0210	0.0249	0.0002	0.0005	0.0003	0.0252	0.0328	0.0239		
		$RMSE\text{-}OP_{tot}$	79	49	70	82	50	59	57	45	63	63	59	67	743	2228
D Optimization of the Kd_i (i=1-5)	yes	Kd_1=Kd_2 (SOL)	0.0	1.4	0.1	0.0	2.7	10.0	68.4	38.5	42.2	3.0	9.1	8.5		
		Kd_3 (HEM)	0.3	0.0	0.0	0.0	8.9	6.8	14.3	28.4	15.0	12.2	0.0	0.0		
		Kd_4 (CEL)	0.0	0.0	4.5	8.7	0.0	0.0	26.7	29.0	15.4	0.0	1.0	4.0		
		Kd_5 (LIC)	3.0	2.5	0.0	0.0	0.0	0.0	0.0	0.0	0.0	0.0	6.7	0.0		
		Fr	0.0062	0.0061	0.0090	0.0012	0.0017	0.0011	0.0007	0.0016	0.0014	0.0062	0.0056	0.0047		
		Dr	0.0028	0.0043	0.0087	0.0175	0.0210	0.0249	0.0002	0.0005	0.0003	0.0252	0.0328	0.0239		
		$RMSE\text{-}OP_{tot}$	75	48	68	79	43	57	57	44	60	56	58	66	711	4268

[a] In all runs, *Fr* and *dr* were optimized.
[b] Total mean square error of the OP module, $RMSE\text{-}OP_{tot}$
[c] Sum of $RMSE\text{-}OP_{tot}$ multiplied by the number of parameters requiring optimization

Coupling with the OC module enabled the best improvement in simulation. Indeed, the most marked decrease in the sum of RRMSE-OP_{tot} was found between Runs A (without coupling) and B (with coupling), both of which used experimental Kd as fixed values for the Kd parameter, while Fr and dr were optimized. For both Runs A and B, the evolution of fluoranthene speciation was the best simulated (average RRMSE-OP_{tot} of 78 and 61, respectively) and NP gave the poorest fits (average RRMSE-OP_{tot} of 117 and 87, respectively), probably because the experimental Kd was too high.

When optimizing a single Kd parameter for all C_i pools (Run C), the optimized Kd values were twice as low as the experimental values for NP and the simulated amount of soluble NP matched the experimental observations. This was also the case for LAS, while for fluoranthene and glyphosate, a small difference was observed between the experimental Kd (used in Runs A and B) and the optimized Kd (Run C). For the two surfactants (LAS and NP), the experimental Kd measured on mature compost was too high when compared with the experimental results of the water extraction of OP from OP speciation. Moreover, the experimental Kd of mature compost was lower than that seen in more immature compost (Lashermes et al., 2010).

The optimization of four Kd_i parameters for the C_i pools (Run D) further improved the simulation when compared with Run C. Nevertheless, the benefits were not so important when considering the number of parameters (six) optimized in Run D by comparison with Run C (only three optimized parameters). Moreover, the Kd_i parameters were correlated and several different combinations produced simulations of similar quality, inducing a difficult interpretation of values for the sorption coefficient Kd_i related to each C_i pool.

3.6.3.2 Selection of the optimum run to calibrate the model

Run B appeared to produce the most efficient simulations. Indeed, when requesting the optimization of only two parameters (dr and Fr), it produced the lowest weighted sum of RMSE-OP_{tot}. The simulated amounts of soluble and sorbed fractions, NER and mineralized OP with Run B accounted for more than 86% of the variability of the corresponding experimental values (Fig.3.4), thus testifying that the COP-Compost

model was able to predict satisfactorily the experimental behavior of each OP studied. The best simulated pools were the NER and mineralized ^{14}C-CO_2, with average E_f values of 0.99 ± 0.01 and 0.93 ± 0.07, respectively (Table 3.4). In addition, both the low average and their related standard errors of 0.7 ± 1.3% of the initial 14C for NER simulations and 0.9 ± 1.1% for mineralized ^{14}C-CO_2 indicated no bias in the simulations of these pools using the model. The simulations also agreed with the experimental evolution of sorbed OPs, with an average E_f of 0.85 ± 0.19. However, values indicated that the model over-estimated the sorbed amount of LAS by comparison with experimental data. The quality of fit of the soluble pool was satisfactory for glyphosate (average E_f = 0.89), intermediate for fluoranthene (average E_f = 0.20) (mainly because of heterogeneous experimental data) and poor for the two surfactants (average E_f = -1.03 for LAS and E_f = -6.04 for NP) because of the excessively high Kd values used for simulation and corresponding to experimental measurements on mature composts. The experimental Kd determination on mature compost was proposed to calibrate the model since this constitutes an easily accessible characteristic that can be assessed without ^{14}C-labeled OPs. Nonetheless, in the case of surfactants, analyses must be performed with particular care.

Table 3.4: Statistical evaluation of model efficiency in the simulations obtained using the model coupling OC and OP modules, and with Run B.

	OP fraction	Glyphosate			LAS			Fluoranthene			NP		
		GLY-1	GLY-2	GLY-3	LAS-1	LAS-2	LAS-3	FLT-1	FLT-2	FLT-3	NP-1	NP-2	NP-3
RMSE-OP	Soluble	7	30	17	38	44	35	20	12	31	53	38	59
	Sorbed	15	7	20	24	18	30	3	2	9	4	24	12
	NER	21	7	31	25	4	6	16	7	28	12	4	9
	^{14}C-CO_2	38	6	16	29	2	4	19	24	11	13	10	23
	$RMSE\text{-}OP_{tot}$	81	51	84	115	68	75	58	45	80	81	75	103
$\overline{D}$ [a]	Soluble	1.6	6.4	2.0	-3.3	-3.6	-2.4	0.2	-0.1	-1.1	-2.6	-1.6	-3.3
	Sorbed	-1.0	0.2	-3.4	4.7	5.9	9.0	0.2	0.6	3.1	-0.2	3.0	0.4
	NER	0.5	0.4	2.9	0.7	0.2	0.2	-0.3	-0.1	-1.6	2.7	0.6	2.1
	^{14}C-CO_2	0.7	0.7	1.6	3.0	0.1	0.4	0.0	0.0	0.0	1.5	0.2	2.7
E_f [b]	Soluble	0.96	0.76	0.94	0.22	-2.89	-0.42	0.48	0.69	-0.57	-11.63	-0.94	-5.56
	Sorbed	0.82	0.98	0.87	0.89	0.95	0.90	0.58	0.96	0.36	1.00	0.94	0.98
	NER	0.99	1.00	0.98	0.99	1.00	1.00	0.99	1.00	0.98	1.00	1.00	1.00
	^{14}C-CO_2	0.77	0.99	0.95	0.88	1.00	1.00	0.93	0.92	0.97	0.96	0.97	0.85

[a] Mean difference (as a % of initial ^{14}C)

[b] Efficiency coefficient

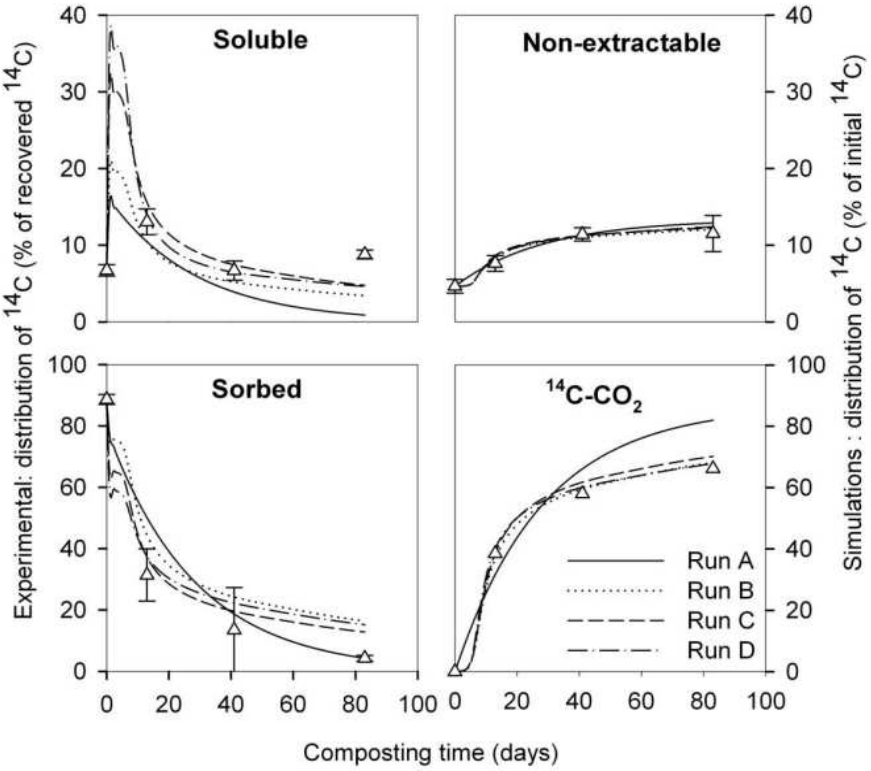


Figure 3.4: Experimental (symbols) and simulated (lines) data on soluble, sorbed, non-extractable, and mineralized LAS during composting. The simulations were obtained successively with Runs A, B, C, D for compost LAS-3 which presented a median quality of fitting. Symbols represent experimental values ± standard errors.

Median values for the Fr and dr parameters (Table 3.3) were proposed to calibrate the model for the four studied OPs: Fr = 0.0066 d^{-1} and dr = 0.0044 d^{-1} for glyphosate, Fr = 0.0011 and dr = 0.0335 for LAS, Fr = 0.0013 and dr = 0.0004 for fluoranthene, Fr = 0.0044 and dr = 0.0500 for NP. The simulated evolutions of OP speciation during composting obtained with this calibration were in agreement with experimental data (Fig.3.5 and 3.6). In some cases, the sum of the experimental pools was lower than 100% where volatilization and lixivation were observed experimentally but not taken into account by the model which explained the differences between simulated and experimental pools in these cases. NER formation from glyphosate was slightly over-estimated by the model at the beginning of composting, but the predicted amount of NER in mature compost (39% of initial ^{14}C) remained realistic, as did the sorbed amount of ^{14}C-residues (14%) and the mineralized ^{14}C -CO_2 (30%). However, soluble

^{14}C-residues of glyphosate in mature compost were over-estimated by the model (17% of initial ^{14}C) by comparison with experimental data (median of 9% of recovered ^{14}C). For LAS, the predicted amount of sorbed ^{14}C -residues in mature compost was over-estimated (18% of initial ^{14}C) while the corresponding experimental median value was 5% of recovered ^{14}C. The predicted amounts of soluble ^{14}C -residues in mature compost (4% of initial ^{14}C), the NER (13%) and the mineralized ^{14}C-CO_2 (65%) all matched with the experimental observations. The evolution of fluoranthene speciation was well simulated: no mineralization was predicted, soluble ^{14}C-residues accounted for 3% of initial ^{14}C, the sorbed fraction for 68% and NER for 29%. For NP, the NER was slightly over-estimated in mature compost (54% of initial ^{14}C) while only 45% of recovered ^{14}C was seen to form NER under experimental conditions. However, the amounts of soluble ^{14}C-residues in mature compost (1% of initial ^{14}C), sorbed fraction (5%) and mineralized ^{14}C-CO_2 (39%) were satisfactorily predicted. The amount of water soluble residues considered as being directly available (Benoit and Barriuso, 1997) was globally small, suggesting a low risk linked with direct OP assimilation by plants or leaching in soils.

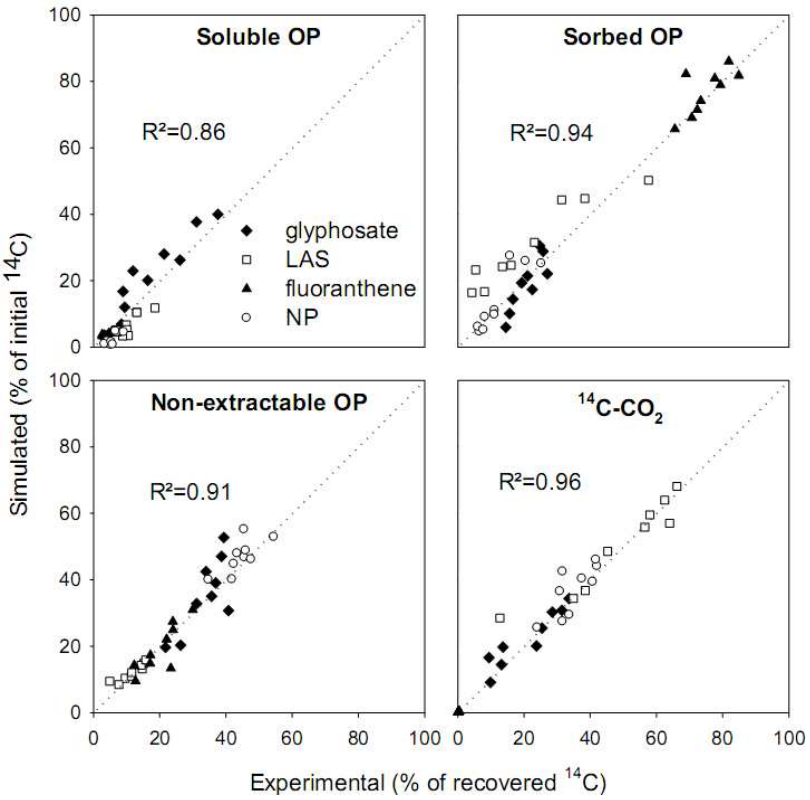


Figure 3.5: Relationships between experimental and simulated values for soluble, sorbed, non-extractable and mineralized OPs for the four OPs, with Run B. The dotted line is the 1: 1 line.

3.6.3.3 Evaluation of OC-OP coupling hypotheses

The assumption of the overall sorption coefficient Kd as the sum of Kd_i sorption coefficient in different OC pools (hypothesis 1) could not be supported by the results of this study. However, the sorption properties of organic substrates do undergo change during composting. Contradictory results have been found, with either an increase in sorption properties (Benoit et al., 1996) or a decrease (Lashermes et al., 2010). Thus, taking account in the model of variations in the sorption properties of the organic matter undergoing composting would certainly improve the simulations of the soluble and sorbed pools. Further research on the influence on OP behavior of an initial waste mixture with contrasted biochemical properties during composting should help to evaluate this hypothesis.

On the other hand, it was possible to validate the hypothesis of microbial biomass being active in OP degradation and NER formation (hypotheses 2 and 3). The description of the composting process, as initially proposed by Kaiser (1996), was proved to be relevant to the simulation of OP behavior. When account was taken of the influence of total microbial biomass size, the mineralization of the four studied OPs could be satisfactorily predicted by the coupled model. The limitation of considering a single microbial biomass has already been underlined (Sole-Mauri et al., 2007), especially if one considers that the different microbial populations that occur during the process have contrasted capacities for OP mineralization (Haderlein et al., 2006). The model would thus be improved by the addition of microbial populations with different growing conditions and contrasted abilities to degrade OPs.

3.7 Conclusions

Using an innovative approach, the COP-Compost model combines the dynamics of OC and OPs during composting by coupling two modules. The model simulated satisfactorily the evolution of OC and OPs. For the OC module, only data on the biochemical composition of the initial waste mixture was required for the simulation, which is a relatively accessible analysis. For the OP module, further research is now necessary to assess the parameters using pollutants with different initial waste mixtures. Correlations need to be determined between the estimated parameters and

data that would be more easily available than those obtained from ^{14}C-labeled experiments.

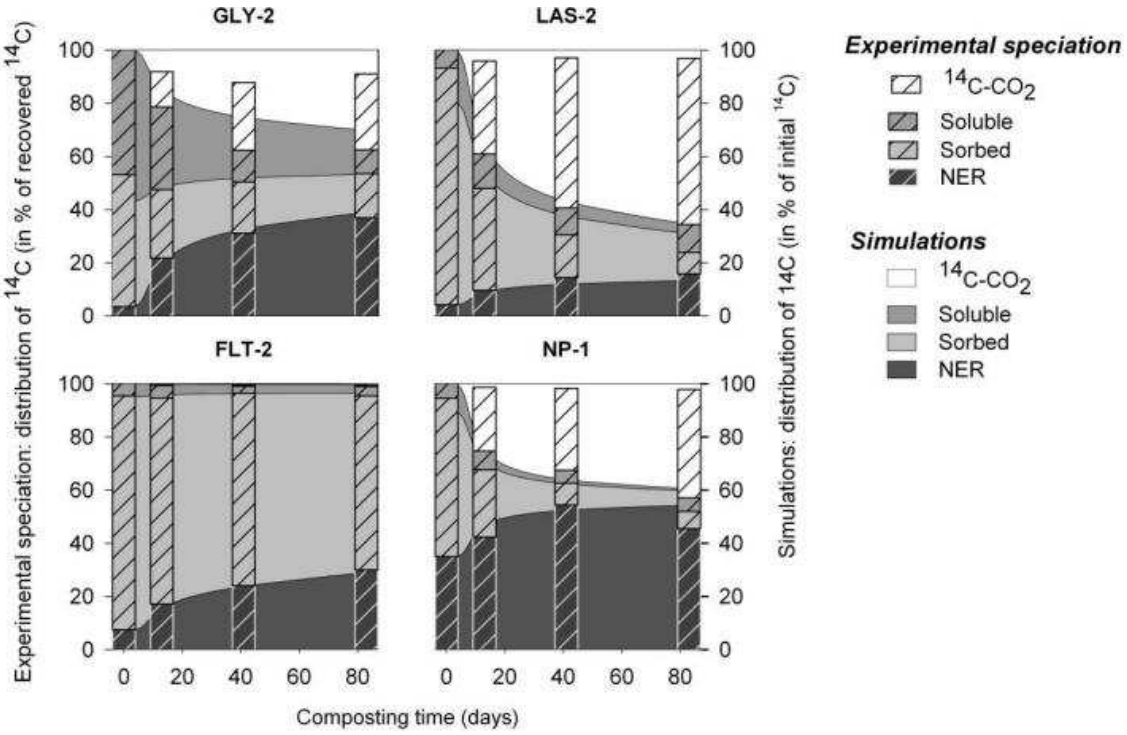


Figure 3.6: Experimental and simulated distribution kinetics during the composting of ^{14}C between mineralized, soluble, sorbed and NER fractions, from ^{14}C-labeled glyphosate, LAS, fluoranthene and NP applied at the beginning of composting experiments. Simulations were obtained using the proposed calibration of the model coupling OC and OPs. GLY-2, LAS-2, FLT-2, and NP-1 represent the median quality of simulations. Area plots represent simulations and hatched histograms represent experimental values.

3.8 Acknowledgements

We would like to thank ADEME (French Environment and Energy Management Agency) as well as the Environment and Agronomy Division of INRA (French National Institute for Agricultural Research) for their grants and Veolia Environment, Research and Development, for providing financial support for the experiments. We also thank Laurent Lardon and Maelenn Le Villo-Poitrenaud for their constructive comments.

3.9 References

AFNOR, 1999. Norme française NF ISO 10694. Qualité du sol - Dosage du carbone organique 349 et du carbone total après combustion sèche (analyse élémentaire). AFNOR, Paris, France.

AFNOR, 2005. Norme Française NFU 44-162. Amendements organiques et supports de culture – Fractionnement biochimique et estimation de la stabilité biologique. AFNOR, Paris, France.

Barker, A.V., Bryson, G.M., 2002. Bioremediation of heavy metals and organic toxicants by composting. Sci. World J. 2, 407-20.

Barriuso, E., Benoit, P., Dubus, I.G., 2008. Formation of pesticide non-extractable (bound) residues in soil: Magnitude, controlling factors and reversibility. Environ. Sci.Technol. 42, 1845-1854.

Benoit, P., Barriuso, E., 1997. Fate of C-14-ring-labeled 2,4-D, 2,4-dichlorophenol and 4-chlorophenol during straw composting. Biol. Fert. Soils 25, 53-59.

Benoit, P., Barriuso, E., Houot, S., Calvet, R., 1996. Influence of the nature of soil organic matter on the sorption-desorption of 4-chlorophenol, 2,4-dichlorophenol and the herbicide 2,4-dichlorophenoxyacetic acid (2,4-D). Eur. J. Soil Sci. 47, 567-578.

Benoit, P., Madrigal, I., Preston, C.M., Chenu, C., Barriuso, E., 2008. Sorption and desorption of non-ionic herbicides onto particulate organic matter from surface soils under different land uses. Eur. J. Soil Sci. 59, 178-189.

Bright, D.A., Healey, N., 2003. Contaminant risks from biosolids land application: Contemporary organic contaminant levels in digested sewage sludge from five treatment plants in Greater Vancouver, British Columbia. Environ. Pollut. 126, 39-49.

Brändli, R.C., Bucheli, T.D., Kupper, T., Furrer, R., Stadelmann, F.X., Tarradellas, J., 2005. Persistent organic pollutants in source-separated compost and its feedstock materials - A review of field studies. J. Environ. Qual. 34, 735-760.

Bertrand, I., Chabbert, B., Kurek, B., Recous, S., 2006. Can the biochemical features and histology of wheat residues explain their decomposition in soil? Plant and Soil 281, 291-307.

Corbeels, M., Hofman, G., Van Cleemput, O., 1999. Simulation of net N immobilisation and mineralisation in substrate-amended soils by the NCSOIL computer model. Biology and Fertility of Soils 28, 422-430.

Doublet, J., 2008. Influence du co-substrat carboné sur la nature des matières organiques et les formes d'azote des composts de boue ; conséquences sur la disponibilité de cet azote. Dissertation. AgroParisTech, Paris, France.

European Communities, 2005. Waste Generated and Treated in Europe 1995–2003. Office for Official Publications of the European Communities, Luxembourg.

Francou, C., 2003. Stabilisation de la matière organique au cours du compostage de déchets urbains: Influence de la nature des déchets et du procédé de compostage – Recherche d'indicateurs pertinents. Thesis of doctorat INA P-G, 388p.

Francou, C., Linères, M., Derenne, S., Villio-Poitrenaud, M.L., Houot, S., 2008. Influence of green waste, biowaste and paper-cardboard initial ratios on organic matter transformations during composting. Bioresour. Technol. 99, 8926-8934.

Garnier, P., Néel, C., Aita, C., Recous, S., Lafolie, F., Mary, B., 2003. Modelling carbon and nitrogen dynamics in soil with and without straw incorporation. European Journal of Soil Science 54, 555–568.

Gaillardon, P., Gaudry, J.C., Calvet, R., 1983. Effect of organic-Matter added to Soil on the adsorption of herbicides-influence of the composition of the organic-matter. Weed Research 23, 333-338.

Gevao, B., Semple, K.T., Jones, K.C., 2000. Bound pesticide residues in soils: a review. Environ. Pollut. 108, 3-14.

Haderlein, A., Legros, R., Ramsay, B.A., 2006. Pyrene mineralization capacity increases with compost maturity. Biodegradation 17, 293-302.

Kaiser, J., 1996. Modelling composting as a microbial ecosystem: A simulation approach. Ecol. Model. 91, 25-37.

Kästner, M., Streibich, S., Beyrer, M., Richnow, H.H., Fritsche, W., 1999. Formation of bound residues during microbial degradation of [C-14]anthracene in soil. Appl. Environ. Microbiol. 65, 1834-1842.

Kocamemi, B.A., Çeçen, F., 2005. Cometabolic degradation of TCE in enriched nitrifying batch systems. J. Hazard. Mater. 125, 260-265.

Laine, M.M., Haario, H., Jorgensen, K.S., 1997. Microbial functional activity during compostingof chlorophenol-contaminated sawmill soil. Meeting on Substrate Use for Characterization of Microbial Communities in Terrestrial Ecosystems (SUBMECO). Elsevier Science Bv, Innsbruck, Austria, pp. 21-32.

Lashermes, G., Houot S., Barriuso E., 2010. Sorption and mineralization of organic pollutants during different stages of composting. Chemosphere, 79, 455-462.

Mason, I.G., 2006. Mathematical modelling of the composting process: A review. Waste Manag. 26, 3-21.

Nicolardot, B, Recous, S, Mary, B., 2001. Simulation of C and N mineralisation during crop residue decomposition: A simple dynamic model based on the C:N ratio of the residues. Plant & Soil 228, 83-103

Rosso, L., Lobry, J.R., Flandrois, J.P., 1993. An unexpected correlation between cardinal temperatures of microbial-growth highlighted by a new model. J. Theoretical Biol.162, 447-463.

Sabljić, A., Gusten, H., Verhaar, H., Hermens, J., 1995. Qsar modeling of soil sorption - improvements and systematics of LogK-oc vs Log K-ow correlations. Chemosphere, 31, 4489-4514.

Saffih-Hdadi, K., Bruckler, L., Barriuso, E., 2003. Modeling of sorption and biodegradation of parathion and its metabolite paraoxon in soil. . J. Environ. Qual. 32, 2207-2215.

Shelton, D.R., Doherty, M.A., 1997. A model describing pesticide bioavailability and biodegradation in soil. Soil Sci. Soc. Am. J. 61, 1078-1084.

Smith, P., Smith, J.U., Powlson, D.S., McGill, W.B., Arah, J.R.M., Chertov, O.G., Coleman, K., Franko, U., Frolking, S., Jenkinson, D.S., Jensen, L.S., Kelly, R.H., Klein-Gunnewiek, H., Komarov, A.S., Li, C., Molina, J.A.E., Mueller, T., Parton, W.J., Thornley, J.H.M., Whitmore, A.P., 1997. A comparison of the performance of nine soil organic matter models using datasets from seven long-term experiments. Geoderma 81, 153-225.

Sole-Mauri, F., Illa, J., Magri, A., Prenafeta-Boldu, F.X., Flotats, X., 2007. An integrated biochemical and physical model for the composting process. Bioresour. Technol.98, 3278-3293.

Tremier, A., De Guardia, A., Martel, J.L., 2005. Evaluating the biodegradability of an organic waste thanks to a respirometric characterization. 1st International conference on engineering for waste treatment, beneficial waste and by-products, Albi, 17-19 May 2005.

Wauchope, R.D., Yeh, S., Linders, J., Kloskowski, R., Tanaka, K., Rubin, B., Katayama, A., Kordel, W., Gerstl, Z., Lane, M., Unsworth, J.B., 2002. Pesticide soil sorption parameters: theory, measurement, uses, limitations and reliability. Pestic. Manag. Sci. 58, 419-445.

Xing, B.S., McGill, W.B., Dudas, M.J., Maham, Y., Hepler, L., 1994. Sorption of phenol by selected biopolymers - isotherms, energetics, and polarity. Environ. Sci.Technol. 28, 466-473.

CHAPTER 4: SENSITIVITY ANALYSIS OF COP_COMPOST MODEL FOR THE DEGRADATION OF ORGANIC MICROPOLLUTANTS DURING COMPOSTING PROCESS

4.1 Abstract

A kinetic partitioning model called COP-Compost model coupled the organic matters (OC) module and organic pollutants (OP) module. The model was applied to simulate the changes in organic matters, organic pollutants, as well as the microbial activities during composting process. For model calibration, 12 composting experiments varying in initial organic matter characteristics were chosen from literature to estimate OC module parameter and composting experiments describing two different organic pollutants (simazine and pyrene) were also chosen from literature to optimize OP module parameters. For the model evaluation, in OC module, seven fixed parameters were obtained from the literature or calculated directly from the measurements, while six were estimated by inverse modelling of the OC module; in OP module, adsorption coefficient (Kd) values were calculated and estimated directly on the basis of experimental data, while the other parameters were optimised by the model. In order to assess the relative importance of individual parameters on the overall model performance, a sensitivity analysis was also conducted. A good agreement was achieved between simulated and experimental results describing the evolution of different organic fractions except a poor simulation of the cellulosic and soluble pools. The sensitivity analysis demonstrated that the assimilation yield (Y), the death rate (m), adsorption coefficient (Kd_i) and the degradation rate (dr) greatly influenced the evolution of all the OP fractions.

4.2 Introduction

In recent years, a huge growth of organic waste treatment by composting has been seen across Europe (European Communities, 2005). However, a wide range of organic contaminants may be introduced into compost (Brändi et al., 2005) by the pathways of

atmospheric deposition and direct application of pesticides. These organic pollutants (OP) have been observed to persist in the environment, bioaccumulate in human and animal tissue, and to have potential significant impacts on human heath and the environment.

On the other hand, composting has been demonstrated to be effective in biodegrading polycyclic aromatic hydrocarbons (PAHs) (Potter et al., 1999; Canet et al., 2001; Antizar-Ladislao et al., 2006, Zhang et al., 2011a), chlorophenols (Laine and Jorgensen, 1997), polychlorinated biphenyls (PCBs) (Block, 1998) and some other OP. All these organic pollutants can be either degraded through the microbial activity that develops during composting or be stabilized through the formation of associations with the organic matter of the waste. Various potentials for compost microflora to degrade OP have been observed (Harlieb et al., 2003).

During the composting process, there are a number of potential fates for organic pollutants. These include mineralization to carbon dioxide, conversion to humic matter, incorporation into microbial biomass, adsorption, biotransformation, volatilization, and leaching (Michel et al., 1995). The transformation of OP is function of the evolution of organic matters (Benoit et al., 1996), the microbial activities (Haderlein et al., 2006) and the specific property of OP (Hartlieb et al., 2003).

As we know, the fates of OP showed complexity during the composting system. In order to better understand the behaviours of composting systems and predict the dynamics of OP during composting, modelling is considered as a good tool. Since 1976, mathematical modelling of composting process has appeared in literature. Most of modellers have typically looked at the composting system on a macro-scale, in which the couple of heat and mass balance, the effect of temperature, moisture, oxygen and evolution of organic matters have been focused on (Mason, 2006, Sole-Mauri et al., 2007, Lin et al., 2008, Vlyssides et al., 2009). However, until now no model of composting considers the dynamics of OP. Models describing the dynamic of OP exist specifically in soil science (Saffih-Hdadi et al., 2003). Most of these models focused on the sorption-desorption process (Ma and Selim, 1994; Brusseau et al., 1991; Xue et al., 1997) or biodegradation kinetics (Soulas, 1997). Few of these models took into account the microbial activities (Soulas and Lagacherie,

1990; Shelton and Doherty, 1997). Models describing the OP dynamics in composting system calibrated by experimental data have still not been proposed.

Therefore, the objective of our research were i) to build a model describing the dynamics of organic micro-pollutants and considering the decomposition of organic matters in order to better understand the composting system performance to degrade OP and ii) to test it using the data of literature using C14 labelled organic pollutants. In the following sections, we presented the COP-Compost model with its calibration and evaluation for each OC and OP modules first, and with their interaction, secondly. At the end, a sensitivity analysis is presented.

4.3 Materials and methods

4.3.1 Presentation of COP_Compost model

This section briefly presents the structure of COP_Compost model (see Fig.4.1). It consists in 2 parts: OC module which presents the dynamics of organic carbon (OC) and OP module presenting the evolution of organic micro-pollutants (OP). The model COP_Compost can run each module separately or together.

The OC module was already presented in Zhang et al. (2011b). The OC pool was divided into 4 pools with increasing degradability. These 4 pools were characterized into soluble fraction (SOL), hemicelluloses (HEM), cellulose (CEL) and lignin (LIC) by using the method of Van Soest (1967), where the SOL fraction was divided into 2 pools with fast degradability (SOL-F) and slow degradability (SOL-S) based on their different performance. Such heterogeneities and evolution of the SOL fraction characteristics during composting have been evidenced in several works (Lichtfouse et al., 1998; Pascual et al., 1999; Francou et al., 2008) which have already detected the presence of easily degradable substrates and more recalcitrant substances simultaneously in soluble fractions. These OM fractions were hydrolyzed into available substrates (H2O) for microbial growth according to specific hydrolysis constants. A maximum of 3 microbial biomasses, each with particular substrate specificity and optimum temperature for growth, can be activated. The microbial degradation of the hydrolyzed substrate is modelled with Monod kinetic, modulated with a temperature growth-limiting function. Microbial biomasses died according to a decay rate and then became either available substrates (H2O) once more for growth of

living micro-organisms or join a resistant OC pool (SOL-S). The equations of OM module were already given in Zhang et al. (2011b).

The OP module describes the organic pollutants behavior. It considered three pools of the OPs: soluble, sorbed and bound to organic matter. This module also considered a compartment of CO_2 issued from the mineralization of OPs which was degraded by a specific microbial population. The OP compartments were characterized by successive extractions with water (soluble fraction), then with another solvent adapted to the OP properties (sorbed fraction). Finally, NER were measured after extractions and represented the OP bound to organic matter. The model assumed that: i) the NER were produced from the sorbed OPs and ii) the OP biodegradation occurred in the soluble phase only. The NER formation and OP biodegradation rates were Fr and dr, respectively. Moreover, OP allocation between the soluble and sorbed pools was an instantaneous equilibrium described with a sorption coefficient (Kd).

For the OC-OP coupling model, three types of interactions between OC and OP were proposed as hypotheses formulated based on literature. First, the sorption coefficients of the OP on OC are function of the quality of the OC, represented by the proportions of the different biochemical fraction of OC pools. Second, OPs were degraded by co-metabolism with micro-organisms whose growth rate and quantity are mainly driven by OC decomposition. A specific degradation rate of OP may also be used. It supposed a specific microbial population which could degrade the OP without the nutrition of OC. Third, the formation of bound residues was influenced by a specific rate of bound residues formation and the growth rate of the microbial population. The equations of the model are given in Table 4.1.

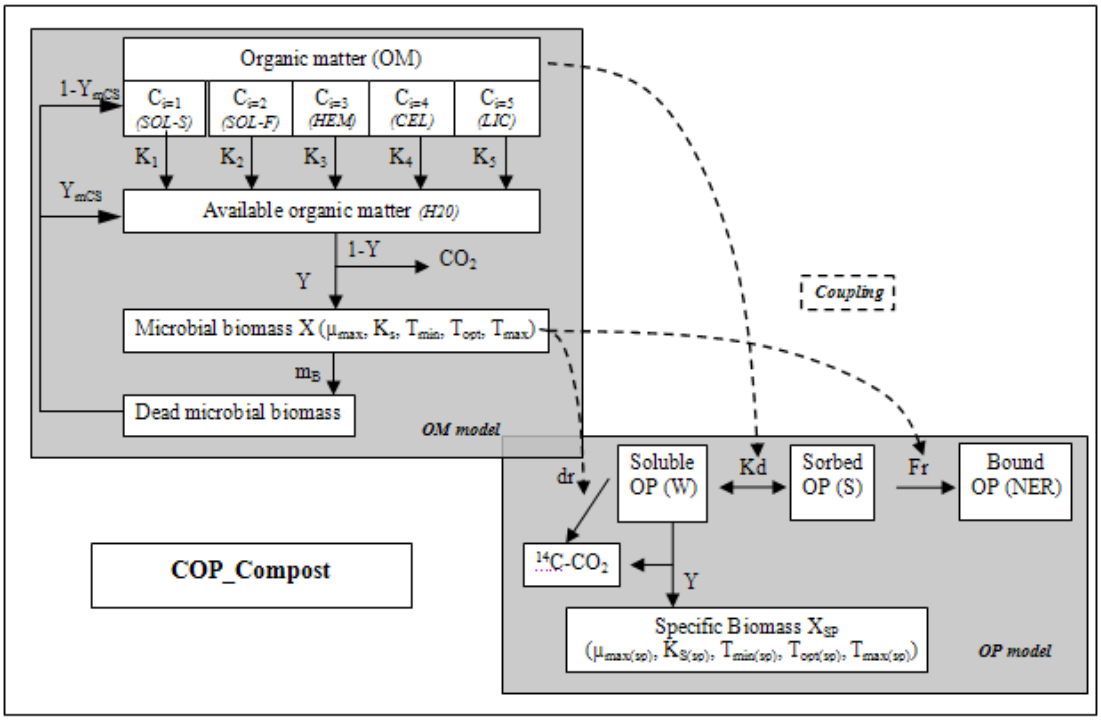


Figure 4.1: The presentation of COP_Compost model

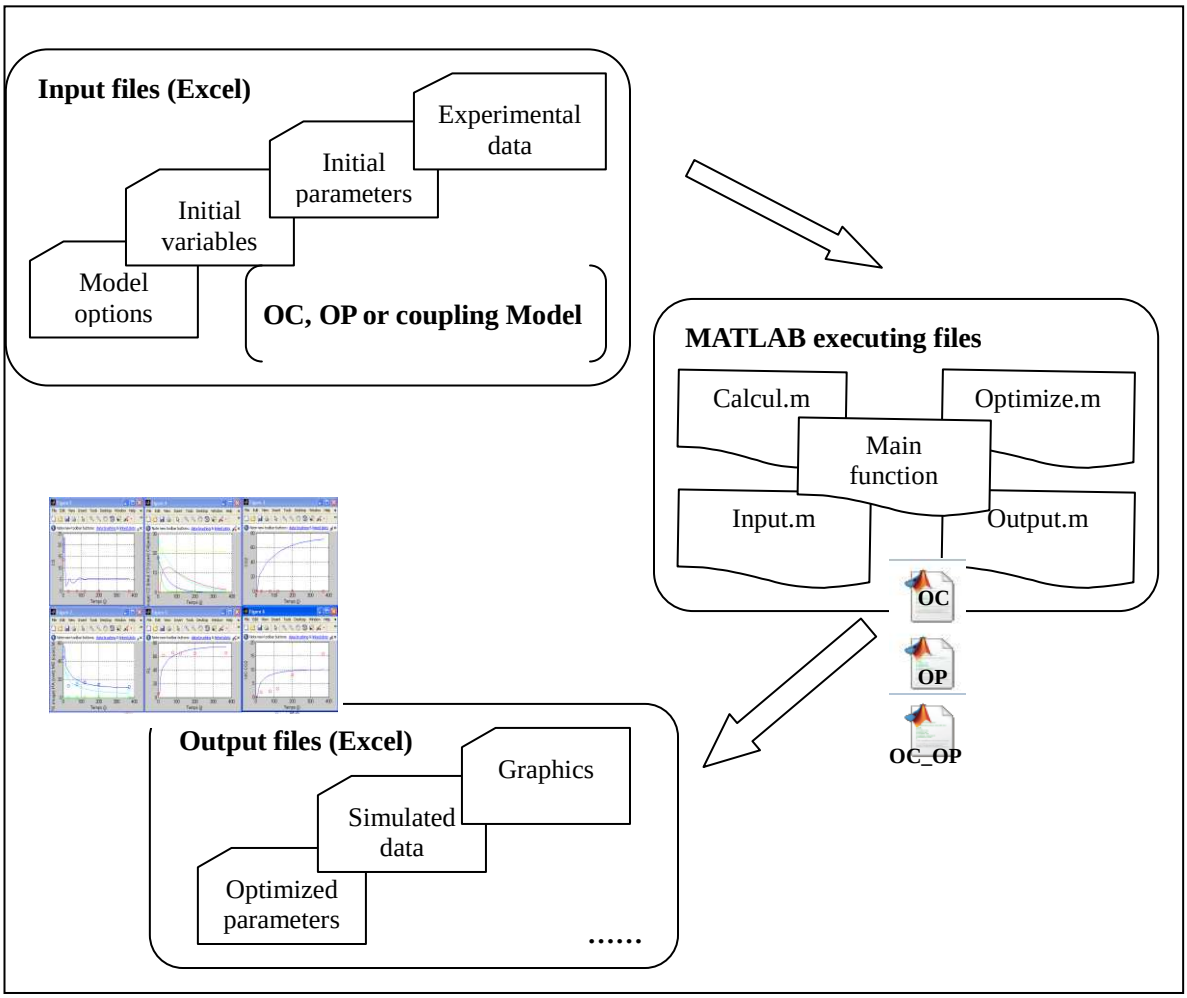


Figure 4.2: The structure of MATLAB interface

4.3.2 Software / Interface (MATLAB & Excel)

Our numerical model was developed using MATLAB software, assisted by Excel files. In order to be convenient for users and much easier to familiar the program without the knowledge on MATLAB, we took Excel files as the input and output files, so that users needn't to do the changes in MATLAB interface. Optimization toolbox for solving non-linear least square problems has been used to estimate the model parameters. The model is organized in three main parts (Fig.4.2): Executing files, Input Excel files and Output Excel files. The Matlab platform was chosen to realize the executing files, because it provides a good environment not only to do the programming, but also to show the simulation figure immediately at each running, which can give us a visual judgement. This section presents the 3 parts in details.

4.3.2.1 MATLAB executing files

Our software was implemented in the Matlab platform (The MathWorks, Natick, Mass, USA, version 7.9.0.529 R2009b) to perform the dynamical simulations either for one run or for several runs if the option "parameter estimation" was activated. The program is divided into 5 functions:

- The function 'main.m' is the principal executing function which contains the declaration of variables and parameters, the concerned function calls and exportation of the graphics of simulation in MATLAB.
- 'Calcul.m' is the function for calculating all the variables according to the mathematical equations (for OP module, see Table 4.1 and for OC module see Zhang et al., 2011) of COP_Compost model.

Table 4.1: Equations for OP module

	Process	Process equations
OP Module	Decomposition of soluble OP (W)	$\frac{dW}{dt} = -dW$
	Balance between soluble (W) and sorbed OP (S)	$S = KdW$ Where, $Kd = \sum_{i=1}^{5} Kd_i \frac{C_i}{\sum_{i=1}^{5} C_i}$ for OM_OMP coupling model
	Formation of non extractible residues (NER)	$\frac{dNER}{dt} = NER_0 + FrS$ Where, $Fr = Fr_C + Fr_B \cdot \sum_{h=1}^{3} X_h$ for OM_OMP coupling model, Fr_C is a constant and is considered to be zero in coupling model
	Mineralisation of OP (^{14}C-CO_2)	$\frac{d\,^{14}C - CO_2}{dt} = drW$ Where, $dr = \sum_{h=1}^{3} (X_h \cdot dr_h)$ for OM_OMP coupling model And $\frac{d\,^{14}C - CO_2}{dt} = \sum_{h=1}^{3} (X_h \cdot dr_h) \cdot W + (1 - y) \cdot \frac{\mu_{sp} X_{sp}}{y}$ for coupling model with specific microbial population Where, $\mu_{sp} = \mu_{max\,(sp)} \frac{W}{K_{S(sp)} + W} f_{T(sp)}$

- 'Optimize.m' contains the estimation algorithm using the minimization function which attempts to find a constrained minimum of a scalar function of several variables starting at an initial estimate. Our program used the function 'fmincon'. This is generally referred to as constrained nonlinear optimization or nonlinear programming which has the form below.

x = fmincon (fun, x0, A, b, Aeq, beq, lb, ub, nonlcon, options)

Which starts at x0 and minimizes the function 'fun' with the optimization options specified in the structure options. Variable x is defined by a set of lower and upper bounds, so that the solution is always in the range $lb \leq x \leq ub$.

- 'Input.m' is used to import the initial values of experimental data from Excel
- 'Output.m' is used for exporting the results (data and figures) into Excel

4.3.2.2. Input files (Excel)

In order to use the model more easily without having MATLAB, we applied Microsoft Office Excel as an interface of data input. The input files enclose the experimental data, the initial conditions, the initial parameters values, the parameter constraints, and the different options.

The Excel interface was built with a set of worksheets:

- The worksheet "main menu" concludes all the indicate information for program operation.
  - The "Options" gives the choices for users: form of execution: simulation or optimisation; model of operation: OC, OP or coupling model; number of microbial populations to be applied in the model; type of kinetics used for microbial growth…
  - Several buttons with indicate information: different input parameter worksheets according to different models; different output results, for example, optimised parameters, output simulation results, output graphs, etc.
- The worksheet "Guide" is a user's manual with all operation details

- The worksheet “Initial_OC”, “Initial_OP” and ‘Initial_OP_couple” are used for the parameters of OC, OP and OC_OP coupling model respectively to provide the initial values of parameters, the lower limit, upper limit and also the choice for optimisation of parameters (choose the ones to be optimised and the others to be kept in initial values) for the model program.
- The worksheet “Data_Exp” is filled with the experimental data, using ‘0’ or ‘1’ to control the operation of optimisation in the model.
- The worksheet “Schema” shows the diagram of the model COP_Compost.

4.3.2.3 Output files (Excel)

The output data were also conserved in this Excel interface:

- The sheet “Optimised parameters” is used for the exit of optimised parameters;
- The sheet “Results_Simul” is the exit of the simulation results for each pool;
- The sheet “Print” is used as the print page with all details about optimised parameters, model efficiency and simulation figures in order to be convenient for users

4.3.3 Experimental Data for model calibration and evaluation

The calibration of the OC module was already presented in Zhang et al. (2011b) using the data of Francou et al. (2008) and Doublet et al. (2010). For the calibration of OP module, we used the data of Hartlieb et al. (2003). These authors carried out a composting experiment using biowaste. However, the data necessary to simulate with COP-Compost the OM dynamic during composting, like the biochemical fractions, were not available. In the following, we used one of the composting experiments used to calibrate our OM module and described in Zhang et al. (2011b).

4.3.3.1 Data acquisition for calibration and evaluation of the OP module

The data for calibration of OP model were collected from the article of Hartlieb et al. (2003) with 2 types of OP: pyrene and simazine. In his experiments, the composting of contaminated municipal biowastes was performed during 370 days in pilot-scale

bioreactors of 1.8 m^3. The ^{14}C-labelled pollutants were used to follow the dynamic of OPs with the composting performance. The application of each model substance (^{14}C-pyrene, ^{14}C-simazine) to the biowaste was carried out individually prior to composting. Initially applied concentrations were 0.56 mg pyrene (kg dry mass)$^{-1}$ = 5.6 MBq pyrene (kg dry mass) $^{-1}$; 1.17 mg simazine (kg dry mass) $^{-1}$ = 9.5 MBq simazine (kg dry mass) $^{-1}$. Sequential extractions were carried out to differentiate the ^{14}C activity between extractable fractions and non-extractable residues. The NER was measured by combustion from the exhaustively extracted material.

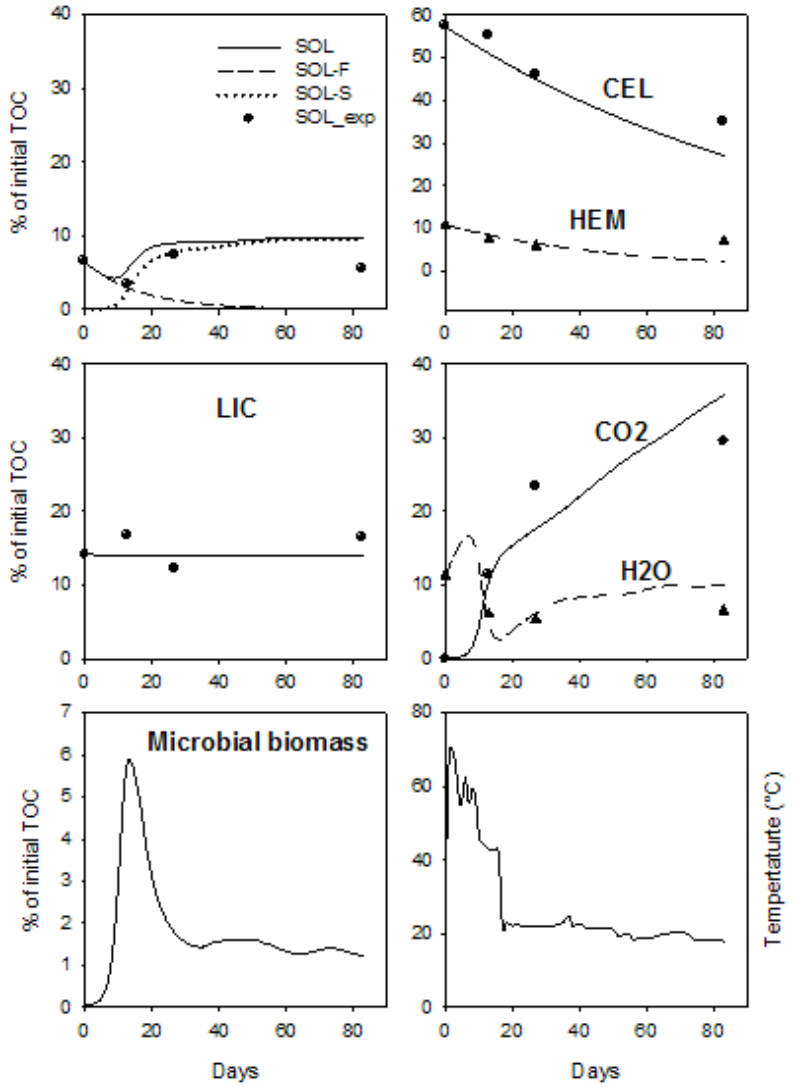


Figure 4.3: Example of simulation (curves) of the experimental data (points) set corresponding to the composting mixture R4 used for the evaluation of the model. The simulations were done using the average estimated parameters of Table 4.2.

4.3.4 Model calibration for OP module

To calibrate the model and study the parameter sensitivity, the results of Hartlieb et al. (2003) were used to simulate the OP, and then coupling with one of the organic mixtures P3 described in Zhang et al. (2011). The mixture P3 (green wastes=64%; sewage sludge=14%; branches=17%; grass clippings=5%) was made initially from 4 organic fractions (SOL = 16.15, HEM = 13.8, CEL = 26.6 LIC = 28.33 and H2O = 15.12, with a unit: % of initial TOC). Fig.4.3 gave the experimental and simulated dynamic of the organic pools during the composting of P3.

One microbial population was applied at first for the calibration process. Totally there were 13 parameters for the OC module given in Table 4.2. For the OP module, we need to fit either 8 or 4 parameters: one or 4 adsorption coefficients (Kd_i) depending if we consider of the different biochemical fractions of the OM, 2 bound residue formation rates (Fr_B related to biological activity, Fr_C for chemical activity) and one OP degradation rate dr.

In a first calibration, the adsorption coefficient was fixed to the same value calculated as the ratio between the initial experimental concentration of sorbed OP and soluble OP (Kd (%) = Concentration of sorbed OP / concentration of soluble O). Then, the coefficient Fr and dr were estimated by model inversion. In a second calibration, the Kd_i were estimated with the constraint: Kd (LIC)> Kd (HEM, CEL) > Kd (SOL). Gaillardon et al. (1983) showed that the organic substrates adding into the soil lead to an increase in the quantity of adsorbed herbicides with the following order: substrates ≤ membrane ≤ lignocellulose ≤ lignin. Furthermore, Xing et al. (1994) found the following order for adsorption coefficients of (benzene, toluene and oxylene): cellulose ≤ humic acid ≤ lignin.

Parameter estimation was performed using the fmincon function of Matlab. The objective function was $RRMSE_{tot}$, the sum of RRMSE (%) calculated between the experimental and simulated values of each compartment of OP module; i.e. (W, S, NER, and CO_2. (Smith et al., 1997), as follows:

$$\text{RRMSE} \quad (\%) \;=\; \frac{100}{\overline{O}} \sqrt{\sum_{i=1}^{n} \frac{(S_i - O_i)^2}{n}} \qquad [1]$$

Where n is the number of measurement, Si and Oi are respectively the simulated and observed values, and O is the average of n experimental values. The best simulation was that producing the lowest RRMSEtot.

The efficiency coefficient, E_f, and the mean difference, $\overline{D}$, of the model were used in addition to evaluate the simulations (Smith et al., 1997):

$$E_f = \frac{\sum_{i=1}^{n} (O_i - \overline{O})^2 - \sum_{i=1}^{n} (S_i - \overline{O})^2}{\sum_{i=1}^{n} (O_i - \overline{O})^2} \quad [2]$$

$$\overline{D} = \frac{\sum_{i=1}^{n} (S_i - O_i)}{n} \quad [3]$$

4.3.5 Sensitivity analysis

A sensitivity analysis of the model was conducted i) to identify the most sensitive parameters and ii) to study the importance of the initial organic matter quality of the compost and iii) to study the initial quantity of microbial biomass.

In order to assess the relative importance of individual parameters on the overall model performance, a first sensitivity analysis was conducted. Each parameter was successively modified to the ±20% of its default value. The effect of these individual changes was investigated on 4 variables: soluble fraction (W), sorbed fraction (S), bound residues (NER) and carbon dioxide gas (^{14}C-CO2).

In this study, the sensitivity coefficient was expressed by the form below:

$$\sigma_{20\%} = \frac{1}{t_f} \int_0^{t_f} \frac{S(p + 20\%, p_0, \tau) - S(p, p_0, \tau)}{S(p, p_0, \tau)} d\tau \quad [4]$$

Where time τ ranged from 0 to t_f; S (p, p0, τ) denotes the simulated value of variable S at time τ associated with the parameter equal to its initial value p_0 (Bernard et al. , 2001).

A second sensitivity analysis was conducted in order to study the sensitivity of the pyrene and simazine dynamics to initial quality of OC. We used 3 realistic materials

found in literature (Francou et al., 2008; Doublet et al., 2010) and calibrated in Zhang et al. (2011). The first compost P3 (in Zhang et al., 2011) was the mixture of green wastes (64% on dry weight), sewage sludge (14%), branches (17%) and grass clippings (5%); the second one R4 was the mixture of green wastes (26% on dry weight), biowastes (16%) and papers (58%); and the third one (in Doublet, 2008) was Fum_bovin_6388 was the mixture based on manures and sewage sludge (SS). These 3 mixtures showed high variability. The 5 biochemical fractions in P3 showed identical proportion; CEL gave a higher percentage in R3, while Fumier_Bovin_6388 was rich in H2O fraction.

Finally, a model sensitivity of the initial quantity of microbial biomass to the pollutant behaviour was conducted. The values of 0.005, 0.05, 0.5, and 5 (g C 100 g^{-1} initial TOC), were tested. These values were comparable with the review of Eiland et al. (2001) who found a range from 1.4 to 8.6 mg microbial carbon per g of organic matter (approximated to be 0.056 to 0.430 (g C 100g^{-1} dry mass)).

4.4 Results and discussion

4.4.1 Calibration of OP module

The simulations of pyrene (see Fig.4.4-A) and simazine (Fig.4.4-B) were obtained by optimising the parameters of OP (Table 4.3) for one microbial population.

The efficiency coefficients of Table 4.4 indicated a good agreement between simulated and observed data for the 3 fractions of pyrene (with a low E_f value for soluble fraction). While for simazine, we found a good agreement between simulated and observed data for 3 fractions except ^{14}C-CO_2, which had a negative E_f value.

Figure 4.4-A: **Figure 4.4-B:**

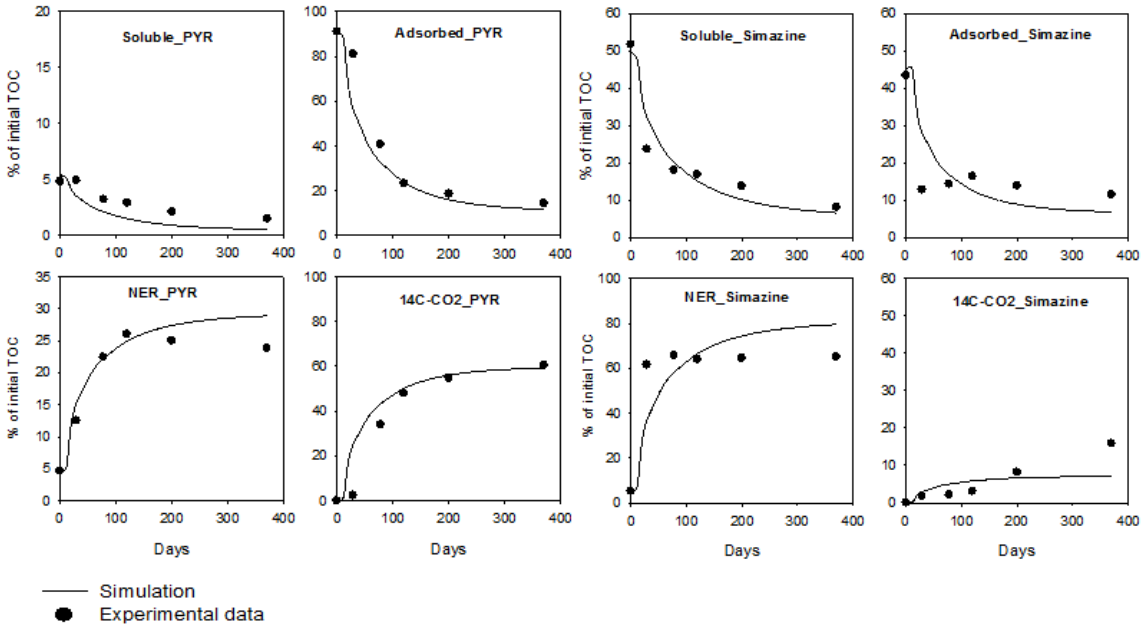


Figure 4.4: Comparison between simulated results and observed data (obtained from Hartlieb et al., 2003) for the 4 fractions (soluble, sorbed, NER and mineralised fraction) of pyrene (Fig.4-A) and simazine (Fig.4-B).

Table 4.2: Variables and parameters in the COP-Compost model

	Symbol	Description	Value proposed*	Unit
Variables of the model				
OM model	C_{i-1}	Proportion of OM in the SOL fraction with slow degradation (SOL-S)		% of initial TOC
	C_{i-2}	Proportion of OM in the SOL fraction with fast degradation (SOL-F)		% of initial TOC
	C_{i-3}	Hemicellulose (HEM)		% of initial TOC
	C_{i-4}	Cellulose (CEL)		% of initial TOC
	C_{i-5}	Lignin (LIC)		% of initial TOC
	C_a	OM soluble in hot water (H20)		% of initial TOC
	X	Microbial biomass		% of initial TOC
	CO_2	Carbon dioxide gas		% of initial TOC
OP model	W	soluble OP in which is water extractable		% of initial ^{14}C
	S	Sorbed OP which is solvent extractable		% of initial ^{14}C
	NER	Bound residues non extractible		% of initial ^{14}C
	^{14}C-CO_2	^{14}C-labeled carbon dioxide gas		% of initial ^{14}C
Parameters of the model				
OM model	K_1	Rate of transformation in available C_{i-1} (SOL-S)	0.018	day^{-1}
	K_2	Rate of transformation in available C_{i-2} (SOL-F)	0.061	day^{-1}
	K_3	Rate of transformation in available C_{i-3} (HEM)	0.019	day^{-1}
	K_4	Rate of transformation in available C_{i-4} (CEL)	0.009	day^{-1}
	K_5	Rate of transformation in available C_{i-5} (LIC)	0.001	day^{-1}
	Y	Assimilation rate of the available OM for X	0.5	
	μ_{max}	Maximal specific growth rate for microbial biomass	5.996	day^{-1}
	K_s	Saturation constant for Monod kinetic	101.1	% of initial TOC
	T_{min}	Minimum temperature for microbial growth	0	°C
	T_{max}	Maximum temperature for microbial growth	49	°C
	T_{opt}	Optimum temperature for microbial gorwth	83	°C
	m_B	Death constant for microbial biomass	0.2290	day^{-1}
	Y_{met}	Availability rate for dead microbial biomass	0.4	
OP model	Kd	Adsorption coefficient of OM		g C ads g^{-1} C sol
	Kd_1	Adsorption coefficient of C_{i-1} (SOL-S)		g C ads g^{-1} C sol
	Kd_2	Adsorption coefficient of C_{i-2} (HEM)		g C ads g^{-1} C sol
	Kd_3	Adsorption coefficient of C_{i-3} (CEL)		g C ads g^{-1} C sol
	Kd_4	Adsorption coefficient of C_{i-4} (LIC)		g C ads g^{-1} C sol
	Fr_B	NER formation rate related to biological activity		day^{-1}
	Fr_C	NER formation rate related to chemical reactivity of the compost organic matter		day^{-1}
	dr	OP degradation rate		day^{-1}

According to observed data, the mineralization of simazine was much lower than that of pyrene, with a different kinetic. While using the actual equations, the simulation can not be improved. A specific microbial population was added to simulate the mineralization of this organic pollutant. This result is supported by Kästner (1999), who detected that after inhibition of fungi; slower metabolism and an increased in the formation of bound residues compared to the uninhibited control. After inhibition of bacteria, no metabolism occurred. This indicated that bacteria made the major contribution to the metabolism of organic micro-pollutants. As a result, in the following simulations, the same parameters were applied besides a specific microbial population added for the degradation of soluble OP, with the optimized value of 3.5 day^{-1} for μ_{sp} (see the equation for μ_{sp} in table 1). The set of temperature parameters for specific biomass were obtained from literature (Rosso et al., 1993): $T_{min(sp)}$ = 5.1°C, $T_{max(sp)}$ = 47.1°C and $T_{opt(sp)}$ = 36.8°C. This set of temperature differed from the one for microbial population of OC, who had a larger range of temperature profile of microbial growth. The simulations of simazine were regenerated with the new equations which fitted better the experimental data especially for the mineralisation fraction (shown in Fig.4.5).

Table 4.3: Parameter values and evaluation statistics of OP simulations (units given in Table 4.2)

	One microbial population		**Two microbial population**
	Simazine	**Pyrene**	**With a specific biomass**
NER_0	5.100	4.800	5.100
Kd_1	0.001	0.001	0.001
Kd_2	0.93	19.800	0.93
Kd_3	0.93	15.197	0.93
Kd_4	1.167	24.716	1.167
Kd_5	0.000	0.000	0.000
Fr_B	0.012	0.002	0.012
dr	0.001	0.080	0.001
RRMSE-OP_{tot}	138	124	98

According to the evolution of observed data, the mineralization of simazine seemed to be different from that of pyrene, because it showed an exponential kinetic. While with the existing equations, the dynamics can’t be simulated better, so a specific microbial

population was proposed in our model to simulate the mineralization of these organic pollutants. This hydrolysis could be supported by Kästner (1999), who detected that after inhibition of fungi; slower metabolism and increased formation of bound residues were observed compared to the uninhibited control. After inhibition of bacteria, no metabolism occurred. This indicated that bacteria made the major contribution to the metabolism of OP. As a result, in the following simulations, the same parameters were applied besides a specific microbial population added for the degradation of soluble OP, with the optimized value of 3.5 day^{-1} for μ_{sp} (see the equation for μ_{sp} in Table 1). The set of temperature parameters for specific biomass were obtained from literature (Rosso et al., 1993): $T_{min(sp)}$ = 5.1°C, $T_{max(sp)}$ = 47.1°C and $T_{opt(sp)}$ = 36.8°C. This set of temperature differed from the one for microbial population of OC, who had a big range of temperature profile of microbial growth. The simulations of simazine were regenerated with the new equations which fitted better the experimental data especially for the mineralisation fraction (shown in Fig.4.5 and Table 4.3).

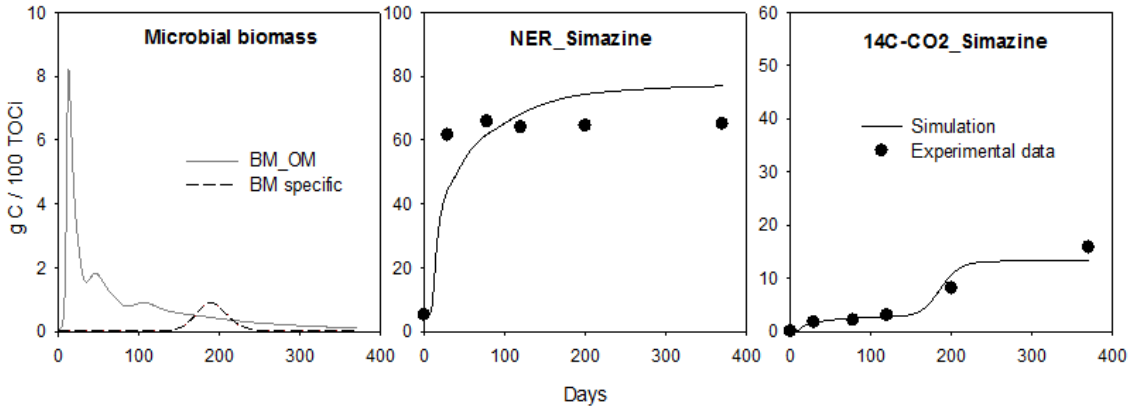


Figure 4.5: Comparison of observed data of simazine (obtained from Hartlieb et al., 2003) and simulated results using the model with adding a specific microbial population.

Table 4.4: Statistical evaluation of model efficiency in the simulations obtained using model coupling

	OP fractions	One microbial population		Two microbial populations (with an Xsp)
		Simazine	Pyrene	Simazine
RMSE-OP	Soluble	12	34	17
	Sorbed	28	24	34
	NER	18	14	18
	14C-CO2	80	31	29
	RMSE-OP_{tot}	138	108	98
$\overline{D}^{a}$	Soluble	-0.24	-1.0	-0.7
	Sorbed	0.51	-6.2	-0.1
	NER	-0.73	1.5	0.8
	14C-CO2	0.49	5.9	0.0
E_f^{b}	Soluble	0.96	-0.39	0.91
	Sorbed	0.75	0.82	0.64
	NER	0.99	0.99	0.99
	14C-CO2	**-0.98**	0.72	**0.74**

[a] Mean difference (as a % of initial ^{14}C)

[b] Efficiency coefficient

4.5 Sensitivity analysis

4.5.1 Sensitivity of pyrene and simazine to all parameters

The sensitivity coefficients were performed for 10 parameters of the model for Pyrene and 12 parameters for Simazine (the 2 extra parameters describing the specific biomass were included). Fig.4.6-A and Fig4.6-B, show the sensitivity to each parameter of each compartment of pyrene and simazine, respectively.

The Fig.6-A indicated that the soluble fraction of pyrene was sensitive to the model parameter Y (assimilation rate), m (death rate) and dr (degradation rate), while sorbed fraction of pyrene was sensible not only to these three parameters, but also to Kd_i (adsorption coefficient). It seems that the parameters linked to microbial population of OC had a significant influence on the evolution of soluble and sorbed fractions of OP. The first parameter influencing NER fraction of pyrene was Fr_B (NER formation rate related to biological activity), and followed by Y, m, Kd_i and dr. The parameter which

had strong influence on the mineralisation of pyrene was Y, and then followed by dr, Kd_i and m.

En comparison, for simazine (see Fig.4.6-B), after the specific microbial population was added, the parameters Y, m and Fr still played an important role on the dynamics of all OP fractions but the parameter $u_{max(sp)}$ (maximal growth rate for specific microbial biomass) and in a certain proportion $K_{S(sp)}$ (saturation constant for specific microbial biomass) showed the strongest influence on the soluble, sorbed and mineralised fraction of simazine except NER fraction.

The parameter Ks (saturation constant for Monod kinetic) exhibits a low influence to all fractions of either pyrene or simazine. Two possible explanations are suggested by Sole-Mauri (2007) to justify behaviour: if the saturation constant for hydrolysis is too low, the effect on objective function is only noticeable when it reaches a value which is high enough but, if this value is appropriate, the effect of this constant is only detected when it takes a large value.

The results illustrated in this section demonstrated that the parameter linked the specific organic pollutant and the microbial activity by co-metabolism had a strong effect on model output.

Figure 4.6-A: Figure 4.6-B:

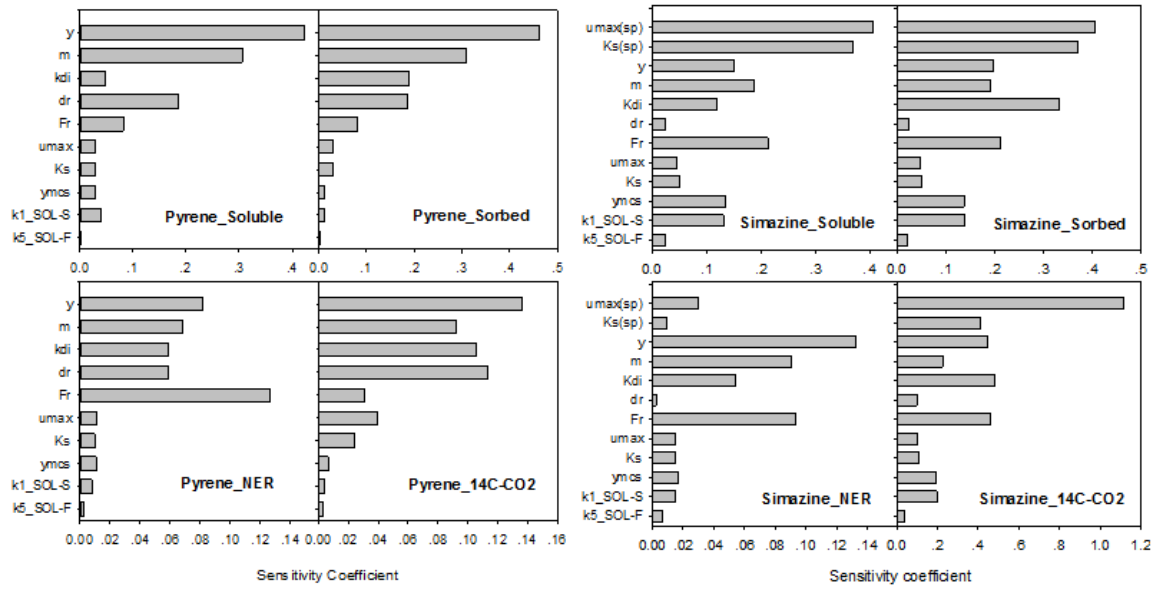


Figure 4.6: Sensitivity coefficient of the different model parameters for the 4 fractions of pyrene (Fig.4.6-A) and simazine, with adding the specific microbial population (Fig.4.6-B).

4.5.2 Sensitivity to initial conditions

The four other sets of experimental data obtained in 170-L pilots (R2, R4, P4, P6), were used to evaluate the model. The average RMSE-OC_{tot} of the validation datasets (with a value of 155) was lower than that of the calibration datasets (with a value of 184), thus showing an improvement in the simulations for validation (see the details in Zhang et al., 2011). The simulations obtained were within the range of variation of the experimental measurements in the six composting replicates.

4.5.2.1. Sensitivity to initial quality of OC

As mentioned by Tester et al. (1978) and Angers and Recous (1997), the carbon degradation of dry fractions of composts and crop residues had the potential to be changed because of the organic fraction quality of organic matters. Moreover, the repartition of no-extractable residues varies as a function of particle-size fraction of soil, which can be linked to the sorption quality of OP that will be influenced by the quality of these fractions (Loiseau and Barriuso, 2002).

According to these researches, it is interesting to study the influence of initial quantity of OC. Two examples by using pyrene and simazine showed the model sensitivity to initial quality of OC. As shown in Fig.4.7 and Fig.4.8, different existing quality of organic substrates with varied initial Van Soest compositions were applied for the sensitivity analysis. Consequently, the microbial biomass gave different growth dynamics, which led to slightly different evolutions of OP fractions, especially at the beginning of composting process, while no strong influence could be observed among the 3 different organic mixtures. Obviously, organic substrates which were degraded to a significant extent during composting have only small effect on residue formation.

4.5.2.2. Sensitivity to initial quantity of microbial biomass

As portrayed in Fig.4.9, we did not found significant influence of initial quantity of microbial biomass (varied from 0.005 to 5 (g C 100 g^{-1} initial TOC)) on each fraction of OP, except the effect observed at the early stage of OP mineralisation. The mineralisation rate increased with the initial microbial biomass. That could be explained by the evolution of microbial growth: no matter how much the initial

quantity of biomass was, the microbial growth climbed quickly and the quantity reached to the peak just before the 20th day of composting and then it decreased rapidly and after 30 days it has returned to a mall quantity of biomass.

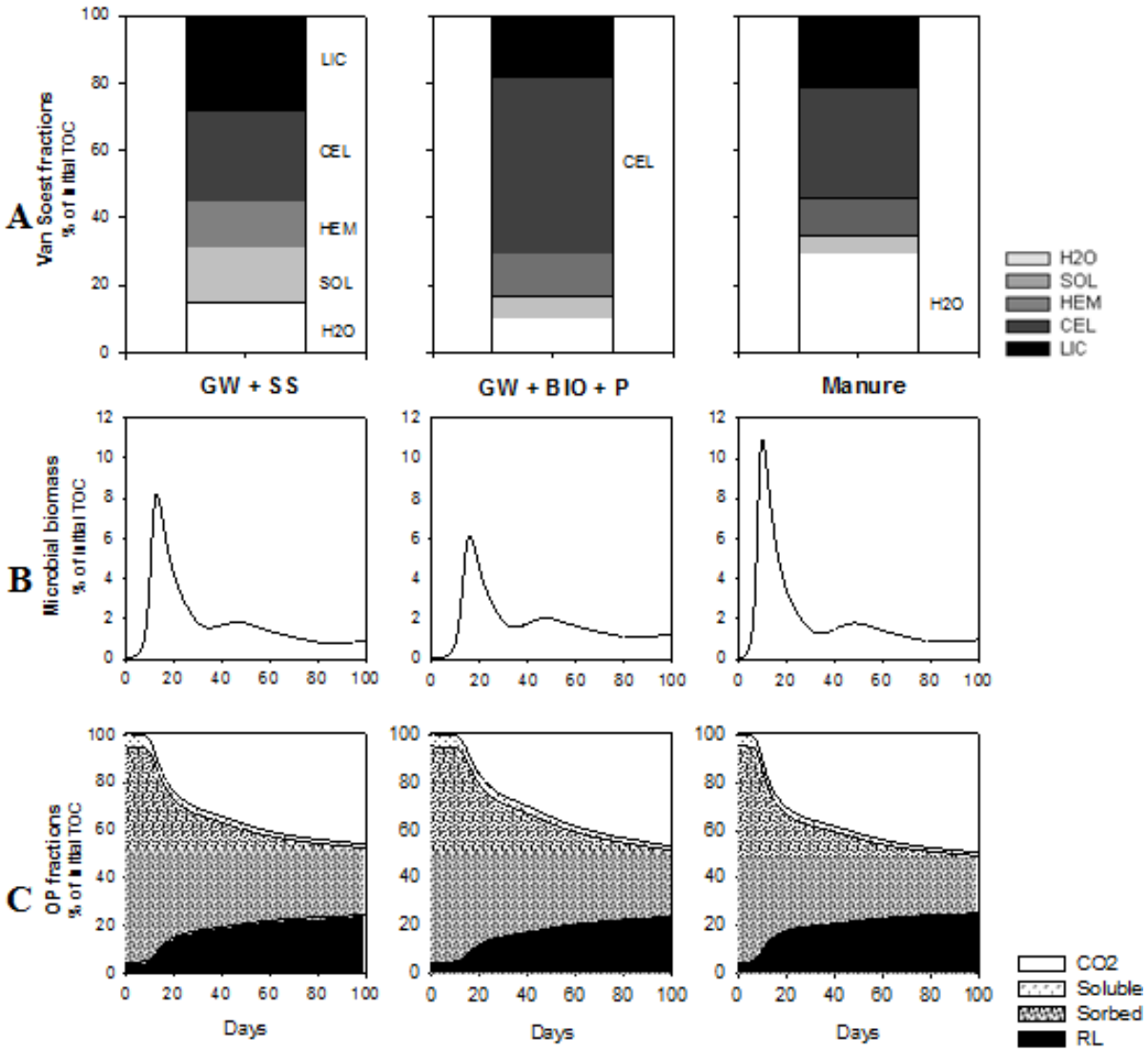


Figure 4.7: The sensitivity of pyrene to the initial quality of organic matters. Initial quantity of fraction of pyrene was: W_0 (Soluble) = 4.8; S_0 (Sorbed) = 91; NER_0 (non extractable) = 4.6 (gC / 100g TOCi). GW+SS = mixture of P3 (Doublet, 2008); GW+BIO+P = R4 (Francou, 2003); Manure =Fumier_Bovin. GW: Green wastes; SS: Sewage sludge; BIO: biowastes; P: Papers. Figures in line A represent the organic compositions characterized by the method of Van Soest. Figures in line B are the evolution of microbial biomasses in each organic waste. Line C shows the evolution of 4 OP fractions coupled with different organic wastes.

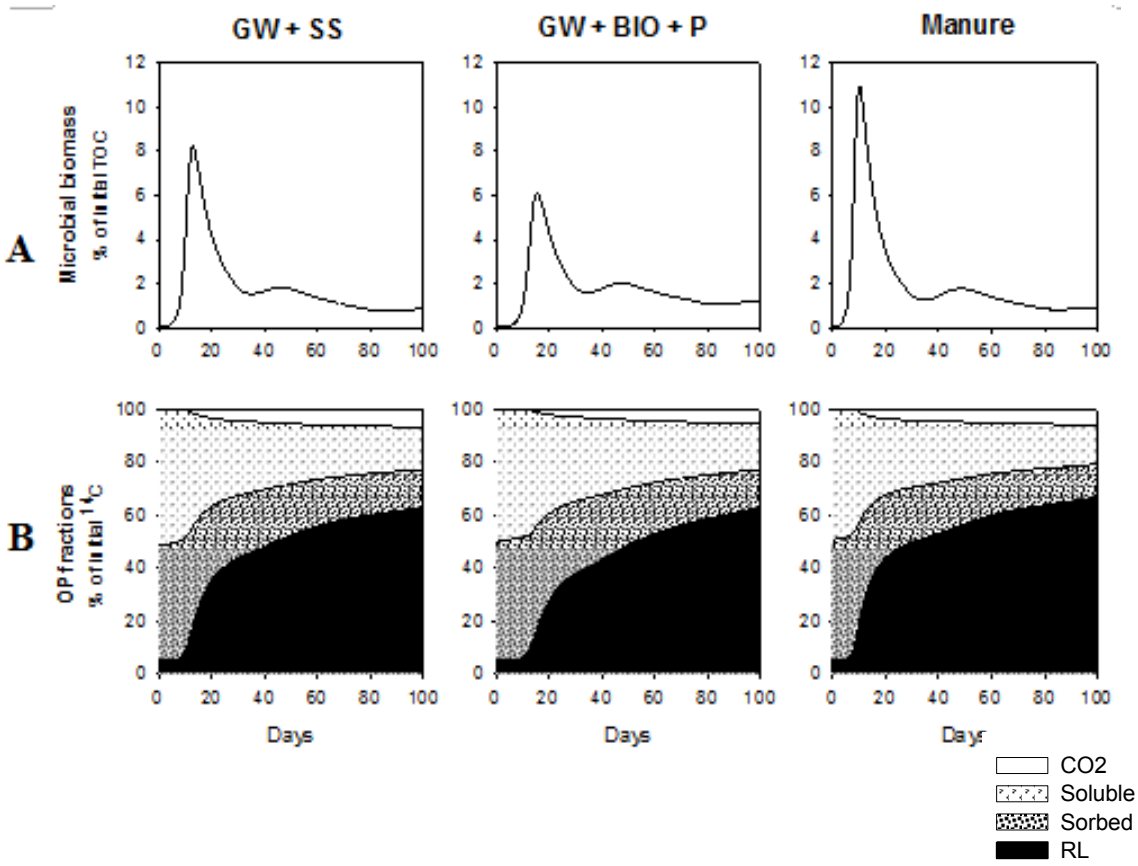


Figure 4.8: The sensitivity of simazine to the initial quality of organic matters. Initial quantity of fraction of pyrene was: W_0 (Soluble) = 51.6; S_0 (Sorbed) = 43.3; NER_0 (non extractable) = 5.1 (gC / 100g TOCi). Figures in line A are the evolution of microbial biomasses in each organic waste. Line B shows the evolution of 4 OP fractions coupled with different organic wastes.

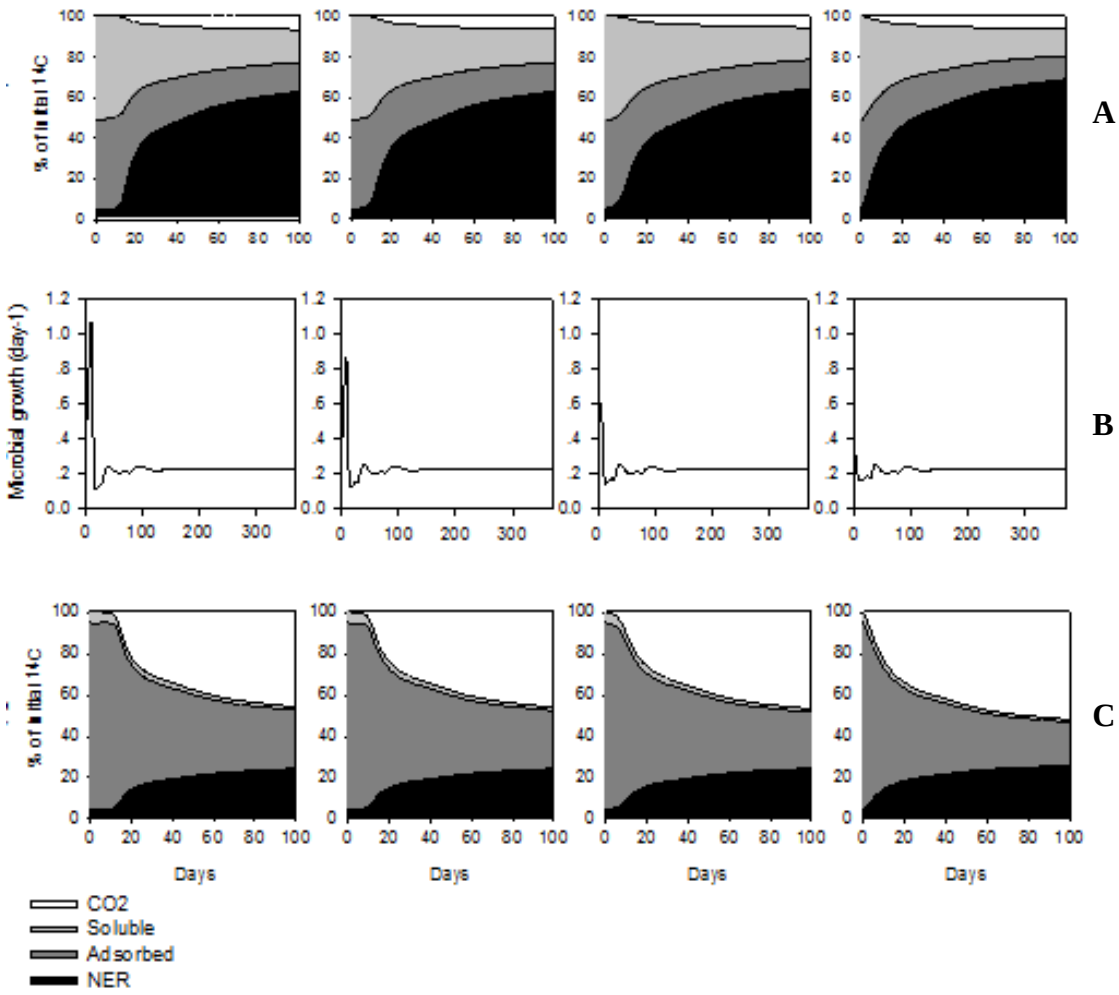


Figure 4.9: The sensitivity of each fraction (soluble, sorbed, non-extractable and mineralized fraction) of simazine (Line A) and pyrene (Line C) to the initial quantity of microbial biomass; Line B corresponds the evolution of microbial biomass.

4.6 Conclusion

A new model, coupling the dynamic of organic matter and organic pollutants during composting was built. The coupling model has been calibrated and its simulations could well fit the observed data taken from literature where labelled pyrene and simazine were studied during composting. By adding a specific microbial population into the coupling model, the simulations showed improvement especially for the mineralisation of simazine.

The sensitivity analysis demonstrated that the parameters linked to the activity of the microbial biomass degrading pollutants by co-metabolism and the adsorption coefficients (Kd_i) greatly influenced the evolution of all the fractions of either pyrene or

simazine, as well as the specific microorganisms for simazine; while a low sensitivity was found for parameters linked to the growth of microorganisms under standard operating conditions. These results are consistent with those found by Stombaugh and Nokes (1996) or Hamelers (2001), and contribute to the understanding the interactions between the different substrates and microbiota, and their relative importance to the composting process.

4.7 Acknowledgements

We are grateful to Egide, the French ministry of Foreign Affairs for providing financial support for this study through the program PHC-PFCC. We thank for supplying the PAH. We also would like to thank Dr. C. Francou from Veolia Environment, Research and Development and Dr. J. Doublet graduated from AgroParisTech-ABIES, for allowing us to use his data and for supplying additional information.

4.8 References

Angers, D.A., Recous, S., 1997. Decomposition of wheat straw and rye residues as affected by particle size. Plant and Soil, 189, 197-203.

Antizar-Ladislao, B., Lopez-Real, J., Beck, A.J., 2006. Degradation of polycyclic aromatic hydrocarbons (PAHs) in an aged coal-tar contaminated soil under in-vessel composting conditions. Environmental Pollution 141, 459–468.

Benoit, P., Barriuso, E., Houot, S., Calvet, R., 1996. Influence of the nature of soil organic matter on the sorption-desorption of 4-chlorophenol, 2, 4-dicholorophenol and herbicide 2, 4-dechlorophenoxyacetic (2, 4-D). Eur. J. Soil Sci. 47, 567-578.

Bernard, O., Hadj-Sadok, Z., Dochain, D., Genovesi, A., Steyer, J.P., 2001. Dynamical Model Development and Parameter Identification for an Anaerobic Wastewater Treatment Process. John Wiley & Sons, Inc.

Block, D., 1998. Degrading PCBs through composting. Biocycle 39, 45–48.

Brändli, R.C., Bucheli, T.D., Kupper, T., Furrer, R., Stadelmann, F.X., Tarradellas, J., 2005. Persistent organic pollutants in source-separated compost and its feedstock materials e a review of field studies. J. Environ. Qual. 34, 735-760.

Brusseau, M.L., Jessup, R.E. and Rao, P.S.C., 1991. Nonequilibrium sorption of organic chemicals: Elucidation of rate-limiting processes. Environ. Sci. Technol. 25:134–142.

Canet, R., Birnstingl, J.G., Malcolm, D.G., Lopez-Real, J.M., Beck, A.J., 2001. Biodegradation of polycyclic aromatic hydrocarbons (PAHs) by native microflora and combinations of white-rot fungi in a coal-tar contaminated soil. Bioresource Technology 76, 113–117.

Doublet, J., 2008. Influence du co-substrat carboné sur la nature des matières organiques et les formes d'azote des composts de boue ; conséquences sur la disponibilité de cet azote. Thesis of doctorat AgroParisTech, Paris, France. 280p.

Doublet, J., Francou, C., Poitrenaud, M. and Houot, S., 2010. Sewage sludge composting: Influence of initial mixtures on organic matter evolution and N availability in the final composts. Waste Management, accepted.

Eiland, F., Klamer, M., Lind, A.M., Leth, M., Baath, E., 2001. Influence of initial C/N ratio on chemical and microbial composition during long term composting of straw. Microbial Ecology, 41, 272-280.

European Communities, 2005. Waste Generated and Treated in Europe 1995-2003. Office of Official Publications of European Communities, Luxembourg.

Francou, C., 2003. Stabilisation de la matière organique au cours du compostage de déchets urbains: Influence de la nature des déchets et du procédé de compostage – Recherche d'indicateurs pertinents. Thesis of doctorat INA P-G, 388p.

Francou, C., Linères, M., Derenne, S., Le Villio-Poitrenaud, M., Houot, S., 2008. Influence of green waste, biowaste and paper-cardboard initial ratios on organic matter transformations during composting. Bioresource Technology 99, 8926-8934.

Gaillardon, P., Gaudry, J.C. and Calvet, R., 1983. Effet des matières organiques ajoutées au sol sur l'adsorption des herbicides. Influence de la composition des matières organiques. Weed Research, 23, 333-338.

Haderlein, A., Legros, R., Ramsay, B.A., 2006. Pyrene mineralization capacity increases with compost maturity. Biodegradation 17, 293-302.

Hamelers, H.V.M. 2001. A mathematical model for composting kinetics, Ph.D. Dissertation. Wageningen University.

Hartlieb, N., Ertunc, T., Schaeffer, A., Klein, W., 2003. Mineralization, metabolism and formation of non-extractable residues of 14C-labelled organic contaminants during pilot-scale composting of municipal biowaste. Environmental Pollution 126, 83–91.

Kästner, M., Streibich, S., Beyrer, M., Richnow, H.H., Fritsche W., 1999. Formation of Bound Residues during Microbial Degradation of [14C]Anthracene in Soil. Applied and Environmental Microbiology, May 1999, p.1834–1842.

Laine, M.M., Jorgensen, K.S., 1997. Effective and safe composting of chlorophenol-contaminated soil in pilot scale. Environmental Science & Technology 31, 371–378.

Lichtfouse, E., Chenu, C., Baudin, F., Leblond, C., Da Silva, M., Behar, F., Derenne, S., Largeau, C., Wehrung, P., and Albrecht, P., 1998. A novel pathway of soil organic matter formation by selective preservation of resistant straight-chain biopolymers: chemical and isotope evidence. Organic Geochemistry 28, 411-415.

Lin, Y.P., Huang, G.H., Lu, H.W., He, L. 2008. Modeling of substrate degradation and oxygen consumption in waste composting processes. Waste Management 28,

1375-1385.

Loiseau, L., Barriuso, E., 2002. Characterization of the atrazine's bound (nonextractable) residues using fractionation techniques for soil organic matter. Environmental Science & Technology, 36, 683-689.

Ma, L., and Selim, H.M., 1994. Predicting atrazine adsorption-desorption in soils:Amodified second-order kinetic model. Water Resour. Res. 30:447–456.

Mason, I.G., 2006. Mathematical modelling of the composting process: A review. Waste Management 26, 3-21.

Michel, F.C., Reddy, C.A., Forney, L.J., 1995. Microbial-degradation and humification of the lawn care pesticide 2, 4-dichlorophenoxyacetic acid during the composting of yard trimmings. Applied and Environmental Microbiology, 61, 2566-2571.

Pascual, J.A., Garcia, C., Hernandez, T., 1999. Comparison of fresh and composted organic waste in their efficacy for the improvement of arid soil quality. Bioresource Technology 68, 255-264.

Payne, W.J., 1970. Energy yields and growth of heterotrophs. 419 Annual Review of Microbiology 24, 17-52.

Potter, C.L., Glaser, J.A., Chang, L.W., Meier, J.R., Dosani, M.A., Herrmann, R.F., 1999. Degradation of polynuclear aromatic hydrocarbons under bench-scale compost conditions. Environmental Science & Technology 33, 1717–1725.

Rosso, L., Lobry, J.R., Flandrois, J.P., 1993. An unexpected correlation between cardinal temperatures of microbial growth highlighted by a new model. Journal of Theoretical Biology 162 (4), 447–463.

Saffih-Hdadi, K., Bruckler, L. and Barriuso E., 2003. Modeling of Sorption and Biodegradation of Parathion and Its Metabolite Paraoxon in Soil. J. Environ. Qual. 32:2207–2215.

Shelton, D.R., and M.A. Doherty. 1997. A model describing pesticide bioavailability and biodegradation in soil. Soil Sci. Soc. Am. J. 61:1078–1084.

Smith, P., Smith, J.U., Powlson, D.S., McGill, W.B., Arah, J.R.M., Chertov, O.G., Coleman, K., Franko, U., Frolking, S., Jenkinson, D.S., Jensen, L.S., Kelly, R.H., Klein-Gunnewiek, H., Komarov, A.S., Li, C., Molina, J.A.E., Mueller, T., Parton, W.J., Thornley, J.H.M., Whitmore, A.P., 1997. A comparison of the performance of nine soil organic matter models using datasets from seven long-term experiments. Geoderma 81, 153-225.

Sole-Mauri, F., Illa, J., Magry, A., Prenafeta-Boldu, F.X., Flotats, X., 2007. An integrated biochemical and physical model for the composting process. Bioresource Technology 98, 3278–3293.

Soulas, G. 1997. Modeling of biodegradation of pesticides in the soil. p. 117–140. In J. Tarradellas et al. (ed.) Soil ecotoxicology. CRC Press, Boca Raton, FL.

Soulas, G., and B. Lagacherie. 1990. Modelling of microbial processes that govern degradation of organic substrates in soil, with special reference to pesticides. Philos. Trans. R. Soc. London, Ser. B 329, 369–373.

Stombaugh, D.P., Nokes, S.E., 1996. Development of a biologically based aerobic composting simulation model. Transactions of the ASAE 39 (1), 239–250.

Tester, C.F., Sokora, L.J., Taylor, J.M. and Parr, J.F., 1978. Decomposition of sewage sludge compost in soil: III. Carbon, nitrogen, and phosphorus transformations in different sizes fractions. Journal of Environmental Quality, 8: 1979-1982.

Xing, B., McGill, W.B. and Dudas M.J., 1994. Sorption of benzene, toluene and o-xylene by collagen compared with non-protein organic sorbents. Can. J. Soil Sci. 74: 465-469.

Xue, S.K., Chen, S. and Selim, H.M., 1997. Modeling alachlor transport in saturated soils from no-till and conventional tillage systems. J. Environ. Qual. 26:1300–1307.

Vlyssides, A., Mai, S., Barampouti, EM., 2009. Source: An integrated mathematical model for co-composting of agricultural solid wastes with industrial wastewater. Bioresource Technology 100, 4797-4806.

Van Soest P.J., Wine R.H., 1967. Use of detergents in the analysis of fibrous feeds. IV. Determination of permanganate. Journal of A. O. A. C., 50, 1: 50-55.

Zhang, Y., Zhu, Y.G., Houot, S., Qiao, Min., Nunan, N., Garnier, P., 2011. Remediation of polycyclic aromatic hydrocarbon (PAH) contaminated soil through composting with fresh organic wastes. Environ Sci Pollut Res. DOI 10.1007/s11356-011-0521-5.

Zhang, Y., Lashermes, G., Houot,S., Doublet, J., Steyer, J.P., Zhu, Y.G.. Endrique Barriuso, Patricia Garnier, 2011. Modelling of organic matter dynamics during the composting process. Waste Management. DOI:10.1016/j.wasman.2011.09.008.

PART II: APPLICATION OF COP_COMPOST MODEL TO BIOREMEDIATION OF PAH CONTAMINATED SOIL TROUGH COMPOST

CHAPTER 5: REMEDIATION OF POLYCYCLIC AROMATIC HYDROCARBON (PAH) CONTAMINATED SOIL THROUGH COMPOSTING WITH FRESH ORGANIC WASTES

Yuan Zhang[1, 2], Yong-Guan Zhu[1], Sabine Houot[2], Min Qiao[4], Naoise Nunan[3], Patricia Garnier[2*]

1 - Chinese Academy of Sciences, Institute of Urban Environment, Xiamen, Peoples R. China

2 - INRA-AgroParisTech, UMR 1091 Environnement et Grandes Cultures, F-78850, Thiverval-Grignon, France

3 - CNRS, UMR7618 - Biogéochimie et Ecologie des Milieux Continentaux, F-78850, Thiverval-Grignon, France

4 - Chinese Academy of Sciences, Research Center for Eco-Environment Sciences, Beijing, Peoples R. China

***Corresponding author:** INRA-AgroParisTech, UMR1091 Environnement et Grandes Cultures, 78850 Thiverval-Grignon, France. Tel: +33 1 30 81 53 14; Fax: +33 1 30 81 53 96.

E-mail address: pgarnier@grignon.inra.fr (Patricia Garnier)

Accepted by **Environmental Science and Pollution Research, 2011**

5.1 Abstract

Composting may enhance bioremediation of PAH-contaminated soils by providing organic substrates that stimulate the growth of potential microbial degraders. However, the influence of added organic matter (OM) together with the microbial activities on the dissipation of PAHs has not yet been fully assessed. An in-vessel composting-bioremediation experiment of a contaminated soil amended with fresh wastes was carried out. Four different experimental conditions were tested in triplicate during 60 days using laboratory-scale reactors: Treatment S (100% soil), W (100% wastes), SW (soil/waste mixture) and SWB (soil/waste mixture with inoculation of degrading microorganisms). A dry mass loss of 35±5% was observed in treatments with organic wastes during composting in all the treatments except Treatment S. The dissipation of the 16 USEPA-listed PAHs was largely enhanced from no significant change to 50.5±14.8% (for SW) / 63.7±10.0% (for SWB). More obvious dissipation was observed when fresh wastes were added at the beginning of composting to the contaminated soil, without significant difference between the inoculated and non inoculated treatments. Phospholipid fatty acid (PLFA) profiling showed that fungi and

G- bacteria dominated at the beginning of experiment and were probably involved in PAH dissipation. Subsequently, greater relative abundances of G+ bacteria were observed as PAH dissipation slowed down. The results suggest that improving the composting process with optimal organic compositions may be a feasible remediation strategy in PAH contaminated soils through stimulation of active microbial populations.

5.2 Introduction

Polycyclic aromatic hydrocarbons (PAHs) are one of the main contaminant classes in soils of former coal gasification sites, tar oil distillation plants, or wood-preserving industries (Wischmann and Steinhart, 1997). Such highly polluted soils lead to ecotoxicological risks and have to be cleaned up. Various remediation and in particular bioremediation procedures are available (Alexander, 1999; Wilson and Jones, 1993). Since PAHs are hydrophobic compounds with low solubility in water, they have a great tendency to bind to organic matter or soil, limiting their availability to microorganisms (Volkering et al., 1992; Pignatello and Xing, 1996; Carmicheal et al., 1997; Zhang et al., 1998). The addition of organic materials can enhance biodegradation by improving soil texture and oxygen transfer and by providing energy sources to rapidly establish a large microbial population (Englert et al., 1993). Several studies have shown that the degradation of PAHs in contaminated soils is significantly higher after addition of compost (Kästner et al., 1994; Wischmann and Steinhart, 1997). Kästner and Mahro (1996) found that adding compost enhanced the removal of soil-associated PAHs and suggested that the presence of microorganisms capable of degrading natural humic substances were responsible for the co-metabolic degradation of the PAHs. Moreover, microbial activity has been shown to form bound residues in soil-compost system (Kästner et al., 1999). PAH dissipation has been frequently observed during composting of various contaminated substrates including sewage sludge (Cai et al., 2007) and organic wastes (Brändli et al., 2005). The composting of contaminated soils has also been demonstrated to enhance the biodegradation of PAHs using both conventional windrow composting systems (Amir et al., 2005; Atagana, 2004) and in-vessel composting systems (Antizar-Ladislao et al., 2006; Sasek et al., 2003). In-vessel composting techniques are easier to operate than conventional

composting systems as temperature, moisture content, ventilation, etc. can all be controlled. Composting after addition of fresh green wastes would appear to be more efficient than the addition of matures compost for decreasing PAH concentrations in contaminated soil (Antizar-Ladislao et al., 2006).

In the field of bioremediation, most studies have applied final composting products and these studies have established the fate of PAHs (Cai et al., 2007) and the effect of fungal-bacterial culture on PAH degradation (Boonchan et al., 2000). However, few investigations have focused on the effect of fresh organic matter addition and microbial inoculation on PAH dissipation during composting of contaminated soil. Only a few reports have described the degradation of contaminants in soil after addition of complex organic materials such as composts (Stegmann et al., 1991; Sims et al., 1990). Research on biodegradation has demonstrated the potential of white-rot fungi to degrade PAH (Canet et al., 1999) and using the PLFA as a biomarker it has been found that the Gram-negative bacteria are more sensitive to PAHs than Gram-positive bacteria or fungi (Yang et al., 2007).

Therefore, our objective was to study how the addition of fresh waste mixtures might enhance PAH dissipation in a contaminated soil during composting in an in-vessel composting system and to identify the relationship between PAH dissipation and the evolution of organic matter characteristics, PAH retention and changes in microbial community structure.

5.3 Materials and methods

5.3.1 Experimental design

Four experimental conditions were tested in triplicate during 60 days using laboratory-scale reactors. **Treatments S** with 100% contaminated soil and **W** with 100% waste mixtures were considered as control treatments. In **treatment SW** the contaminated soil was blended with the mixture of wastes (see below) with an optimal ratio of 0.8:1 (dry-wt soil / dry-wt wastes) (Antizar-Ladislao et al., 2005). The **treatment SWB** was similar to SW with the addition of two PAH degrading micro-organisms (Bacillus sp. & Fusarium sp.).

Treatments S (control), SW and SWB aimed at studying the degradation of PAHs in the soil during the composting process. The three treatments were conducted with the same amounts of soil. The treatment W was used to study the decomposition of waste organic matter (OM) during composting.

5.3.2 Contaminated soil

The contaminated soil was collected from a site located in Beijing (39.85°N, 116.54°E) which was highly polluted by the coal industry. The soil was sieved to 2mm and then air-dried before analysis. The soil was a loamy-sand with 12.4% clay, 33.2% silt and 54.4% sand. The initial total concentration of 16 USEPA PAHs ($\sum_{PAHs}$) was 69.7±2.2 mg kg^{-1} soil (on dry-wt basis). The initial carbon content of contaminated soil was 1.5±0.3% (g. 100 g^{-1} dry wt).

5.3.3 Mixture of wastes

The mixture of wastes included leaves, branches and bio-wastes consisting of green vegetables such as cabbage, spinach and celery (60%, 28% and 12% of total mixture on dry matter basis, respectively). All waste materials were crushed to 2mm before mixing. The initial C/N ratio of a composting mixture should range between 25 and 40 to provide suitable composting conditions (Leclerc, 2001). Therefore, the initial proportions in the waste mixture were calculated to get an initial C/N ratio of 29.3 in the initial mixture.

The initial concentration of ∑ 16 USEPA listed PAHs in the mixture of wastes was 5.0±0.2 mg kg^{-1} dry-wt. The initial content of total carbon content in the mixture of wastes was 42.8±0.2% (g.$100g^{-1}$ dry-wt^{-1}).

5.3.4 Initial soil/waste mixtures

The mixture of wastes was added to the contaminated soil with a ratio of 0.8:1 (dry-wt soil/ dry-wt wastes) as used in Antizar-Ladislao et al. (2005). The TC content in the initial mixture was 24.5±0.7%. The C/N ratio of the initial soil/waste mixture was 25.6. The initial total concentration of 16 USEPA PAHs ($\sum_{PAHs}$) was 74.6±2.4 mg kg^{-1}

dry-wt. The $\sum_{PAHs}$ concentration was higher than that in contaminated soil, because PAHs were also detected in the mixture of fresh wastes.

5.3.5 Specific added microorganisms

Bacillus sp., a Gram-positive rod-shaped bacterium and Fusarium sp., a filamentous fungus widely distributed in soil and in association with plants, were isolated from the contaminated soil and cultured at 30°C and 175 rpm in basal salt-glucose medium supplemented with pyrene (50mg $liter^{-1}$) before application to the soil-waste mixture of the SWB treatment. The population density was determined before inoculation using the dilution and spread plate method. The initial concentration of the two microbial populations (Bacillus sp and Fusarium sp.) were $1x10^8$ and $4.8x10^8$ (colony forming units, CFU/ml), respectively.

Bacillus sp. was chosen because it represents a genus of bacteria that can survive during the thermophilic phase of composting. The Fusarium sp. offers other advantages: (i) most filamentous fungi are adapted to contaminated environments allowing the inoculum to survive and (ii) Fusarium sp., preferentially degrades the high-molecular-weight PAHs with 5- and 6-rings (Olivier et al. 2004).

5.3.6 Bioreactors

Beakers with a volume of 1L (diameter of 106mm and a height of 150mm) were used (see details in Fig.5.1) and placed in water-bathes to control the temperature. Each treatment was run in triplicate in 3 separate beakers. During composting, the optimal aeration during the active phrase varied from 3L.h^{-1}.kg^{-1} dry-wt (Lau et al. 1992; Sadaka and Taweel 2003) to 150L.h^{-1}.kg^{-1} dry-wt (Mathur et al. 1993). The used aeration rate decreased during composting from 12-25 L. h^{-1}.kg^{-1} dry-wt. at the beginning to 3-6 L.h^{-1}.kg^{-1} dry-wt at the end as proposed by Francou el al. (2008).

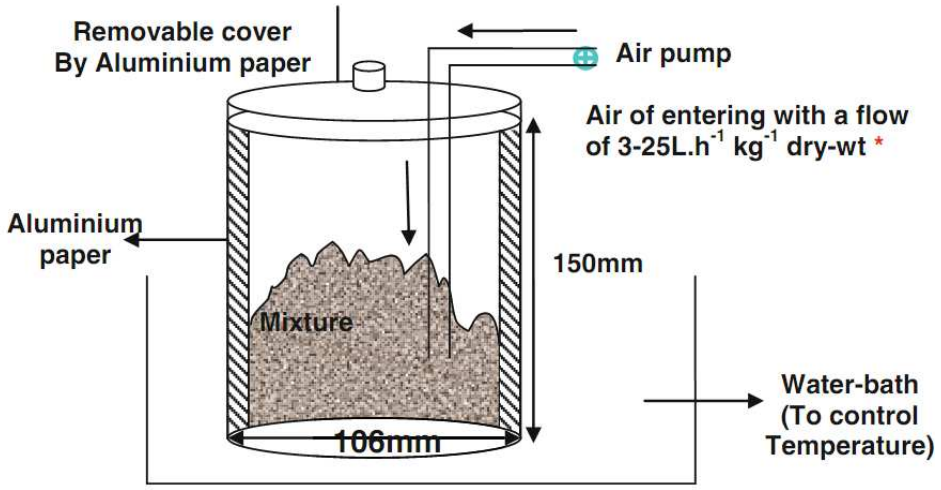


Figure 5.1: Design of bioreactor (volume of 1L).

5.3.7 Temperature and moisture

The variation temperature profile for the time periods Days 0–14 at 38°C, Days 15–35 at 55°C, Days 36–42 at 70°C and Days 43–60 at 38°C was chosen according to Antizar-Ladislao et al. (2005). The temperature profile simulated natural composting systems and was achieved using the water-bathes. The optimal moisture content during composting generally varies between 50 and 80% of total wet mass (Willson, 1989; Richard et al., 2002). The moisture content (100*mass of water / mass of wet mixture) in treatments W, SW and SWB were maintained to 50% by adding water into the bioreactors after each sampling event. In the control treatment S, a moisture content of 50% made the contaminated soil too wet to be in aerobic condition, and a moisture content of 15% in Treatment S was chosen within the maximum water content of soil. Li et al. (2006) also found that submerged conditions can inhibit the degradation of B[a] P in soil.

5.3.8 Sample collection

With the exception of the beginning and the end of composting (Day 0 and 60), sampling ocurred immediately prior to each change of temperature at days 14, 35 and 42. At every sampling date, the beakers were emptied, mixed thoroughly and sub-sampled in triplicate. The sub-samples with about 20g (wet weight) per

sub-sample were frozen at -80°C for the analysis of total organic matter (TOM), PAHs, phospholipid fatty acid (PLFA) and adsorption coefficient (Kd) of FLT and PHE on soil and on soil/waste mixture.

5.3.9 Organic matter analysis

The samples were dried in an oven at 105°C to obtain the dry weight. The evolution of biochemical fractions was measured using the Van Soest method (Van Soest and Wine, 1967), but just for the treatment W because of the limits of the Van Soest method. Successive extractions of water soluble (H_2O), soluble substances in neutral detergent (SOL), hemicellulose-like (HEM), cellulose-like (CEL) and lignin & cutin-like (LIC) fractions were carried out as described in the French XPU 44-162 standard (AFNOR, 2009).

5.3.10 PAHs analysis

The PAHs were extracted from 4g samples which were dried by lyophilisation and then weighed in triplicate into the pressure tubes used for accelerated solvent extractor (Dionex ASE-300). The solvent was a dichloromethane/acetone (1:1) mixture. The sample and solvent were heated to 100°C; pressure 10.35 MPa using the standard ASE program. The extracts were purified on chromatographic columns packed with 12 cm SiO_2 (100/200 mesh; conditioned at 180°C during 12 h before use), 6 cm Al_2O_3 (100/200 mesh; 250°C; 12 h), and 1 cm Na_2SO_4 (450°C; 4 h). In order to remove hydrophobic impurities, the columns were previously washed with 10 ml hexane, then 5 ml of extracts were eluted, and the columns were left to dry for 1 min. The PAHs were then eluted with 70 ml solvent (hexane: dichloromethane, 7:3 v/v). The extracts were concentrated to 1ml by flux of N_2.

PAHs were analyzed using a GC-MS Chemstation (6890N/5975C, Agilent, USA) using a HP-5MS column (19091S-433, 30 m×0.25mm×0.25µm). The injection volume was 1 µl. The temperature programme was 50°C for 2 min, 20°C min^{-1} to 200°C, which was maintained for 2 min, 4.5°C min^{-1} to 240°C which was maintained for 2 min and then 2.5°C min^{-1} to 290°C. The MS was operated in selective ion

monitoring (SIM) mode according to chemical ionization.

The 16 PAHs were grouped into three groups, according to the number of rings: small PAHs with 2- and 3-ring (naphthalene, acenaphthylene, acenaphthene, fluorine, anthracene); medium PAHs with 4-ring (fluoranthene, pyrene, benzo[a]anthracene, chrysene) and large PAHs with 5- and 6-ring (benzo[b]fluoranthene, benzo[k]fluoranthene, benzo[a]pyrene, ideno[1,2,3-c,d]pyrene, dipbenzo[a,h]anthracene, benzo[g,h,i]perylene).

5.3.11 PAH sorption

The sorption of PAHs was measured on fresh samples of the feedstock materials, the initial mixtures, the homogenized soil/waste mixture at each sampling event and the initial contaminated soil. Two PAHs were used: fluoranthene (FLT) and phenanthrene (PHE) were used. Average sample weight of soil/waste mixture was 1.0 g (soil)/0.06g (wastes) ±0.003 g dry-wt, 1.0 g dry-wt for waste and 3.0±0.003 g dry-wt for the soil samples. Each measurement was done in triplicate. The equivalent PAH concentration in soil/waste mixture samples (expressed in mg kg^{-1} dry-wt) was 1.95 and 1.98 for FLT and PHE. Volumes of 9, 15 or 15 ml of ^{14}C-PAH solution (methanol and alkaline solvents) prepared for the soil/waste mixture, wastes or soil sorption experiments, respectively, were added to the samples in glass corex tubes which were then shaken for 24h at 20°C and then centrifuged for 10 min at 1644 g. The final concentration of ^{14}C-PAH in the supernatants was determined by liquid scintillation counting (Tri-Carb 2100 TR, Perkin Elmer Ins., Courtabeuf, France) using Ultima Gold XR (Packard) as scintillation cocktail. The amount of ^{14}C-PAH sorbed on the soil/waste mixture samples or soil sample (Qs in mg kg^{-1} dry-wt) was calculated from the difference in concentration between the initial PAH solution and the corresponding centrifuged supernatant after 24h of equilibration. The sorption coefficients Kd (in L kg^{-1} dry-wt) were determined as $Kd = Q_s Q_w^{-1}$ where Q_w (in mg L^{-1}) was the PAH concentration in supernatant solution after equilibration.

5.3.12 PLFA analysis

The lipids were extracted and stored under an atmosphere of N_2. Soil and composting material lipids were extracted on 4g samples in 30 ml of chloroform/methanol/buffer (1:2:0.8 v/v/v) by shaking for at least 2 h (biofilm) or overnight (soil and composting materials) at 21°C. The chloroform phase was reduced by evaporation. Fatty acid methyl esters were quantified and identified by mass spectral comparison using a MS Chemstation (G1034C Version C.02.00) fitted with a HP-5MS column (19091S-433, 30 m×0.25mm×0.25µm). The injection volume was 1 µL. The initial oven temperature was set at 120°C for 5 min and then increased at a rate of 20°C min^{-1} to 180°C followed by a 4°C min^{-1} increase to 240°C. The MS was operated in selective ion monitoring (SIM) mode. Fatty acid nomenclature used was that described by Frostegård et al. (1993). Mono-unsaturated and cyclopropyl fatty acids were deemed to be gram-negative bacterial (G-) biomarkers (Zelles et al. 1999), iso- and anteiso-fatty acids gram-positive bacteria (G+) biomarkers (Zelles et al. 1999), C18:2(9,12) a fungal biomarker (Frostegard et al. 1993) and carboxylic acids with a methyl function on the carbon chain were treated as biomarkers of actinobacteria (Zelles et al. 1994). The ratio of cyc-C17:0 to C16:1(7)cis, the trans-to-cis ratio and the i:a ratio were calculated as stress indicators (Navarrete et al. 2000; Smithwick et al. 2005). The ratio of fungal-PLFA to bacterial-PLFAs (as specified above) was used as an estimate of the relative importance of the bacterial and fungal energy channels (Parekh and Bardgett 2002). The fungal to bacterial PLFA and G+ / G- bacterial ratios are considered as indicators of microbial community changes during in-vessel composting (Antizar-Ladislao et al. 2007).

5.3.13 Statistical analysis

Statistical procedures used to describe and evaluate the results were appropriate for the data of our study. The differences between treatments were tested by one-way analysis of variance using SAS (Version 8.1). The paired groups were evaluated using Burtlett's test. The comparison method Fisher's LSD with a significance level of 0.05 was used to test the significance of pairwise differences.

5.4 Results & Discussion

5.4.1 Dry mass

The soil dry mass in treatment S remained constant during composting while dry mass losses were observed in the treatments W, SW and SWB (Fig.5.2). This occurred mainly during the first 14 days. A mean dry mass loss of 34.9±4.6%, 19.4±2.0% and 26.0±14.3% was found in Treatments W, SW and SWB, respectively after two months of composting. The dry mass loss in Treatment W (34.9±4.6%) was close to that previously observed during the composting of other organic wastes (Sánchez-Monedero et al., 1999).

The mineralization of total carbon organic (TOC) into CO_2 explained TOC loss which was calculated according to the dry mass loss during composting (Fig.5.3-A). The carbon loss represented 35.2±3.2%, 36.9±5.2% and 44.2±11.6% for treatments W, SW and SWB, respectively. The mineralisation of TOC was calculated according to the carbon loss (see details in Fig.5.3-B). Significant differences were found between treatment W and SW/SWB ($P<0.05$), while, no significant differences could be found between treatments ($p>0.05$). These results indicated that the influence of added degrading bacteria on the decomposition of organic matters was not noticeable.

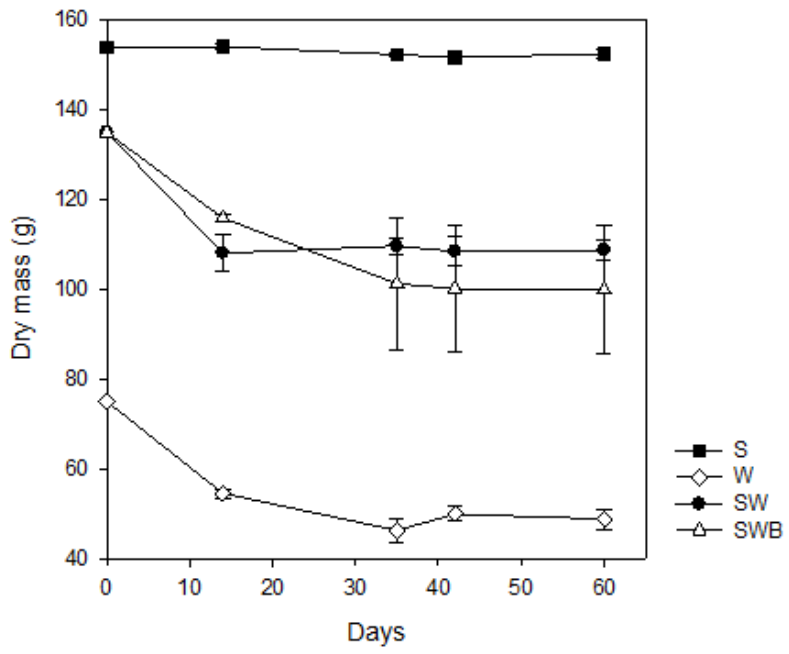


Figure 5.2: Evolution of dry mass during composting for the different treatments (S, W, SW and SWB).

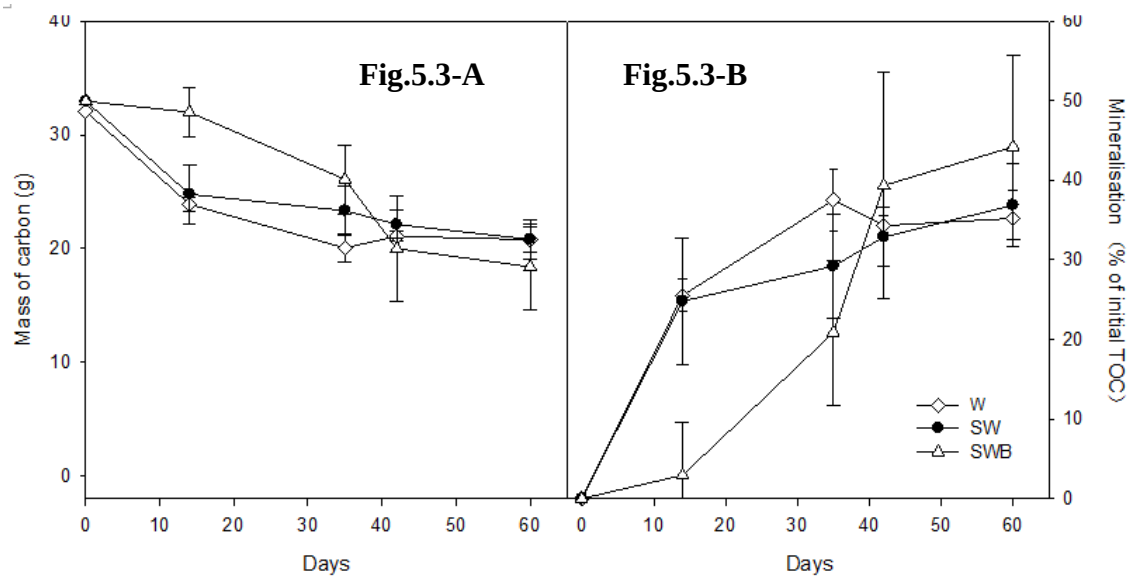


Figure 5.3: Loss of carbon mass (Fig.5.3-A) and percentage of total initial organic carbon mineralisation calculated according to the loss of carbon mass (Fig.5.3-B).

5.4.2 Organic matter analysis

The evolution of Van Soest fractions of OM during the incubation is portrayed for the W treatment in Fig.4. The mineralisation fraction CO_2 was calculated by using the dry mass balance, since the sum of all the organic fractions (SOL, H_2O, HEM, CEL, LIC and CO_2) represented 100% of the initial total dry mass (see details in Fig.5.4). The proportion of HEM and H_2O fractions decreased while LIC, CEL and SOL fractions remained constant. These results have generally been observed in other composting studies (Doulet et al. 2010; Francou et al. 2008) with the exception of the CEL fraction that generally decreases during composting. However, its degradation varies with the substrate of origin because of its spatial interaction with lignin (Doublet et al. 2010). The compost made from leafs may contribute to limit CEL degradation. The SOL fraction remained constant most likely because this pool was replenished by the decomposition of other organic matter pools at the same rate at which it was being degraded. The LIC fraction was always the most recalcitrant compartment for microbial degradation, and it changed least during the composting (Francou et al. 2008; Doublet et al. 2010). The H_2O fraction, which represented the easily degradable compartment, contributed most to the dry mass loss (about 19.7%). We assumed that the degradation of OM mixed with soil in SW and SWB treatments would follow a

similar degradation pattern because at the end of the experiments we found approximatively the same amount of carbon lost (see Fig.5.3).

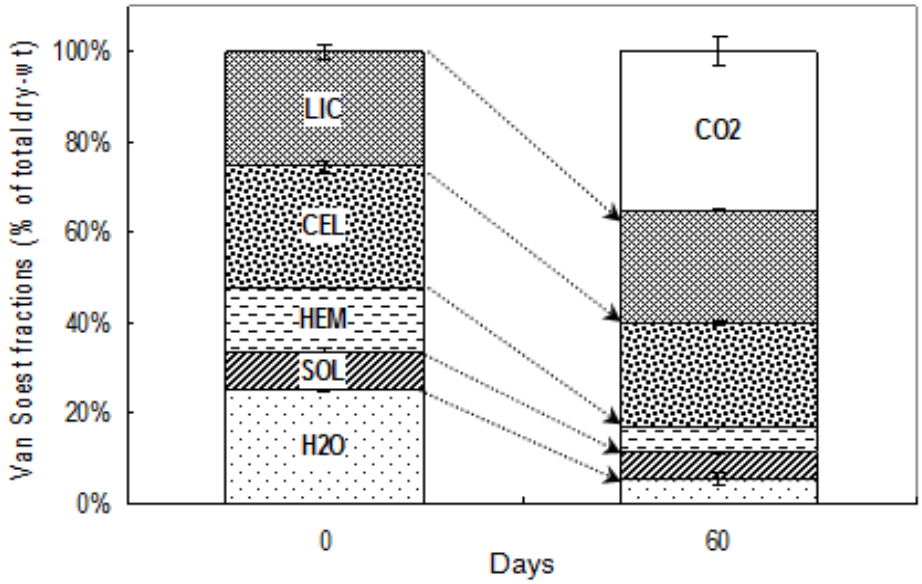


Figure 5.4: Changes of the biochemical fractions during composting in the W treatment (100% wastes) using the Van Soest method.

5.4.3 Fate of PAHs

5.4.3.1. Degradation of PAHs

No significant degradation of PAHs was observed for treatment S during composting (Fig.5.5) and the slight variations of concentrations observed were attributed to experimental variation of moisture content during the composting treatment that would potentially affect PAH concentrations (Antizar-Ladislao et al. 2005). The soil microflora was not able to degrade PAHs as observed by Kästner et al. (1999). On the other hand, total 16 USEPA PAH concentration decreased by 50.5±14.8% and 63.7±10.0% in treatments SW and SWB, respectively (Fig.5.5), without significant difference between these two treatments (P = 0.564). The results indicated that degrading bacteria had no obvious effect on the PAH dissipation. This conclusion is supported by the research of Canet et al. (2001) who suggested that in soil amended by OM system, the use of the autochthonous microflora, with no introduction of foreign microorganisms, offered the greatest potential for PAH degradation. Other evidence has shown that in the experiments with soil from a contaminated site (Mahro

et al., 1994), PAH degradation was most effectively stimulated after addition of compost in comparison to the addition of fertiliser or degrading bacteria.

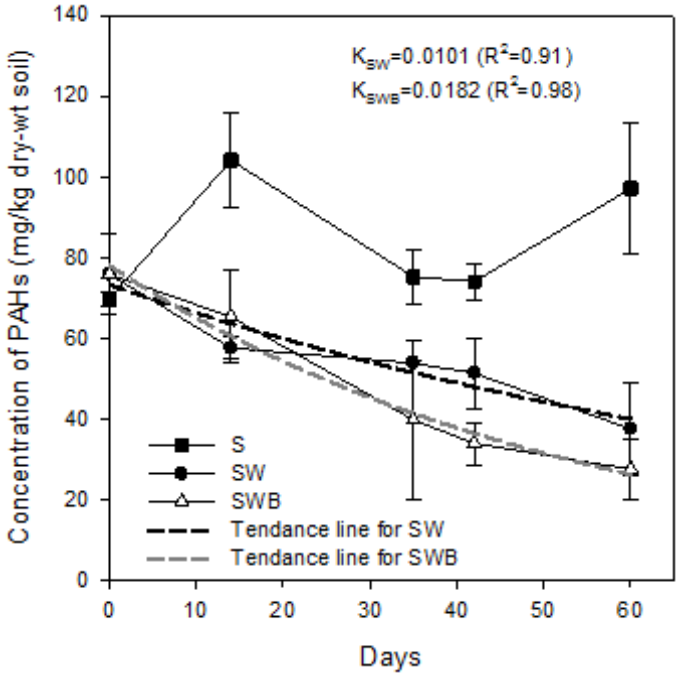


Figure 5.5: Evolution of total PAHs during composting (mean ± standard deviation) in the different treatments (S, W, SW and SWB); first order adjusted kinetics of dissipation in the SW and SWB treatments.

First order kinetic equations were fitted to the kinetics of dissipation of PAHs and the first order rate constants were 0.0102 day^{-1} and 0.0176 day^{-1} for treatments SW and SWB, respectively (Fig.5.5), similar to the value (0.0160 day^{-1}, R^2 = 0.93) reported in Antizar-Ladislao et al. (2007).

The amount and rate of PAHs dissipation varied according to their molecular weights (Fig.5.6). Larger dissipation rates were observed for all PAHs in the SWB treatment compared to the SW treatment, but differences were not significant ($P > 0.05$). Detailed results of PAHs dissipation are showed in Table 5.1. The highest dissipation was observed for medium PAHs in both treatments. This was particularly evident for four-ring PAHs, which are normally less reactive and biodegradable than lighter PAHs (Joner et al., 2010). Generally, large PAHs were more persistent than small and medium PAHs. Since large PAHs have higher octanol-water partition coefficients and

lower water solubility than medium and small PAHs (Antizar-Ladislao et al., 2005), thus bioavailability (Carriere and Mesania, 1995; Potter et al., 1999; Lee et al., 2001) and toxicity (Sverdrup et al., 2002) may have limited their biodegradation, resulting in their persistence.

Figure 5.6: Evolution of small (2- and 3-rings), medium (4-rings) and large (5- and 6-rings) PAHs concentrations in soil during composting.

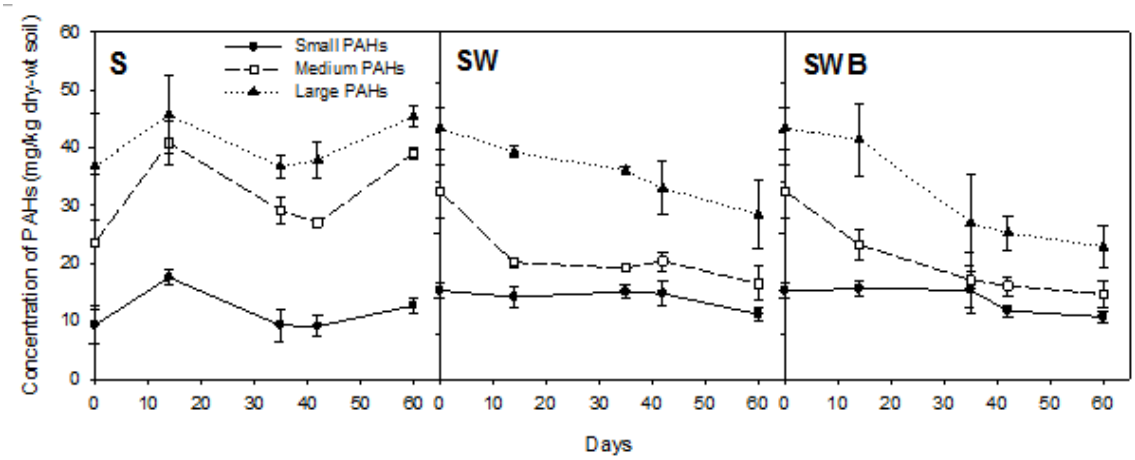


Table 5.1: Small, medium and large PAHs removal percentage for Treatment SW and SWB

Treatment	PAHs Removal (%)			
	Small PAHs	**Medium PAHs**	**Large PAHs**	**Total 16 USEPA PAHs**
SW	55±14	64.9±12.0	42 ± 17	50.5±14.8
SWB	61.3±12.7	72.3±9.3	57.7±10.4	63.7±10.0

5.4.3.2. Evolution of PAH Sorption during composting

In initial materials (S, SW or W), the organic carbon-normalized sorption coefficient (expressed in Log K_{OC}) ranged from 3.4 to 4.1 (L/kg dry-wt) for both PAHs, which confirmed the strong sorption properties of these pollutants (Fig.5.7-A). These values were similar to the value (4.6-4.8) found by He et al. (1995) in soil. Significant differences in Log K_{OC} were observed for FLT between initial materials of S and the other initial materials of SW and W ($p<0.05$). We found a value of 4.1 for S treatment

and 3.7-3.9 for W and SW treatments. Farenhorst (2006) found also that the K_{OC} of pesticide was higher in soil with humified organic matter compared to soil mixed with fresh organic matter. No significant difference could be found in PHE between treatments.

During composting of SW, no difference has been observed for Log K_{OC} of FLT, while for PHE, a slight increase of Log K_{OC} was noted over the time but without significant differences (Fig.5.7-B). These values of Log K_{OC} for SW were agreement with the range from 4.41 to 4.94 found by Zhang et al. (2010) who investigated the Koc values between PHE and biochar-amended soils. These results showed that the organic matter decomposition was not long enough to lead to noticeable changes of reactivity with these PAHs.

Figure 5.7-A:

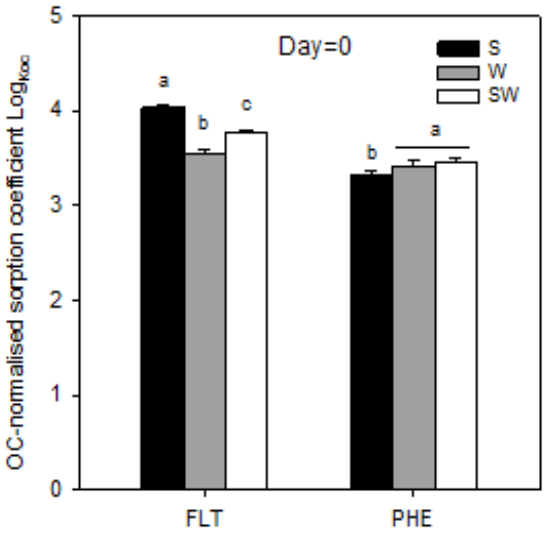


Figure 5.7-B:

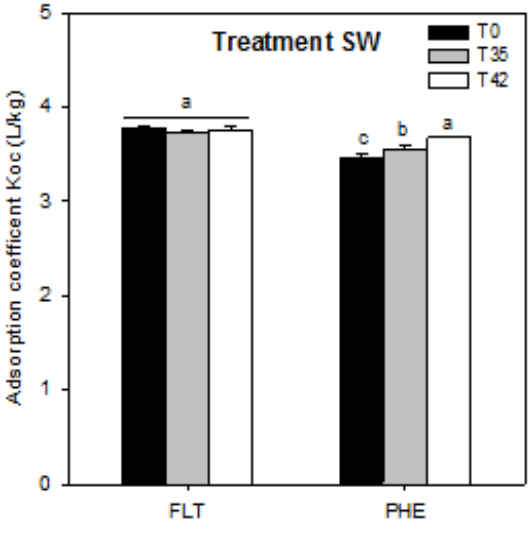


Figure 5.7: (5.7-A) Organic carbon-normalisaed sorption coefficient of FLT and PHE in initial soil, waste and soil-waste mixtures; (5.7-B) Evolution of Organic carbon-normalisaed sorption coefficient during composting in the soil-waste mixture (SW treatment). Different letters (a, b and c) within rows are significantly different ($p < 0.05$) according to one way-ANOVA analysis.

5.4.4 PLFA profiling

The implementation of composting technology as a remediation method requires an understanding of the diversity and ecology of contaminant-degrading microorganisms.

It is for this reason that changes within the microbial community structure were investigated by PLFA profiling to detect the major changes in microbial community structure during composting. The first two ordination axes, representing 83% of the total variability in the data, are presented in Fig.5.8, where principal component (PC1) characterised the stages of composting. Contaminated soil samples were significantly ($P<0.05$) separated from the waste samples and the soil and waste mixture samples along the first ordination axis. Inspection of the loadings revealed that the difference between soil and other samples was primarily due to a higher relative abundance of fatty acids indicative of actinomycetes in the soil samples and higher relative abundance G+ bacterial biomarkers in the other samples. No significant different was observed between the waste samples and the soil-waste mixtures, suggesting that the waste microbial communities dominated in the soil-waste mixture. Microbial community structure also varied significantly ($P<0.05$) with time in all treatments. Variation as a function of time was more pronounced in the contaminated soil than in the waste or soil-waste mixture and it was apparent on the first ordination axis. It was due to an increase in the abundance of actinobacteria. The second ordination axis showed the variation as a function of time in the other treatments. The lipid profiles of these samples were initially dominated by G- bacterial and fungal biomarkers. As the incubation progressed, these treatments saw a distinct increase in the abundance of G+ bacteria (see Fig.5.9-A). It has been suggested that the G+ bacteria like actinomycete may play an important role in the mineralisation of PAHs (Kästner et al. 1994; Larkin et al. 2005), and these are also thermophiles meaning they are likely to be encountered at the higher temperatures (above 38 °C) used during the variable temperature profile. Thus, a higher relative proportion of G+ was expected (Antizar-Ladislao et al. 2008).

According to Fig.5.9-B, the fungal to bacterial PLFA ratio was observed to be in the range of 0.03 to 0.19 which was within the range of 0.01-0.48 found by Antizar-Ladislao (2007). The fungal to bacterial PLFA ratio in treatments SW and SWB displayed a large degree of variation compared to treatment S. The same trends with time were observed for both of these treatments with an increase of the ratio during the first 14 days and a steady decline thereafter. These results corroborate the results of Antizar-Ladislao (2007), which indicated that an increase in temperature in

the bioreactors from 38 to 70 °C reduced the fungal to bacterial PLFA ratio to low values.

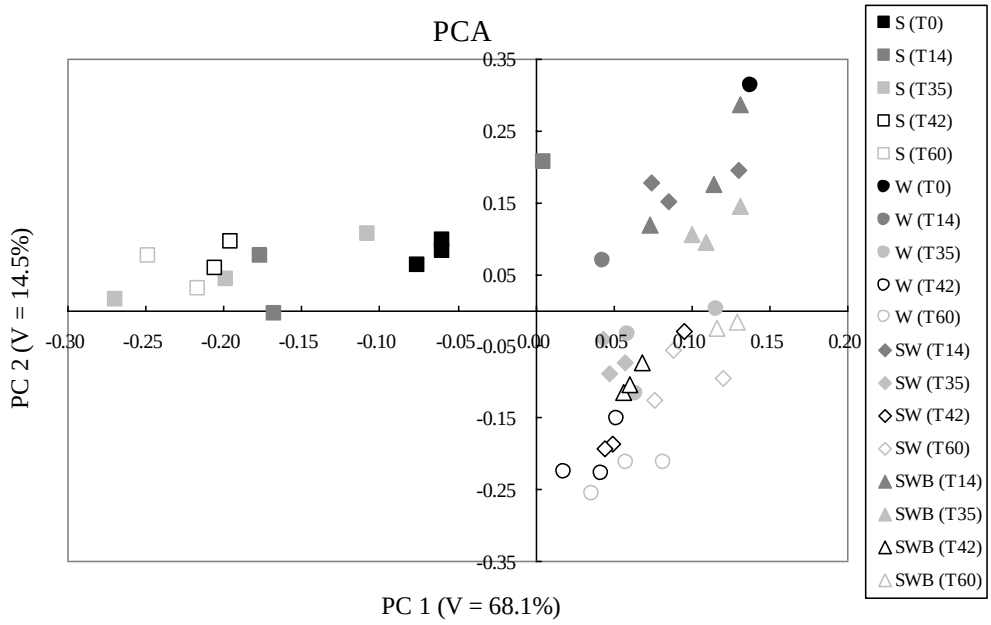


Figure 5.8: Principal component analysis of PLFA data. PC1 & PC2 represents different dates of composting course. Principal component 1 (PC1) explained 68.1% of the variation, while PC2 explained 14.5%. ■: Experimental data of Treatment S; ●: Data of Treatment W; ♦: Data of Treatment SW; ▲: Data of Treatment SWB. Different colours represented data with different date. Black = Day 0; Deep gray = Day 14; Gray = Day 35; Black circle = Day 42 and Gray circle = Day 60.

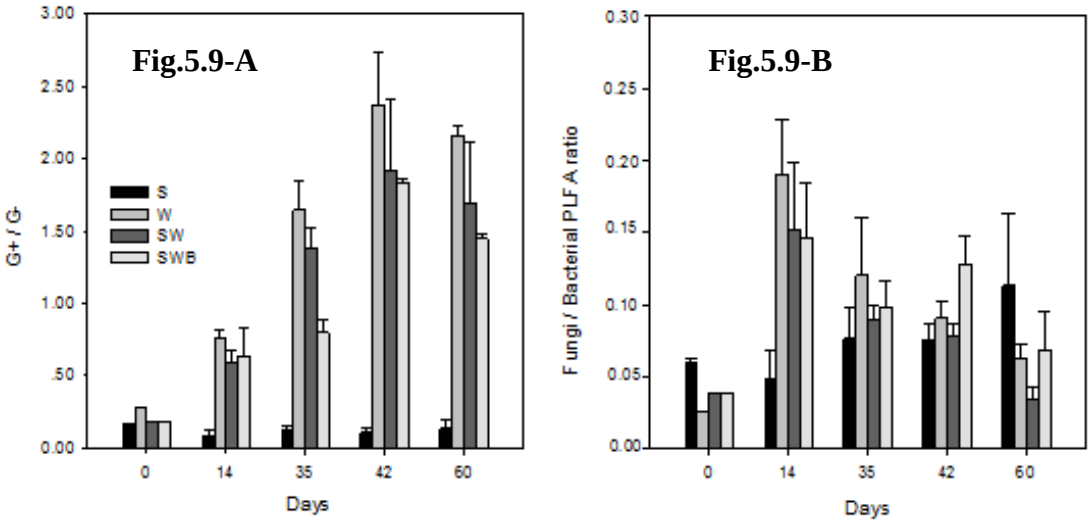


Figure 5.9: G+/G- (Fig.5.9-A) and Fungal/Bacterial PLFA ratio (Fig.5.9-B) in different treatments during composting process.

5.5 Conclusion

In this study, the carbon loss was observed in all treatments W (100% of wastes), SW (soil: wastes = 0.8:1 on dry-wt) and SWB (soil/wastes mixtures with a ratio of 0.8:1 and added by degrading microorganisms). The organic matter degradation occurred due to the decomposition of H_2O (soluble in hot water) and HEM (hemicellulose-like) fractions during the composting, which H_2O contributed most to the total organic matter loss. The composting of contaminated soil amended with fresh waste mixtures can reduce PAH concentrations within a 40^{th} and 70^{th} percentile range by a dissipation rate varied from 0.0101 to 0.0182 day^{-1} for Treatments SW and SWB after 60 days of continuous treatment following a variable temperature profile. No significant influence of degrading bacteria could be found on the dissipation of PAHs. The observation of microbial activity showed that these samples were initially dominated by G- bacterial and fungal biomarkers. Fungal biomarkers were particularly abundant during the first 14 days of composting when the PAHs dissipated most obviously. As was demonstrated by Canet et al. (1999), white-rot fungi have the potential to degrade PAH. These microorganisms naturally decompose lignin and cellulose inside wood fibers using a non-specific enzymatic complex, which also enables them to degrade a wide range of contaminants if they are introduced to soils. As the incubation progressed, these treatments showed a distinct increase in the abundance of G+ bacteria. Thus, using fresh green wastes as composting amendment could achieve a higher dissipation of PAHs than in non amended soil due the organic nutrients provided for microbial communities. However, the active microbial communities in each composting phase have not yet been quantified and qualified in this study, and more research in this direction might be beneficial. The bioremediation in contaminated soil by composting showed a complex system. Therefore, in future studies, we will focus on modelling these connected processes in order to answer the following question: how the PAHs are affected by the composting process with and without foreign degraders; which are the dominant microbial populations responsible for the PAH dissipation during the composting.

5.6 Acknowledgements

We are grateful to Egide, the French ministry of Foreign Affairs for providing financial support for this study through the program PHC-PFCC. We thank for supplying the PAH measurements in contaminated soil and Miss Muriel Jolly for her assistance in the organic matter analysis (Van Soest).

5.7 References

AFNOR, 2005. Norme française NFU 44-162. Amendements organiques et supports de culture – Fractionnements biochimiques et estimation de la stabilité biologique. AFNOR, Paris, France.

Alexander, M., 1999. Biodegradation and bioremediation. 2nd ed. Academic Press, San Diego, CA. 453 p.

Amir, S., Hafidi, M., Merlina, G., Hamdi, H., Revel, J.C., 2005. Fate of polycyclic aromatic hydrocarbons during lagooning sewage sludge. Chemosphere 58: 449-458.

Antizar-Ladislao, B., Lopez-Real, J., Beck, A.J., 2005. Laboratory studies of the remediation of polycyclic aromatic hydrocarbon contaminated soil by in-vessel composting. Waste Management 25: 281-289.

Antizar-Ladislao, B., Lopez-Real, J., Beck, A.J., 2006. Degradation of polycyclic aromatic hydrocarbons (PAHs) in an aged coal-tar contaminated soil under in-vessel composting conditions. Environ. Pollut. 141: 459-468.

Antizar-Ladislao, B., Beck, A.J., Spanova, K., Russell, N.J., Lopez-Real, J., 2007. The influence of different temperature programmes on the bioremediation of polycyclic aromatic hydrocarbons (PAHs) in a coal-tar contaminated soil by in-vessel composting. Journal of Hazardous Materials 144: 340-347.

Antizar-Ladislao, B., Spanova, K., Beck, A.J., Russell, N.J., 2008. Microbial community structure changes during bioremediation of PAHs in an aged coal-tar contaminated soil by in-vessel composting. International Biodeterioration & Biodegradation 61: 357-364.

Atagana, H.I., 2004. Co-composting of PAH-contaminated soil with poultry manure. Lett. Appl. Microbiol. 39: 163-168.

Brändli, R.C., Bucheli, T.D., Kupper, T., Furrer, R., Stadelmann, F.X., Tarradellas, J., 2005. Persistent organic pollutants in source-separated compost and its feedstock materials - A review of field studies. J. Environ. Qual. 34: 735-760.

Boonchan, S., Britz, M.L., Stanley, G.A., 2000. Degradation and mineralization of high molecular-weight polycyclic aromatic hydrocarbons by defined fungal-bacterial cocultures. Applied and Environmental Microbiology 66(3): 1007–1019.

Cai, Q.Y., Mo, C.H., Wu, Q.T., Zeng, Q.Y., Katsoyiannis, A., Ferard, J.F., 2007. Bioremediation of polycyclic aromatic hydrocarbons (PAHs)-contaminated sewage sludge by different composting processes. Journal of Hazardous Materials 142: 535-542.

Canet, R., Lopez-Real, J., Beck, A.J., 1999. Overview of polycyclic aromatic hydrocarbon biodegradation by white-rot fungi. Land Contam. Reclam. 7: 191–197.

Canet, R., Birnstingl, J.G., Malcolm, D.G., Lopez-Real, J.M., Beck, A.J., 2001. Biodegradation of polycyclic aromatic hydrocarbons (PAHs) by native microflora and combinations of white-rot fungi in a coal-tar contaminated soil. Bioresource Technology 76: 113–117.

Carmichael, L.M., Christman, R.F., Pfaender, F.K., 1997. Desorption and mineralization kinetics of phenanthrene and chrysene in contaminated soils. Environ. Sci. Technol. 31(1): 126-132.

Carriere, P.P.E., Mesania, F.A., 1995. Enhanced biodegradation of creosote-contaminated soil. Bioresource Technol. 76: 113-117.

Doublet, J., Francou, C., Poitrenaud, M., Houot, S., 2010. Sewage sludge composting: Influence of initial mixtures on organic matter evolution and N availability in the final composts. Waste Management 30: 1922–1930

Englert, C.J., Kenzie, E.J., Dragun, J, 1993. Bioremediation of petroleum products in soil. In Principles and practices for petroleum contaminated soils (Edited by E. J. Calabrese, P. T. Kostecki), Chap. 8. Lewis Publishers, Boca Raton.

Farenhorst, A., 2006. Importance of soil organic matter fractions in soil-landscape and regional assessments of pesticide sorption and leaching in soil. Soil Science society of America Journal 70(3) : 1005-1012.

Francou, C., Linères, M., Derenne, S., Le Villio-Poitrenaud, M., Houot, S., 2008. Influence of green waste, biowaste and paper-cardboard initial ratios on organic matter transformations during composting. Bioresource Technology 99: 8926-8934.

Frostegård, Å., Tunlid, A., Bååth, E., 1993. Phospholipid Fatty Acid Composition, Biomass, and Activity of Microbial Communities from Two Soil Types Experimentally Exposed to Different Heavy Metals. Appl Environ Microbiol. 59(11): 3605-3617.

He., Y.W., Yediler, A., Sun, T., Kettrup, A., 1995. ADSORPTION OF FLUORANTHENE ON SOIL AND LAVA: EFFECTS OF THE ORGANIC CARBON CONTENTS OF ADSORBENTS AND TEMPERATURE. Chemosphere, Vol.30, No.1, pp.141-150.

Joner, E.J., Hirmann, D., Szolar, O.H.J., Todorovic, D., Leyval, C., Loibner, A.P., 2010. Priming effects on PAH degradation and ecotoxicity during a phytoremediation experiment. Environmental Pollution, accepted.

Kästner, M., Breuer-Jammali, M., Mahro, B., 1994. Enumeration and characterization of the soil microflora from hydrocarbon-contaminated soil sites able to mineralize polycyclic aromatic hydrocarbons. Appl. Microbiol. Biotechnol. 41:267-273.

Kästner, M., Mahro, B., 1996. Microbial degradation of polycyclic aromatic hydrocarbons in soils affected by the organic matrix of compost. Applied Microbiology and Biotechnology 44: 668-675.

Kästner, M., Streibich, S., Beyrer, M., Richnow, H.H., Fritsche, W., 1999. Formation of Bound Residues during Microbial Degradation of [^{14}C]Anthracene in Soil. Applied and Environmental Microbiology, May 1999, p. 1834-1842.

Larkin, M.J., Kulakov, L.A., Allen, C.C.R., 2005. Biodegradation and Rhodococus-masters of catabolic versatility. Current Option in Biotechnology 16: 282-290.

Lashermes, G., Houot, S., Barriuso, E., 2010. Sorption and mineralisation of organic pollutants during different stages of composting. Chemosphere 79: 455-462.

Lau, A.K., Lo, K.V., Liao, P.H., Yu, J.C., 1992. Aeration experiments for swine waste composting. Bioressource Technology, 41:145-152.

Leclerc, B., 2001. Guide des matières organiques. (eds Guide Technique de l'ITAB).

Lee, P.H., Ong, S.K., Golchin, J., Nelson, G.L.S., 2001. Use of solvents to enhance PAH biodegradation of coal tar-contaminated soils. Water Res. 35: 3941-3949.

Li, H., Luo, Y.M., Song, J., Wu, L.H., Christie, P., 2006. Degradation of benzo[a]pyrene in an experimentally contaminated paddy soil by vetiver grass (Vetiveria zizanioides). Environ Geochem Health 28:183-188

Mahro, B., Schaefer, G., Kfistner, M., 1994. Pathways of microbial degradation of polycyclic aromatic hydrocarbons in soil. In: Hinchee AR, Leeson E, Semprini L, Ong SK (eds) Bioremediation of chlorinated and polycyclic aromatic

hydrocarbons. Lewis, Boca Raton, Fla, pp. 203-217

Mathur, S.P., Dinel, H., Owen, G., Schnitzer, M., Dugan, J., 1993. Determination of compost biomaturity. II.Optical density of water extracts of compost as a reflexion of their maturity. Biological Agriculture and Horticulture, 10: 87-108.

Navarrete, A., Peacock, A., Macnaughton, S.J., Urmeneta, J., Mas-Castellà, J., White, D.C., Guerrero, R., 2000. Physiological status and community composition of microbial mats of the Ebro Delta, Spain, by signature lipid biomarkers. Microb. Ecol. 39: 92-99.

Olivier, P., Rafin, C., Reignie, E., 2004. Bioremediation of an aged polycyclic aromatic hydrocarbons (PAHs)-contaminated soil by filamentous fungi isolated from the soil. International Biodeterioration & Biodegradation 54: 45-52.

Parekh, N.R., Bardgett, R.D., 2002. The characterisation of microbial communities in environmental samples. In: Keith-Roach, M.J., Livens, F.R. (Eds.), Interactions of Microorganisms with Radionuclides. Elsevier Science Ltd., pp. 37-60.

Pignatello, J.J., Xing, B.S., 1996. Mechanisms of slow sorption of organic chemicals to natural particles. Environmental Science & Technology, 30: 1-11.

Potter, C.L., Glaser, J.A., Chang, L.W., Meier, J.R., Dosany, M.A., Herrmann, R.F., 1999. Degradation of polynuclear aromatic hydrocarbons under bench-scale compost conditions. Environ. Sci. Technol. 33: 1917-1925.

Richard, T.L., Hamelers, H.V.M., Veeken, A., Silva, T., 2002. Moisture relationships in composting processes. Compost Science & Utilization 10: 286-302.

Sadaka, S., Taweel, A.E., 2003. Effect of aeration and C: N ratio on household waste composting in Egypt. Compost Science & Utilization, 11, 1: 36-40.

Sánchez-Monedero, M.A., Roig, A., Cegarra, J., Bernal, M.P., 1999. Relationships between water-soluble carbohydrate and phenol fractions and the humification indices of different organic wastes during composting. Bioresource Technology, 70: 193-201.

Sasek, V., Bhatt, M., Cajthaml, T., Malachova, K., Lednicka, D., 2003. Compost-mediated removal of polycyclic aromatic hydrocarbons from contaminated soil. Arc. Environ. Contam.Toxicol. 44: 336-342.

Sims, J.L., Sims, R.C., Matthews, J.E., 1990. Approach to bioremediation of contaminated soil. Hazard Waste Hazard Mater 7: 117-149

Sverdrup, L.E., Nielsen, T., Krogh, P.H., 2002. Soil ecotoxicity of polycyclic aromatic hydrocarbons in relation to soil sorption, lipophilicity, and water solubility. Environ. Sci. Technol. 36: 2429-2435.

Van Soest, P.J., Wine, R.H., 1967. Use of detergents in the analysis of fibrous feeds. IV. Determination of permanganate. Journal of A. O. A. C., 50, 1: 50-55.

Wischmann, H., Steinhart, H., 1997. The formation of PAH oxidation products in soils and soil/compost mixtures. Chemosphere 35: 1681-1689.

Wilson, S.C., Jones, K.C., 1993. Bioremediation of soil contaminated with polynuclear aromatic-hydrocarbons (PAHs) – a review. Environ Pollut. 81: 229-249.

Willson, G.B., 1989. Combining raw materials for composting. Biocycle 30: 82-83.

Yang, H., Su, Y.H., Zhu, Y.G., Chen, M.M., Chen, B.D., Liu, Y.X., 2007. Influences of polycyclic aromatic hydrocarbons (PAHs) on soil microbial community composition with or without Vegetation. Journal of Environmental Science and Health Part a- Toxic/Hazardous Substances & Environmental Engineering 42: 65-72.

Zelles, L., Bai, Q.Y., 1994. Fatty acid patterns of phospholipids and lipopolysaccharides in environmental samples. Chemosphere 28: 391-411.

Zelles, L., Bai, Q.Y., Rackwitz, R., Chadwick, D., Beese, F., 1995. Determination of phospholipid- and lipopolysaccharidederived fatty acids as an estimate of microbial biomass and community structures in soils. Biol. Fert. Soil. 19: 115-123.

Zelles, L., 1999. Fatty acid patterns of phospholipids and lipopolysaccharides in the characterisation of microbial communities in soil: a review. Biol. Fertil. Soils. 29: 111-129.

Zhang, H.H., Lin, K,. Wang, H.L., Gan, J., 2010. Effect of Pinus radiata derived biochars on soil sorption and desorption of phenanthrene. Environmental Pollution 158: 2821-2825.

Zhang, W.X., Bouwer, E.J., Ball, W.P., 1998. Bioavailability of hydrophobic organic contaminants: effects and implications of sorption-related mass transfer on bioremediation. Ground Water Monit. Remediat. 18(1): 126-138.

CHAPTER 6: MODELLING REMEDIATION OF POLYCYCLIC AROMATIC HYDROCARBON (PAH) CONTAMINATED SOIL THROUGH COMPOSTING WITH COP-COMPOST MODEL

6.1 Materials and Methods

6.1.1 Contaminated soil

The contaminated soil was collected from the site located in Beijing (39.85°N, 116.54°E) where was highly polluted by the coal industry. The soil was screened into 2mm and then dried in the air before being sent for analysis. The soil was a loam-sandy soil with 12.4% of clay, 33.2% of silt and 54.4% of sand. The initial total concentration of 16 USEPA PAHs ($\sum_{PAHs}$) was 69.7±2.2 mg kg^{-1} soil (on dry-wt basis). The initial carbon content of contaminated soil was 1.5±0.3% (g. 100 g^{-1} dry wt).

6.1.2 Mixture of wastes

For the composting experiment, a prepared mixture of organic wastes was added to the soil. The prepared mixture of wastes included leaves, branches and bio-wastes consisting of green vegetables like cabbage, spinage and celery (60%, 28% and 12% of total mixture on dry matter basis, respectively). All waste materials were crushed into 2mm pieces before being mixed. The initial C/N ratio of a composting mixture should be comprised in a range of 25 to 40 to provide suitable composting condition (Leclerc 2001). Therefore, the initial proportions in the waste mixture were calculated to get an initial C/N ratio of 29.3 in the initial mixture.

The initial concentration of ∑ 16 USEPA listed PAHs in the mixture of wastes was 5.0±0.2 mg kg^{-1} dry-wt. The initial content of total carbon content in the mixture of wastes was 42.8±0.2% (g.$100g^{-1}$ dry-wt^{-1}).

6.1.3 Initial soil/waste mixtures

The mixture of wastes was added to the contaminated soil with a ratio of 0.8:1 (dry-wt

soil/ dry-wt wastes) as used in Antizar-Ladislao et al. (2005). The TC content in the initial mixture was 24.5±0.7%. The C/N ratio of the initial soil/waste mixture was 25.6. The initial total concentration of 16 USEPA PAHs ($\sum_{PAHs}$) was 74.6±2.4 mg kg^{-1} dry-wt. The $\sum_{PAHs}$ concentration was higher than that in contaminated soil, because PAHs were also detected in the mixture of fresh wastes.

6.1.4 Bioreactors

Beakers with a volume of 1L (diameter of 106mm and a height of 150mm) were used (see details in Fig.1) and placed in water-bathes to control the temperature. Each treatment was run in triplicate in 3 separate beakers. During composting, the optimal aeration during the active phrase varied from 3L.h^{-1}.kg^{-1} dry-wt (Lau et al. 1992; Sadaka and Taweel 2003) to 150L.h^{-1}.kg^{-1} dry-wt (Mathur et al. 1993). The used aeration rate decreased during composting from 12-25 L. h^{-1}.kg^{-1} dry-wt. at the beginning to 3-6 L.h^{-1}.kg^{-1} dry-wt at the end as proposed by Francou el al. (2008).

6.1.5 Temperature and moisture

The variation temperature profile: Days 0–14 at 38°C, Days 15–35 at 55°C, Days 36–42 at 70°C and Days 43–60 at 38°C was chosen according to Antizar-Ladislao et al. (2005). The temperature profile simulated the natural composting system and was controlled by the water-bathes. The optimal moisture content during composting process generally varies between 50 and 80% of total wet mass (Willson 1989; Richard et al. 2002). The moisture content in treatments W, SW and SWB were maintained to 40% by adding water into the bioreactors after each sampling event. In the control treatment S, a moisture content of 40% made the contaminated soil too wet to be in aerobic condition, and a moisture content of 15% in Treatment S was chosen in agreement with the maximal water content of soil. Li et al. (2006) also found that submerged conditions can inhibit the degradation of B[a] P in soil.

6.1.6 Sample collection

Except at the beginning and the end of composting (Day 0 and 60), the other sampling

events were performed just before each change of temperature at days 14, 35 and 42. Every time of sampling, the beakers were emptied, well mixed and then sampled in triplicate. The samples were collected and frozen at -80°C for the analysis of TOM, PAHs and adsorption coefficient (Kd) of FLT and PHE on soil and on soil/waste mixture.

6.1.7 Organic matter analysis

The samples were dried in the oven at 40°C and then at 105°C for getting the dry matter. The evolution of biochemical fractions was measured by using the Van Soest method (Van Soest and Wine 1967), but just for the treatment W because of the limit of the Van Soest method. Successive extractions of water soluble (H_2O), soluble substances in neutral detergent (SOL), hemicellulose-like (HEM), cellulose-like (CEL) and lignin & cutin-like (LIC) fractions were proceeded as described in the French XPU 44-162 standard (AFNOR 2009).

6.1.8 PAHs analysis

The PAHs were extracted from 4g samples which were dried by lyophilisation and then weighed in triplicate into the pressure tubes used for accelerated solvent extractor (Dionex ASE-300). Dichloromethane/acetone (1:1) was the solvent. The sample, filler and solvent were heated to 100°C, pressure 10.35 MPa using the standard ASE program. The extracts were purified on chromatographic columns packed with 12 cm SiO_2 (100/200 mesh; conditioned at 180°C during 12 h before use), 6 cm Al_2O_3 (100/200 mesh; 250°C; 12 h), and 1 cm Na_2SO_4 (450°C; 4 h). In order to remove hydrophobic impurities, the columns were previously washed with 10 ml hexane, then 5 ml of extracts were eluted, and the columns were left to dry for 1 min. The PAHs were then eluted with 70 ml solvent (hexane: dichloromethane, 7:3 v/v). The extracts were concentrated to 1ml by flux of N_2.

PAHs were analyzed using a GC-MS Chemstation (6890N/5975C, Agilent, USA) using a HP-5MS column (19091S-433, 30 m×0.25mm×0.25µm). The injection volume was 1 µl. The temperature programme was 50°C for 2 min, 20°C min^{-1} to

200°C, which was maintained for 2 min, 4.5°C min^{-1} to 240°C which was maintained for 2 min and then 2.5°C min^{-1} to 290°C. The MS was operated in selective ion monitoring (SIM) mode according to chemical ionization.

6.1.9 PAH sorption

The sorption of PAHs was measured on fresh samples of the feedstock materials, the initial mixtures, the homogenized soil/waste mixture at each sampling event and the initial contaminated soil. Two PAHs were used: fluoranthene (FLT) and phenanthrene (PHE) were used. Average sample weight of soil/waste mixture was 1.0 g (soil)/0.06g (wastes) ±0.003 g dry-wt, 1.0 g dry-wt for waste and 3.0±0.003 g dry-wt for the soil samples. Each measurement was done in triplicate. The equivalent PAH concentration in soil/waste mixture samples (expressed in mg kg^{-1} dry-wt) was 1.95 and 1.98 for FLT and PHE. Volumes of 9, 15 or 15 ml of ^{14}C-PAH solution (methanol and alkaline solvents) prepared for the soil/waste mixture, wastes or soil sorption experiments, respectively, were added to the samples in glass corex tubes which were then shaken for 24h at 20°C and then centrifuged for 10 min at 1644 g. The final concentration of ^{14}C-PAH in the supernatants was determined by liquid scintillation counting (Tri-Carb 2100 TR, Perkin Elmer Ins., Courtabeuf, France) using Ultima Gold XR (Packard) as scintillation cocktail. The amount of 14C-PAH sorbed on the soil/waste mixture samples or soil sample (Qs in mg kg^{-1} dry-wt) was calculated from the difference in concentration between the initial PAH solution and the corresponding centrifuged supernatant after 24h of equilibration. The sorption coefficients Kd (in L kg^{-1} dry-wt) were determined as $Kd = Q_s Q_w^{-1}$ where Q_w (in mg L^{-1}) was the PAH concentration in supernatant solution after equilibration. By using the Kd value, the total meausred PAH concentration was separated into two parts: concentraiton of soluble fraction and of adsorbed fraction, which would be applied in the COP-Compost model.

6.1.10 Statistical analysis

Statistical procedures used to describe and evaluate the results were appropriate for the data of our study. The differences between treatments were tested by one-way analysis of variance using SAS (Version 8.1). The paired groups were evaluated using

Burtlett's test. The comparison method Fisher's LSD with a significance level of 0.05 was used to test the significance of pairwise differences.

6.1.11 COP_Compost model

The two modules (OC and OP) of the COP-Compost model can be used separately or coupled (Fig. 1, Table 1). The model has been programmed in Matlab® language (The Mathwork, USA). All equations in the two modules are described in Appendix.

6.1.11.1 Organic C module

Briefly, OC is divided into five pools (Ci, i=1-5) with decreasing degradability. Following first order kinetics with specific hydrolysis constants, these organic pools were hydrolyzed into one organic pool, CS, defined as the substrate available for microbial growth. These five pools could be determined using the Van Soest fractionation method (AFNOR, 2005): OC soluble in neutral detergent (SOL) and the hemicellulose-like (HEM), the cellulose-like (CEL) and lignin-like (LIC) fractions. The SOL fraction was further divided into two pools with fast (SOL-F) and slow (SOL-S) degradability (Francou et al., 2008). The available substrate (CS) was defined as being the hot water soluble fraction of total OC (H2O). Microbial biomass growth and its assimilation of the available substrate were modeled using Monod kinetics, modulated by the temperature growth-limiting function proposed by Rosso et al. (1993). The microbial biomass gradually died off, and the dead cells were recycled into either the SOL-S pool (characterized by a slow hydrolysis rate) or the H2O pool of available substrate.

6.1.11.2 Organic pollutant module

The model proposed by Saffih-Hdadi et al. (2003) to describe pesticide behavior in soil was simplified and adapted to compost. The composting OP module considered three pools of OPs: soluble, sorbed and bound to organic matter. The model also considered a compartment of CO2 arising from OP mineralization. The OP compartments were characterized by means of successive extractions with water (soluble fraction), then with another solvent adapted to the properties of OP (sorbed

fraction). Finally, non-extractable residues (NER) were measured after the extractions and represented the OP bound to organic matter. The model assumed that: i) NER were produced from sorbed OPs, and ii) OP biodegradation only occurred in the soluble phase. The NER formation and OP biodegradation rates were represented by Fr and dr, respectively. Moreover, the distribution of OP between the soluble and sorbed pools was an instantaneous equilibrium described using a sorption coefficient (Kd).

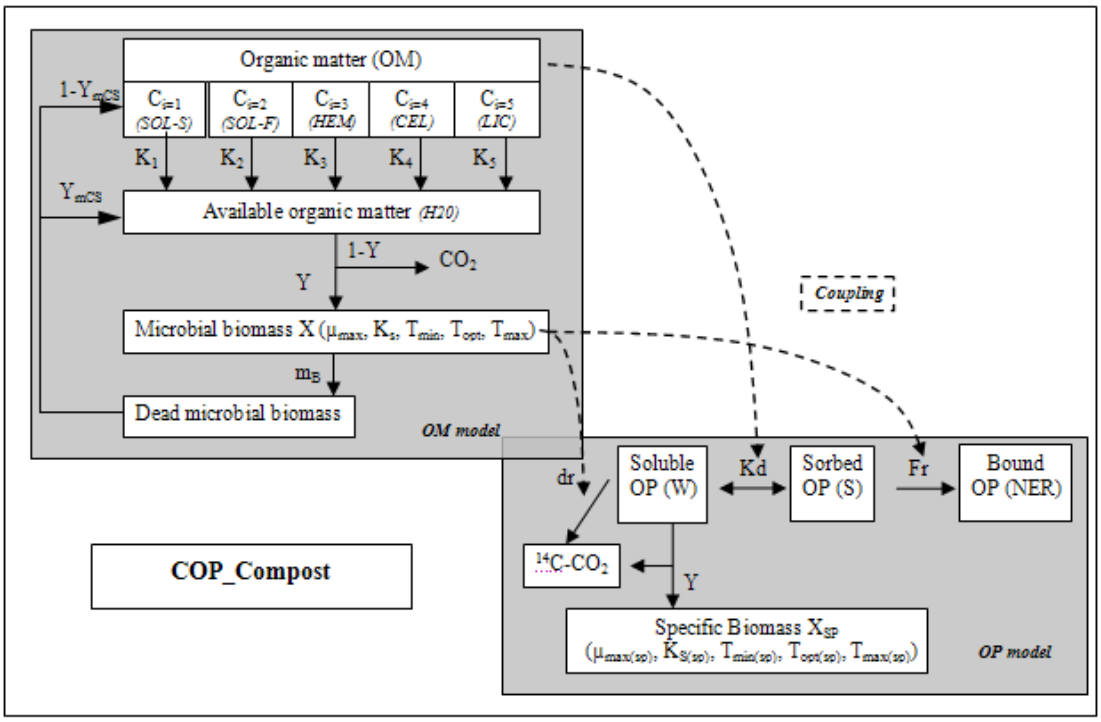


Figure 6.1: Schematical presentation for COP_Compost model

6.1.11.3 Model coupling OC and OP modules

Three coupling hypotheses to describe the interactions between OC and OP modules were proposed:

Hypothesis 1: The overall OP sorption coefficient Kd was assumed to be the sum of the sorption coefficients (Kdi) in the different OC pools (Ci, i=1-5), balanced with the proportions of OC in the pools.

Hypothesis 2: Most OPs were assumed to be degraded by microorganisms through co-metabolism during composting, the microorganisms using compost organic matter

as a primary energy source (Barker et al., 2002). The level of OP degradation was therefore supposed to depend on the potential degradability of the chemicals and on the overall microbial activity driven by organic matter decomposition (Laine et al., 1997).

Hypothesis 3: The formation of NER from sorbed OPs was assumed to depend on the chemical reactivity of the OPs and overall microbial activity.

6.1.12 Model application

Before applying the COP-Compost model, the OM module has been calibrated and evaluated by 12 composting experiments carried out in 170-L pilots using different mixtures of wastes: mixtures R1 to R6 included green waste and biowaste (Francou, 2003; Francou et al., 2008), and mixtures P1 to P6 consisted of sewage sludge and green waste (Doublet, 2008; Doublet et al., 2010). In this study, the averages of optimised parameters in OC part were decided to use for the simulation of OC part. And we did different tests for the part of OP and coupling. The same model efficiency analysis was considered to apply (see details in Zhang et al., 2011).

For the part of OP, no data corresponds the NER and ^{14}C-CO_2 compartments due to the lack of ^{14}C-labelled method application. Two types of OP (FLT and PHE) in our study have been measured the Kd values so that we could identify the W and S fractions. Therefore, in the following, we compared the experimental data of FLT and PHE for W (soluble fraction) and S (sorbed fraction) compartments to compare with the evaluated results, but the simulations of NER and 14C-CO2 have also been shown for better understanding.

In order to do the simulations, firstly the OP model without coupling was applied, and we have done two tests for model evaluation. For test A, the measured value Kd was used, and Fr and dr were decided to take the values optimised by Lashermes (2011); Test B: Kd, Fr and dr optimised by the model.

6.2 Data acquisition for model simulation

6.2.1 Organic matter analysis

The evolution of Van Soest fractions of OM after 60 days of composting is portrayed

for the W treatment in Fig.6.2. By using the dry mass balance considering the mineralisation fraction, all the organic fractions (SOL, H_2O, HEM, CEL, LIC and CO_2) were expressed on % of total dry mass (see details in Fig.4). The proportion of HEM and H_2O fractions decreased while LIC, CEL and SOL fractions remained constant. These results were generally observed in other composting studies like (Doulet et al. 2010; Francou et al. 2008) except for the CEL fraction that generally decreases during composting.

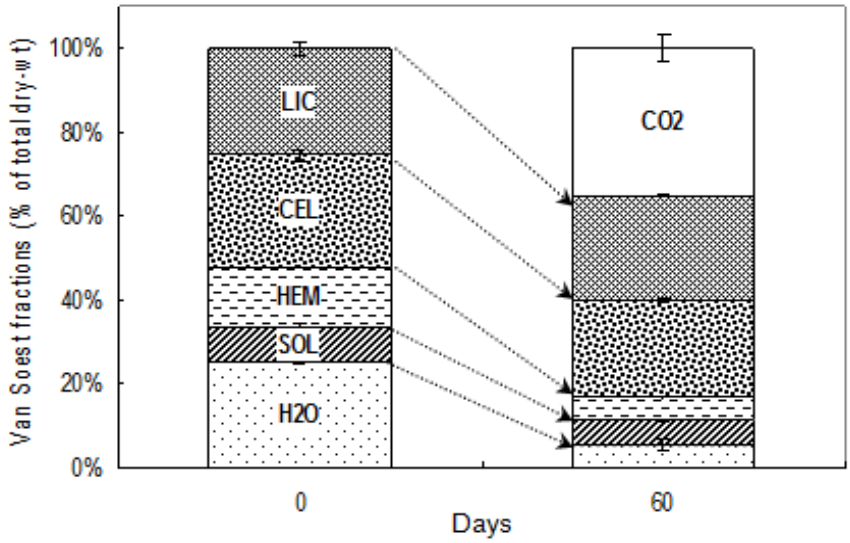


Figure 6.2: Evolution of Van Soest fractions after 60 days of composting

6.2.2 Organic micro-pollutant analysis

6.2.2.1 Evolution of PAHs

The results of PAHs were represented on PAH concentration with the unit of mg/kg dry-wt soil (see Fig.6.3). Total 16 USEPA-PAHs concentration decreased of 50.5±14.8%. The kinetics of dissipation of PAHs were adjusted to first order kinetics with constant rates of degradation of 0.0102 day^{-1}, similar to the value reported in Antizar-Ladislao et al. (2007).

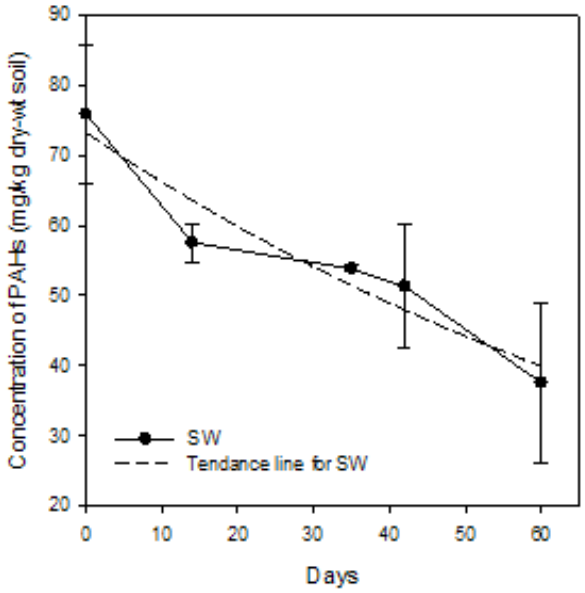


Figure 6.3: Evolution of 16 USEPA-PAHs concentration during composting

6.2.2.2 Evolution of PAH sorption

The Kd values of FLT in soil/waste mixtures decreased slightly from 96 to 73 g sorbed / g soluble and for PHN, the Kd values increased from 44 to 52 g sorbed / g soluble. While in the article of Lashermes et al. (2011), it was found a value of 21.9 g sorbed / g soluble for FLT with OP module, and Kdi ranged from 14 to 68 g sorbed / g soluble for the model of coupling.

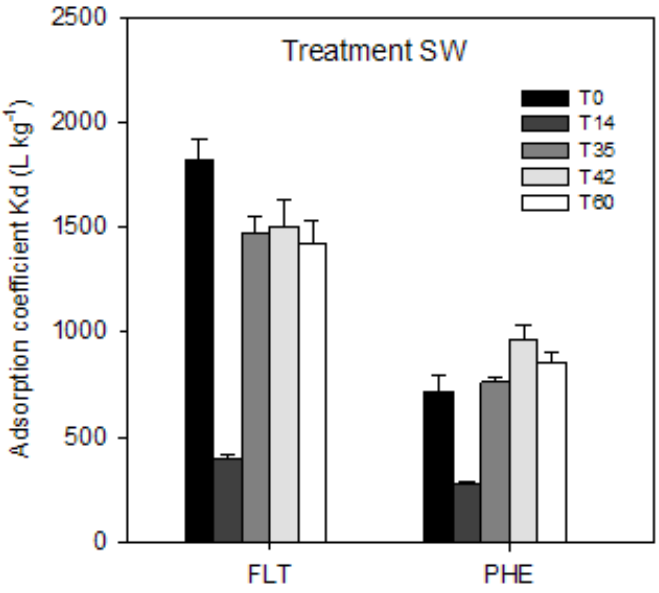


Figure 6.4: Evolution of Kd value for FLT and PHE

6.3 Results and discussion

6.3.1 OM simulation

By applying the results of Van Soest fractions on the day 0 and day 60, we have succeeded to simulate the experimental data by using mean parameter values (see Table 3.1). Shown by Fig.6.5, a good agreement could be found between simulated and observed data for the compartment of H2O, HEM, LIC and CO_2, but not for SOL and CEL. While if we study on the statistics on the modelling efficiency of the simulations which obtained with the calibrated model shown in Table 6.1 for the calibration dataset. The results demonstrate that the SOL compartment was not well simulated and produced the highest RRMSE (221) and a low EF (-2.23). The negative value of EF indicated the model underestimation for experimental data. The use of a unique set of parameters mainly affected the SOL compartment and therefore the mineralization of OC (CO_2 compartment), which displayed much lower EF and higher RRMSE (%) values in Table 6.1. This result was also probably due to a poor prediction of the CEL, which was markedly underestimated during composting, leading to an overestimation of CO_2.

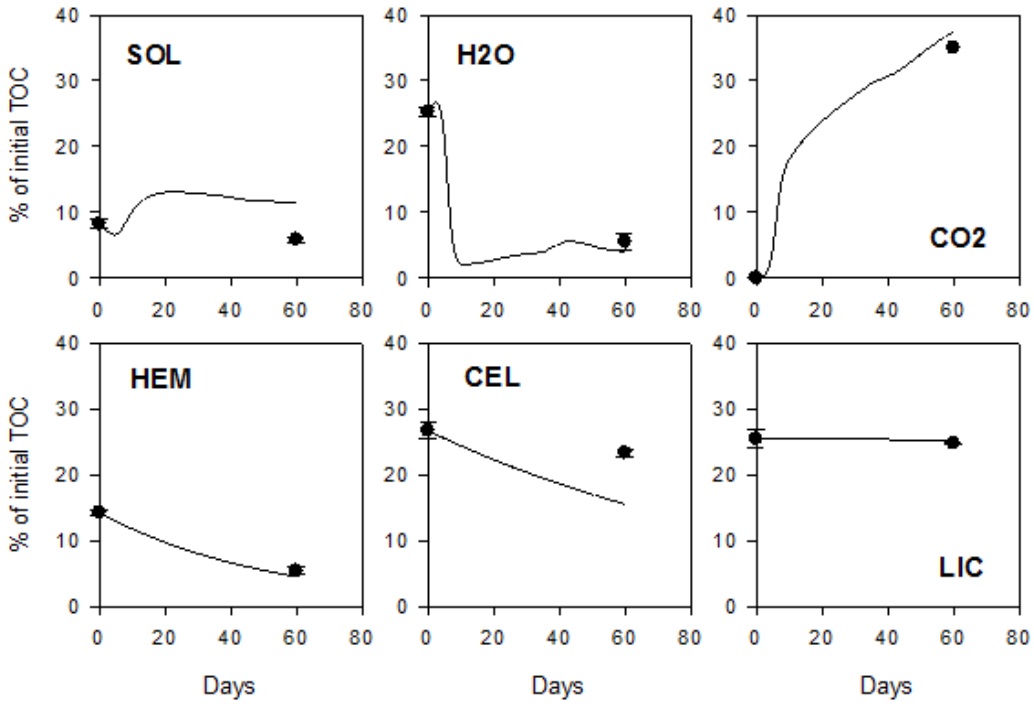


Figure 6.5: Comparison between simulated and observed dataset for the end of composting (Curve: Simulated data; Points: Observed data)

Table 6.1: Statistical evaluation of the goodness-of-fit of the OC module

	RRMSE-OC	$\overline{D}$	E_f
SOL	221	21.2	-2.23
HEM	106	12.0	0.30
CEL	103	26.8	0.29
LIC	124	38.4	-0.02
H2O	34	5.1	0.93
CO_2	193	42.0	-0.86

6.3.2 OP simulation

6.3.2.1 Simulations without coupling model

Table 6.2 showed the different parameter values we applied for model evaluations. According to the Fig.6.6 and 6.7, we can easily find that the simulations would be better enough when the parameters were fitted by the model, either for FLT (Fig.6.6) or for PHE (Fig.6.7). This conclusion could be supported by the statistical evaluations indicated in Table 6.3, which showed that both for FLT or for PHE, after doing optimising the parameters, the RRMSE (%) declined obviously (From 22-30 in Test A, to 4-7 in Test B) and the EF value approached to 1. On the other hand, the simulations of NER and ^{14}C-CO_2, we have no experimental data to calibrate, so that we can give the jugement.

Table 6.2: The parameters applied in the OP module for simulating the observed data

		Test A		**Test B**	
Type of PAH	**Parameters**	**Value**	**Source**	**Value**	**Source**
FLT	**Kd**	81.65	Measured (Zhang et al. 2011)	81.65	Measured (Zhang et al. 2011)
	Fr	0.0037	Ref. (Lashermes et al., 2011)	0.0099	Optimised by the model
	dr	0.0013	Ref. (Lashermes et al., 2011)	0.0011	Optimised by the model
PHE	**Kd**	50.76	Measured (Zhang et al. 2011)	50.76	Measured (Zhang et al. 2011)
	Fr	0.0037	Ref.(Lashermes et al., 2011)	0.0111	Optimised by the model
	dr	0.0013	Ref. (Lashermes et al., 2011)	0.0001	Optimised by the model

Table 6.3: Statistical evaluation of the goodness-of-fit of the OP module

OP type		Model	RRMSE-OP		$\overline{D}$		E_f	
			Test A	Test B	Test A	Test B	Test A	Test B
FLT	**W (Soluble)**	OP	22	4	0.2	0	-1.19	0.92
		Coupling	8.5	20.7	0	0	0.68	0.88
	S (Sorbed)	OP	27	4	16.1	1.0	-0.17	0.97
		Coupling	7.7	28.6	0.4	17	0.91	0.28
PHE	**W (Soluble)**	OP	30	7	0.3	0	0.23	0.96
		Coupling	9.8	27.2	0	0	0.92	0.36
	S (Sorbed)	OP	28	4	16.2	-1.0	-0.21	0.97
		Coupling	7.7	28.6	0.5	16	0.90	-0.31

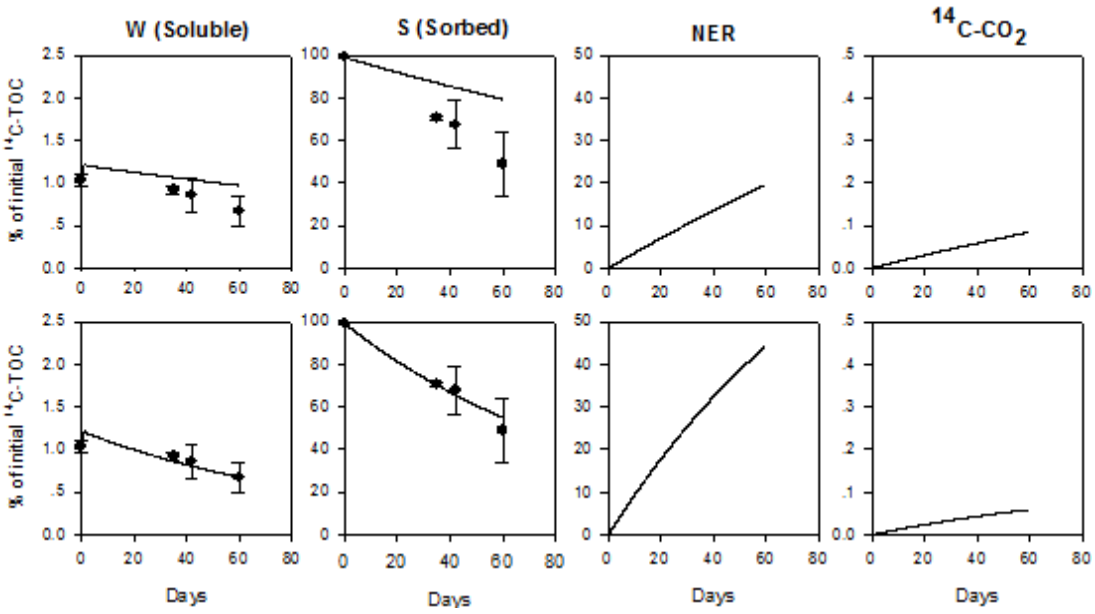


Figure 6.6: Relationships between experimental and simulated values for soluble, sorbed, non-extractable (NER) and mineralized fraction (^{14}C-CO_2) of FLT, with Test A and B. The first line corresponds Test A and second line represents Test B.

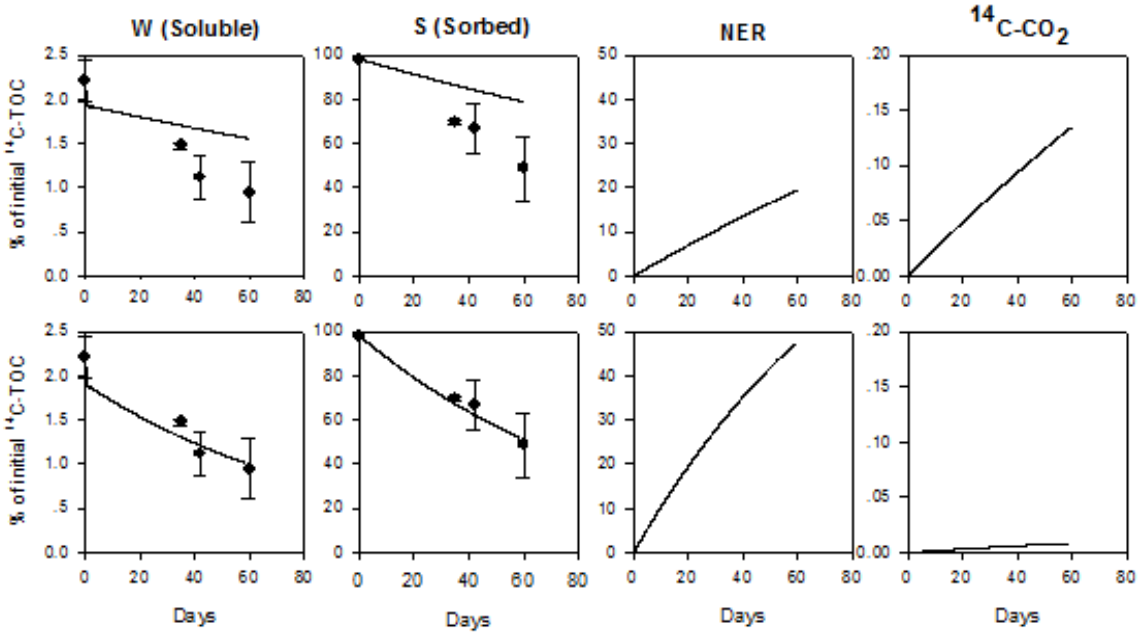


Figure 6.7: Relationships between experimental and simulated values for soluble, sorbed, non-extractable (NER) and mineralized fraction (^{14}C-CO_2) of PHE, with Test A and B. The first line corresponds Test A and second line represents Test B.

6.3.2.2 Simulations with coupling model

Finally we tried to couple the OC part with the OP part. Still two tests were carried out. The averages optimized parameters of OC were always applied for the OC module. For Test A, the parameters of OP were optimized by the model and we applied the average values of Fr_B and dr for both FLT and PHE; for Test B, the average values of Fr_B and dr optimized by Lashermes (2010) were used. The parameters were summarized in Table 6.4.

Fig.6.8 and 6.9 showed that the coupling model can also well simulate the observed data. The efficiency coefficients could support this conclusion, which indicated the low RRMSE (value less than 10 for both FLT and PHE). While, if compare Fig.6.8 and 6.9 with Fig.6.6 and 6.7, the better simulations were observed in OP module with parameters optimised rather than in coupling model. The results were probably due to the bad simulations of SOL and CEL. Therefore influence the simulations of OP fractions (W and S).

Table 6.4: Parameter values and evaluation statistics of OP simulations

	FLT					PHE	
	Zhang, 2011		Lashermes, 2010			Zhang, 2011	
	Test A	Test B	FLT-1	FLT-2	FLT-3	Test A	Test B
Kd_1	73.0	-	68.4	38.5	42.2	44.32	-
Kd_2	79.5	-	68.4	38.5	42.2	49.00	-
Kd_3	79.5	-	14.3	28.4	15.0	51.00	-
Kd_4	96.2	-	26.7	29.0	15.4	59.80	-
Kd_5	0.0	-	0.0	0.0	0.0	0.000	-
Fr_B	0.0030	0.0012	0.0007	0.0016	0.0014	0.003	0.0012
dr	0.0001	0.0003	0.0002	0.0005	0.0003	0.0001	0.0003

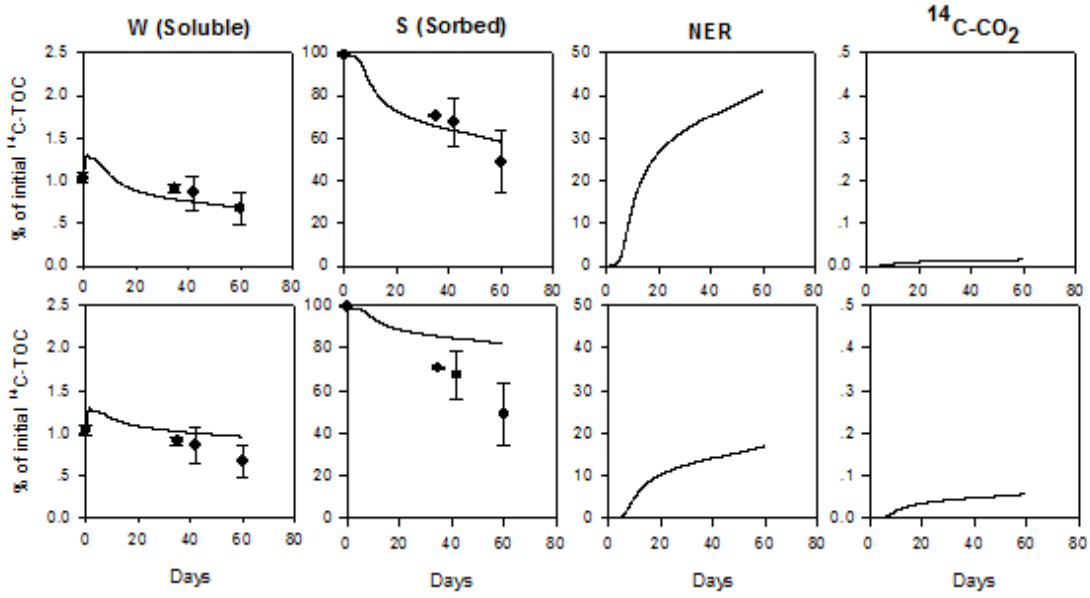


Figure 6.8: Relationships between experimental and simulated values for soluble, sorbed, non-extractable (NER) and mineralized fraction (^{14}C-CO_2) of FLT, with the coupling model. The first line corresponds Test A and second line represents Test B.

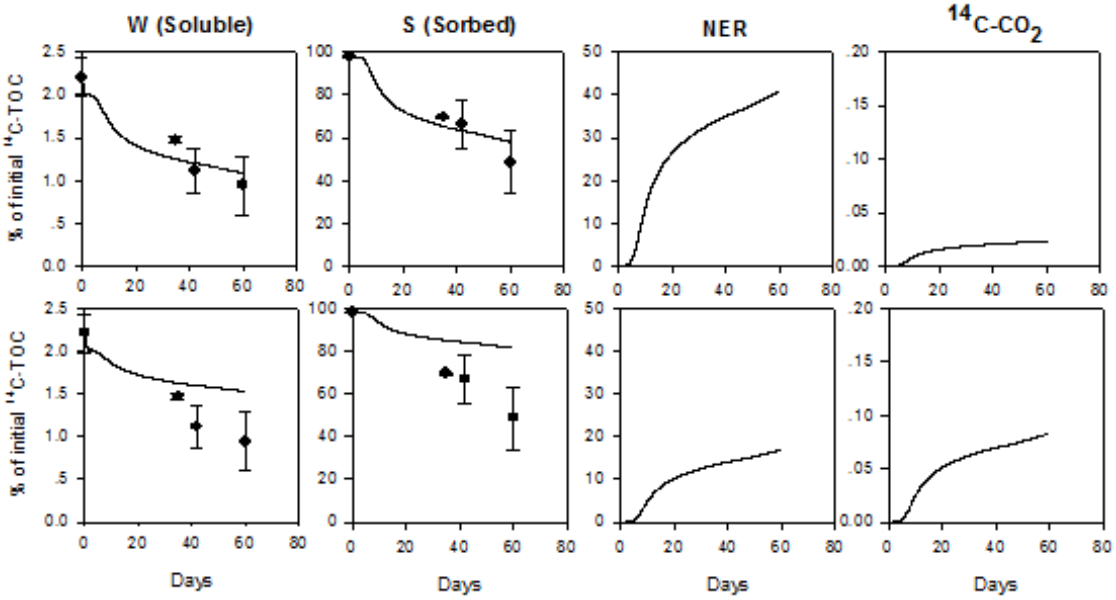


Figure 6.9: Relationships between experimental and simulated values for soluble, sorbed, non-extractable (NER) and mineralized fraction (^{14}C-CO_2) of PHE, with the coupling model. The first line corresponds Test A and second line represents Test B.

PART III: GENERAL CONCLUSION AND PERSPECTIVES

GENERAL CONCLUSION AND PERSPECTIVES

In order to make composting as a continuable field of urban waste recycling and a bioremediation technique for contaminated soil, it is paramount to ensure the quality of compost products guaranteeing of low contents of pollutants and their harmlessness to the agricultural soil. Many studies show a dissipation of OPs during the composting process. However, when traditional chemical analysis is carried out, that corresponds to a reduction in the quantities of extracted OPs and the various ways of dissipation cannot be characterized. During composting, OPs are indeed likely to be volatilized or to be transported into lixiviates, which in fact consists of a pollution displacement. They can also be stabilized by sorption on the organic matter or formation of bound residues. In this case, the availability of OPs is decreased although only the biodegradation of OPs is a real mechanism of elimination. There are few studies focusing on the characterization of the various mechanisms of OPs dissipation during composting and the determination on behalf of the extractable/not-extractable residues. Moreover, no model describing the concerned mechanisms was proposed. The characterization of the availability of OPs during composting and in the final composts are however essential data elements for the risk evaluation related to the practice of spreading of the composts on the agricultural soil.

The objective of this thesis was to propose and parameterize a model simulating the evolution of the speciation of OPs during composting by explicitly taking into account the influence of the nature of composted organic waste. This model can be separated into three parts for using: OM model, OP model and coupling model. The experimental data from literature and my experiment were used to calibrate and validate these three parts. This model is brought to be a tool using the experimental data of the various types of OPs on the function of the nature of composting materials and the process of composting in order to assess the risks of dissemination of OPs at the time of the spreading of the composts onto the agricultural soil.

This work of thesis proceeded in three great stages: I) Construction and parameterize a model describing the mechanisms of the joint evolution of the organic matter and OPs during composting. II) Calibration and validation of the model constructed by using the existent data from literature; sensitivity analysis of key parameters to the model. III) The installation of an in-lab device of composting as pilots of small volume to study the performance of realistic and reproducible composting wastes on soil contaminated with PAHs.

The new COP-Compost model has been developed to simulate the evolution of organic pollutants (OP) availability during composting in interaction with organic matter. It comprises one module for the evolution of organic carbon (OC) and one module for the dynamics of OP, as well as the microbial activities.

A kinetic partitioning model called COP-Compost model coupled the organic matters (OC) module and organic pollutants (OP) module. The model was applied to simulate the changes in organic matters, organic pollutants, as well as the microbial activities during composting process. For model calibration, 12 composting experiments varying in initial organic matter characteristics were chosen from literature to estimate OC module parameter.To calibrate the OP module, the results of Hartlieb et al. (2003) were used to simulate the OP, and then coupling with one of the organic mixtures P3 described in Zhang et al. (2011). The mixture P3 (green wastes=64%; sewage sludge=14%; branches=17%; grass clippings=5%) was made initially from 4 organic fractions (SOL = 16.15, HEM = 13.8, CEL = 26.6 LIC = 28.33 and H2O = 15.12, with a unit: % of initial TOC). An application of COP_Compost model has been tried by Lashermes et al. (2011). In her study, the coupled OC-OPs model was evaluated from composting experiments performed in 4-L pilots using either ^{14}C-labeled fluoranthene, 4-n-nonylphenol, linear alkylbenzene sulfonate or glyphosate. The distribution of organic pollutants between soluble, sorbed and non-extractable fractions was measured by extraction procedures.

For the model evaluation, in OC module, seven fixed parameters were obtained from the literature or calculated directly from the measurements, while six were estimated by inverse modelling of the OC module; in OP module, adsorption coefficient (Kd) values were calculated and estimated directly on the basis of experimental data, while the other parameters were optimised by the model. In order to assess the relative

importance of individual parameters on the overall model performance, a sensitivity analysis was also conducted. A good agreement was achieved between simulated and experimental results describing the evolution of different organic fractions except a poor simulation of the cellulosic and soluble pools.

In summary, using an innovative approach, the COP-Compost model combines the dynamics of OC and OPs during composting by coupling two modules. All the calibration results have demonstrated that coupling the OC and OP modules can improves the simulation of OP speciation during composting. The model simulated satisfactorily the evolution of OC and OPs. For the OC module, only data on the biochemical composition of the initial waste mixture was required for the simulation, which is a relatively accessible analysis. For the OP module, further research is now necessary to assess the parameters using pollutants with different initial waste mixtures. Correlations need to be determined between the estimated parameters and data that would be more easily available than those obtained from ^{14}C-labeled experiments.

In order to assess the relative importance of individual parameters on the overall model performance, a sensitivity analysis was also conducted. A good agreement was achieved between simulated and experimental results describing the evolution of different organic fractions except a poor simulation of the cellulosic and soluble pools. The sensitivity analysis demonstrated that the assimilation yield (Y), the death rate (m), adsorption coefficient (Kdi) and the degradation rate (dr) greatly influenced the evolution of all the OP fractions.

A model, describing the dynamic of organic matter during composting was constructed base on the biochemical characteristics of organic matter. From 12 composting experiments varying in initial organic matter characteristics, we get a unique set of parameters able to correctly simulate the evolution of organic matter characteristics during these 170 L reactor experiments. The dynamic of the soluble fraction could be improved by taking into account the recalcitrant part of the initial soluble fraction but more research is needed to access experimentally this fraction.

The coupling model has been examined that its simulations could well fit with the observed data by using our estimated parameters. By adding a specific microbial population into the coupling model, the simulations showed improvement especially for the mineralisation of OPs. However, it should be tested with more experimental data before the validation.

The sensitivity analysis demonstrated that the assimilation yield (Y), the death rate (m), adsorption coefficient (Kd_i) and the degradation rate (dr) greatly influenced the evolution of all the fractions of either pyrene or simazine, as well as the specific microorganisms for simazine; while a low sensitivity was found for microbial growth rate (μmax), saturation constant (Ks) limiting the relative importance of Monod terms (decomposition of OM) in the growth of microorganisms under standard operating conditions. These results are consistent with those found by by Stombaugh and Nokes (1996) or Hamelers (2001), and contribute to the understanding the interactions between the different substrates and microbiota, and their relative importance to the composting process.

Introduction Composting may enhance bioremediation of PAH-contaminated soils by providing organic substrates that stimulate the growth of potential microbial degraders. However, the influence of added organic matter (OM) together with the microbial activities on the dissipation of PAHs has not yet been fully assessed. **An in-vessel composting-bioremediation experiment of a contaminated soil amended with fresh wastes was carried out.** Four different experimental conditions were tested in triplicate during 60 days using laboratory-scale reactors: treatment S (100%soil), W (100%wastes), SW (soil/ waste mixture), and SWB (soil/waste mixture with inoculation of degrading microorganisms).

A dry mass loss of 35±5% was observed in treatments with organic wastes during composting in all the treatments except treatment S. The dissipation of the 16 USEPA-listed PAHs was largely enhanced from no significant change to 50.5±14.8% (for SW)/63.7±10.0% (for SWB). More obvious dissipation was observed when fresh wastes were added at the beginning of composting to the contaminated soil, without significant difference between the inoculated and non-inoculated treatments. Phospholipid fatty acid (PLFA) profiling showed that fungi and G-bacteria dominated at the beginning of experiment and were probably involved in PAH dissipation. Subsequently, greater relative abundances of G+ bacteria were observed as PAH

dissipation slowed down.

Thus, using fresh green wastes as composting amendment could achieve a higher dissipation of PAHs than in non-amended soil due the organic nutrients provided for microbial communities. However, the active microbial communities in each composting phase have not yet been quantified and qualified in this study, and more research in this direction might be beneficial. The bioremediation in contaminated soil by composting showed a complex system. Therefore, in future studies, we will focus on modeling these connected processes in order to answer the following questions: how the PAHs are affected by the composting process with and without foreign degraders; which are the dominant microbial populations responsible for the PAH dissipation during the composting; moreover, how to apply more compartments to describe the different activities of microbial populations.

At the last phase, **first tests of COP_Compost model were carried out using the results of our composting-bioremediation experiment** for the part of OC, OP as well OC-OP coupling. A good agreement was achieved between simulated and experimental results describing the evolution of different organic fractions using OC module. For OP module, estimation parameter was necessary. More developments will be necessary to conclude. In order to achieve this part, some improvements of the model should be carried out like the simulation of a specific microbial biomass.

In order to better answer these questions above, in the last period of my PHD, a complimentary experiment has been carried out cooperating with the other PHD student PENG Jingjing by using the ^{13}C-Pyrene. With the help of the method molecular analysis and T-RFLP, the active microbial population at different PAH degradation phase will be identified and also quantified. Therefore we can use the results to characterize different compartment of microbial population in the COP_Compost model.

In this composting experiment, the same bioreactors (see Fig.5.1) were used and two treatments were chosen with triplicate per one to study: Treatment A (A1-A3) was the mixture of soil with green wastes with a dry-wt. ratio of 0.8:1, which the soil was contaminated artificially by ^{12}C-pyrene with a concentration of 100mg/kg (dry-wt.); while the treatment B (B1-B3) was the same mixture excepet the soil was polluted

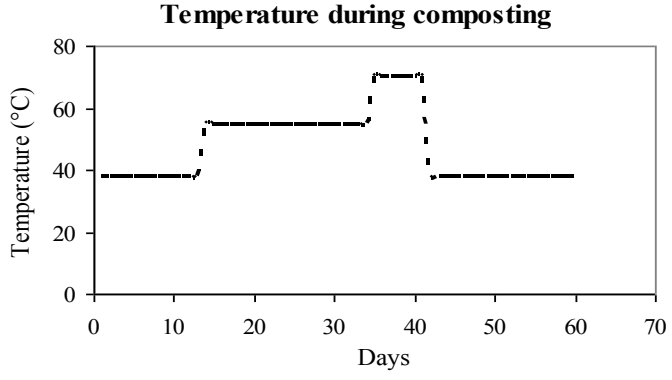
artificially by ^{13}C-pyrene but with the same concentration of 100mg/kg (dry-wt.).

The simulation of composting at a small scale is not obvious since the mass of biodegradable organic matter put into the reactors is not large enough to ensure a thermal inertia leading to thermophilic conditions and to maintain microbial activity over a long period. Bioreactors were placed in temperature-controlled water-bathes to simulate representative thermal stages during in-vessel composting processes.

The variation temperature profile (See Fig.A) for the time periods days 0–14 at 38°C, days 15–35 at 55°C, days 36–42 at 70°C, and days 43–60 at 38°C was chosen according to Antizar-Ladislao et al. (2005). These conditions simulated the operation of a commercial in-vessel operating system by including the minimum thermophilic temperature of 70°C required for pathogen control (Antizar et al. 2007). The optimal moisture content during composting generally varies between 50% and 80% of total wet mass (Willson 1989; Richard et al. 2002). The moisture content (100× mass of water/mass of wet mixture) in treatments A and B were maintained to 50% by adding water into the bioreactors after each sampling event.

This complimentary work sought to identify the microbial communities in each phase of temperature; to better understand which microbial communities are active in the course of evolution of pyrene (PYR) and to apply for our COP-Compost model with more details. The experiment has been just finished at the moment and the results needs to be analysed in the further study.

Figure A: Temperature profile



Appendix: Equations of the COP-Compost model

APPENDIX: EQUATIONS OF THE COP-COMPOST MODEL

Organic carbon module

The OC dynamic during composting is described through equations based on mass balance, using a daily time step. The unit used is the percentage of initial total organic carbon (TOC) (Table 1).

Variables, parameters and units are detailed in Table 1.

Dynamic of microbial biomass X: $$\frac{dX}{dt} = \mu \cdot X - m_B \cdot X$$

with μ, the growth rate of microbial populations: $$\mu = \mu_{max} \cdot \frac{C_S}{K_S + C_S} \cdot f_T$$

with fT, the temperature growth-limiting function (Rosso et al., 1993):

$$f_T = \frac{(T - T_{max}) \cdot (T - T_{min})^2}{(T_{opt} - T_{min}) \cdot [(T_{opt} - T_{min}) \cdot (T - T_{opt}) - (T_{opt} - T_{max}) \cdot (T_{opt} + T_{min} - 2 \cdot T)]}$$

Hydrolysis of organic C pool Ci (i = 2–5): $$\frac{dC_i}{dt} = -K_i \cdot C_i$$

Hydrolysis of organic C pool C1 and recycling of dead microbial biomass in C1:

$$\frac{dC_1}{dt} = -K_1 \cdot C_1 + (1 - Y_{mcs}) \cdot m_B \cdot X$$

Decomposition of available organic carbon CS:

$$\frac{dC_S}{dt} = \sum_{i=1}^{5} K_i \cdot C_i - \frac{\mu X}{Y} + Y_{mcs} \cdot m_B \cdot X$$

Production of CO2: $$\frac{dCO_2}{dt} = (1 - Y) \cdot \frac{\mu X}{Y}$$

Only one microbial population is considered because of lack of experimental data characterizing the succession of microbial populations during composting. Briefly, the equations relating to the dynamic of the microbial biomass (X) are:

$$\frac{dX}{dt} = \mu \cdot X - m_B \cdot X \qquad [1]$$

Where X is the concentration of microorganisms, with a microbial growth rate μ and a death rate m_B. The microbial growth rate μ follows Monod kinetics:

$$\mu = \mu_{max} \cdot \frac{C_S}{K_S + C_S} \cdot f_T \qquad [2]$$

where μmax is the specific maximum growth rate, CS the content of available substrate nad KS the half saturation constant of the available substrate for microbial biomass. The Rosso et al. (1993) function, fT, describing the influence of temperature, is included for correcting the growth rate of microorganisms with respect to the temperature measured in the compost. This function (see Appendix 1) includes few parameters (i.e., maximum, minimum and optimum temperatures) and overall, a total of 13 parameters and 8 variables are needed to run the OC module.

Organic pollutant module

The behavior of OPs during composting is described through equations based on OPs mass balance, using a daily time step. The unit used is the percentage of initial 14C-labeled OPs applied (Table 1). In the OPs module, the instantaneous equilibrium between soluble (W) and sorbed (S) OPs is described with the following equation:

$$S = Kd \cdot W \qquad [3]$$

where Kd is the sorption coefficient of OPs on the compost.

The OPs mineralization (14C-CO2) depends on the amount of soluble OPs and a biodegradation rate (dr):

$$\frac{d(^{14}C - CO_2)}{dt} = dr \cdot W \qquad [4]$$

In the OPs module, the NER formation follows the equation:

$$\frac{dNER}{dt} = NER_0 + Fr \cdot S \quad [5]$$

where NER0 is the initial amount of NER and Fr the NER formation rate. A total of 3 parameters and 4 variables are needed to run the OP module.

Coupling the OC and OPs modules

To couple the OC and OPs modules, the three coupling hypotheses are set down into equations. As in the OPs module considered alone, the equation [3] represents the instantaneous equilibrium between soluble and sorbed OPs. However, in the case of model coupling, the sorption coefficient is expressed as:

$$Kd = \sum_{i=1}^{5} Kd_i \cdot \frac{C_i}{\sum_{i=1}^{5} C_i} \quad [6]$$

where Kd is the sorption coefficient of OPs by total compost OC and Kdi is the sorption coefficients of OPs on the pools Ci.

The influence of microbial activity on the 14C-OP mineralization is described by:

$$\frac{d(^{14}C - CO_2)}{dt} = dr \cdot X \cdot W \quad [7]$$

where X is the content of microbial biomass growing on the OC decomposition and dr is the OPs biodegradation rate.

For coupling the two modules, the following equation of NER formation was first tested:

$$\frac{dNER}{dt} = NER_0 + (Fr_B \cdot X + Fr_C) \cdot S \quad [8]$$

where FrB and FrC are parameters of the NER formation related to biological activity and chemical reactivity of the compost organic matter, respectively. Since the FrC parameter was close from zero in all simulations, the equation of NER formation was simplified:

$$\frac{dNER}{dt} = NER_0 + Fr \cdot X \cdot S \quad [9]$$

where Fr is the rate of NER formation including both chemical and biological origins. To run the coupled model, a total of 21 parameters and 12 variables are needed.